Genetic Classification of Uveal Melanoma

Serdar Yavuzyiğitoğlu

Genetic Classification of Uveal Melanoma

Thesis, Erasmus University Rotterdam, The Netherlands

ISBN: 978-94-6233-919-4

The research project was initiated by the Department of Ophthalmology and Clinical Genetics, Erasmus Medical Centre Rotterdam, the Netherlands and The Rotterdam Eye Hospital, Rotterdam, The Netherlands. This project was financially supported by the Stichting Nederlands Oogheelkundig Onderzoek (SNOO), Combined Ophthalmic Research Rotterdam (CORR), Prof. dr. Henkes Foundation and the Bayer Ophthalmology Research Award 2016 (BORA).

The printing of this thesis was financially supported by: Bayer BV, ZEISS, Chipsoft, Haagse Kunstogen Laboratorium, Laservision, Prof. dr. Henkes Stichting, Rotterdamse Stichting Blindenbelangen, Stichting Blindenhulp, SWOO – Prof. dr. Flieringa, Thea Pharma, Tramedico, UrsaPharm

Genetic Classification of Uveal Melanoma

Genetische classificatie van uvea melanomen

Proefschrift

ter verkrijging van de graad van doctor aan de
Erasmus Universiteit Rotterdam
op gezag van de
rector magnificus

Prof.dr. H.A.P. Pols

en volgens besluit van het College voor Promoties.
De openbare verdediging zal plaatsvinden op

woensdag 18 april 2018 om 15.30 uur

Serdar Yavuzyiğitoğlu
geboren te Hellevoetsluis

Erasmus University Rotterdam

Promotiecommissie:

Promotoren:	Prof. dr. J.R. Vingerling
	Prof. dr. A.D.A. Paridaens
Overige leden:	Prof. dr. E.C. Zwarthoff
	Prof. dr. R.M.W. Hofstra
	Prof. dr. B.J. Klevering
Copromotoren:	Dr. J.E.M.M. de Klein
	Dr. E. Kiliç

Contents

Chapter 4

General discussion

Chapter 5

Chapter 1

General introduction

Chapter 1.1

Clinical presentation and prognosis

Diagnosis and symptoms

Uveal melanoma (UM) is the most common intraocular malignancy in the Western World in adults.[1] UM derive from the melanocytes in the uveal tract of the eye, in which the choroid is the most frequent location for UM (70-80%), followed by the ciliary body (10-20%) and the iris as the least frequent location (5-10%).[2] Diagnosis is made by an ophthalmologist using fundoscopy in which a mass can be observed in the eye (Figure 1). Additional techniques to confirm or make the diagnosis more likely are ultrasonography (US), indocyanine green chorioangiography (ICG), optical coherence tomography (OCT) and fluorescence angiography (FAG).[3-5]

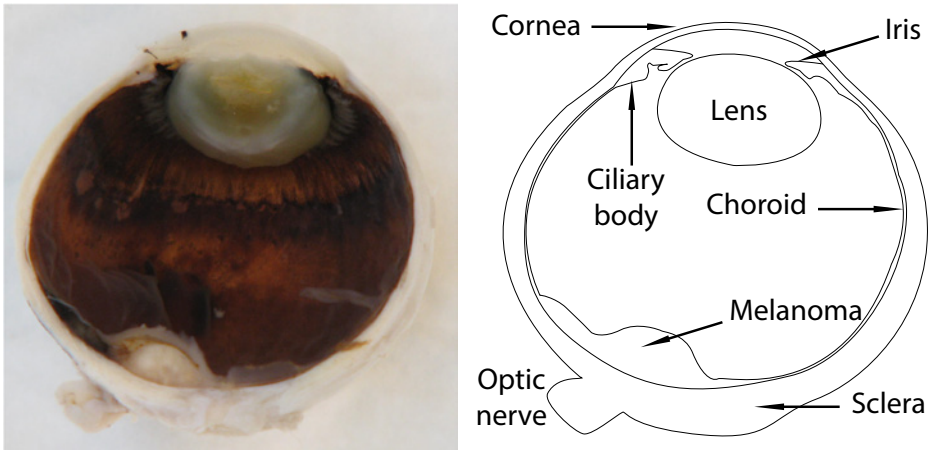

Figure 1. *Cross section of an eye containing a posterior choroidal melanoma. On the right a schematic overview with the anatomical structures.*

UM patients usually present with common ophthalmic symptoms such as decreased sight, visual field defect, floaters and/or flashes.[4,6] In up to 21% of the patients, the UM is missed or misdiagnosed during first examination.[4,7,8] Besides the common ophthalmic symptoms, a large part of UM patients (13-45%) are asymptomatic at the time of diagnosis. These tumors tend to be found during routine ophthalmic examinations co-incidental with other ocular disorders.[4,6,8]

Ocular nevi are benign lesion which occur in approximately 0.2 to 30 % in the Western World.[9,10] Although the prevalence is high, the annual risk for malignant transformation is around 1 in 4300-9000.[9,10] To discriminate between small malignant melanoma and benign nevi, Shields developed the mnemonic 'To Find Small Ocular Melanoma Using Helpful Hints Daily (Figure 2)'.[11,12] The 5-year risk for malignant transformation of a melanocytic lesion with three or more risk factors is more than 50% and thus urges early treatment in these cases.[11,12]

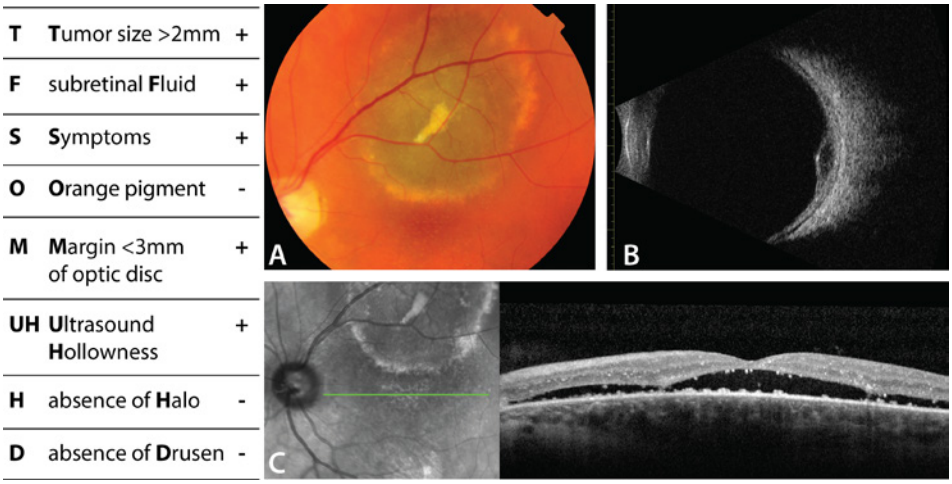

Figure 2. *Clinical presentation of a patient with a choroidal nevus. Listed on the left are the risk factors for malignant transformation (TFSOMUHHD mnemonic from Shields et al. indicated with a '+' if present).*[12] *(**A**) Fundus photo revealed a pigmented lesion with larger and smaller drusen on top of the tumor with a halo surrounding the tumor. The pigmented tumor is located only one disk size (~1.5mm) from the optic disc. (**B**) Ultrasonography showed hollowness and a tumor thickness of 2.5 mm. (**C**) OCT scan of the macula showed subretinal fluid, which was the reason for the newly developed blurry vision. All these risk factors combined give a high-risk for malignant transformation.*

Incidence and risk factors

The incidence of UM ranges from 4.0 to 10.0 in a million in the Western World, with the highest incidence in Scandinavian countries.[1,13] As described before, people with ocular nevi are at risk for the malignant transformation.[9-11] Other predisposing factors for the development of UM are Nevi of Ota which have a 1 in 400 lifetime risk of developing UM.[14,15] Cutaneous nevi and freckles are described in the literature as associated with increased risk for UM.[16] Besides the oculodermal lesions mentioned above, UMs are

also more common among people with a Caucasian ethnicity and light-colored eyes.[17] It is hypothesized that due to the lack of melanin, the melanocytes are more at risk of a malignant turnover caused by damaging UV-light.[17,18] However, despite these risk factors, the role of UV-light in UM remains unclear.[18] Unlike cutaneous melanoma, in which UV-light is proven to be a risk factor, the incidence of UM has not increased in the last several decades, indicating that UV-light does not play a major role in the development of UM.[1,18]

Treatment primary tumor

Treatment of the primary UM depends largely on tumor size. Other factors that play a role are; tumor localization, periorbital growth, general patient condition and patient choice.[19] The treatment options can be divided in tumor irradiation or tumor removal. The main goal of tumor irradiation is primarily to preserve the eye and secondarily the sight. The most commonly used irradiation techniques for small-to-medium sized tumors are proton-beam therapy, stereotactic radiotherapy and episcleral plaque radiation therapy, for which Iodine 125 and Ruthenium 106 are the most used isotopes.[6,20-25] For all irradiation treatment options the success rate of primary tumor control is more than 90%.[20-22,25,26] However, tumors located juxtapapillary are more prone to tumor recurrence and metastatic spread since these tumors are more often radioresistant.[27] Thus for patients with large tumors and tumors located near the optic disc or macula, an enucleation is preferred. For both treatment options, either irradiation or removal, the risk for metastatic disease is similar when corrected for tumor size and location.[4,24]

Prognosis

Despite successful primary tumor treatment, patients still develop metastases in approximately half of the cases (Figure 3A), with a peak at 4 years after diagnosis.[1,28-30] Moreover these metastases have preference for the liver, which is affected in more than 90% of the cases.[31] Since metastasis occurs even after complete removal of the primary tumor with enucleation, it is suggested that micrometastases are present at time of treatment.[28] These micrometastases can grow out to a clinically detectable size even more than 10 years after primary treatment.[28]. Overall survival for patients with metastasis is very poor and most patients die within one year (Figure 3B).[32,33]

Currently, treatment of metastatic disease in UM patients is limited and in general unsuccessful. These metastases seem to be resistant to traditional chemotherapy.[32,34,35] Some patients with single (or limited) solitary liver metastasis may benefit from partial liver resection, however also for these patients the success rate is very low.[36,37] Several clinical trials are conducted in which specific oncogenic pathways are targeted such as the MEK or RAS-ERK kinase pathways. Unfortunately, also for these trials the success rates are very low.[38]

Early diagnoses and thus metastasis treatment could be obtained by more intensive monitoring of high-risk patients. Therefore, it is very important to stratify patients for high-risk and low-risk to develop metastatic disease. For patients with UM, several prognostic markers are already known. These prognostic markers can be divided in clinical, histopathological and genetic markers.

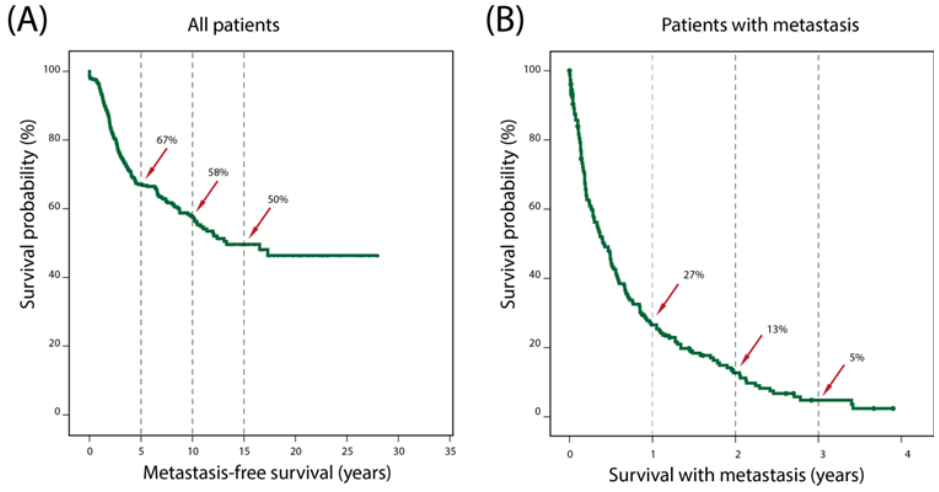

Figure 3. ***(A)*** *Kaplan Meijer curve showing the metastasis-free survival in all uveal melanoma patients (n = 709) in the Rotterdam Ocular Melanoma Study group cohort.* ***(B)*** *Kaplan Meijer curve showing the survival in patients with uveal melanoma metastasis (n = 180). The arrows indicate the survival probability at the given times.*

Chapter 1.2

Clinical and histopathological prognostic markers

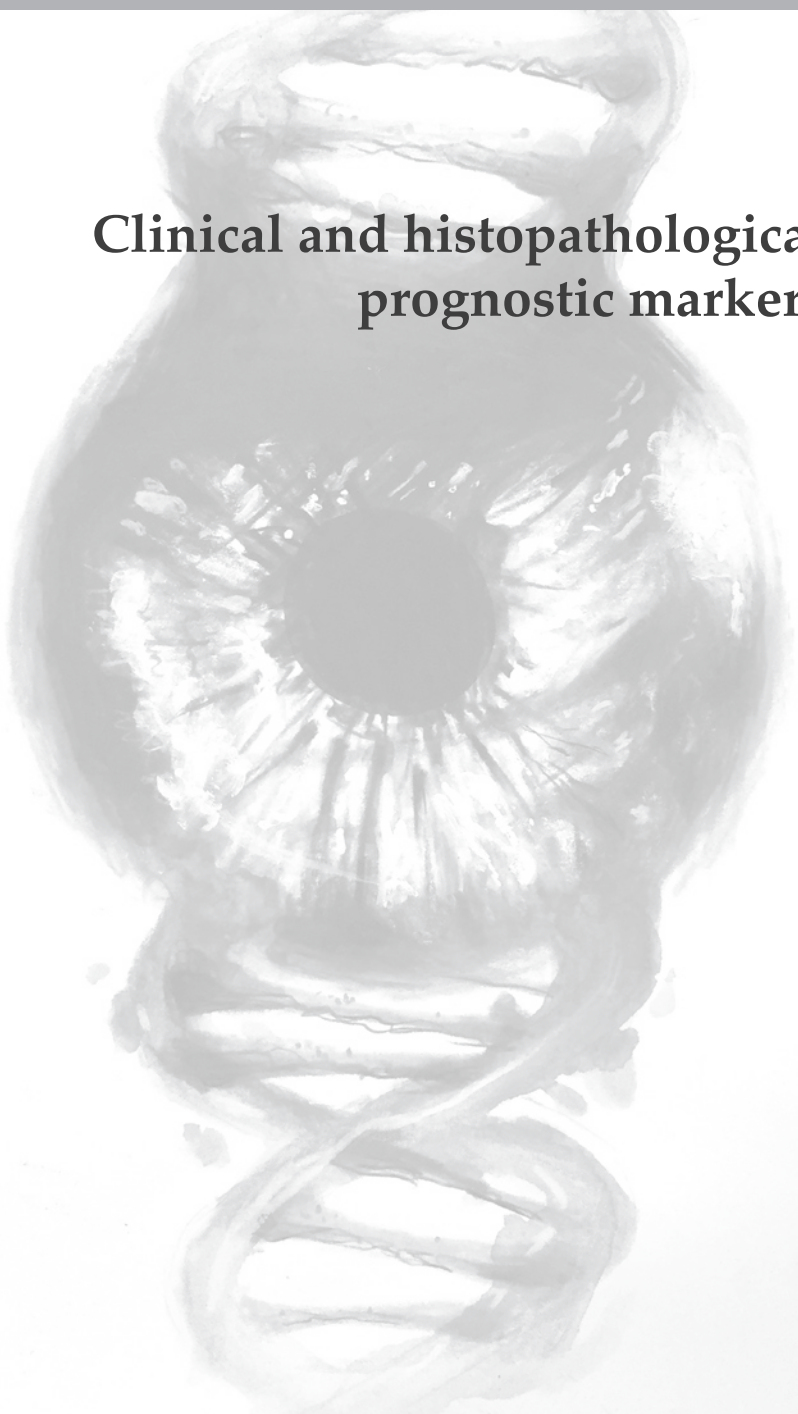

Patient-related prognostic markers

To adequately inform patients about the risk for systemic spread of UM, prognostication is essential. Several patients and tumor characteristics have been associated with metastatic disease in UM patients.

Males and females are affected equally, however the risk for metastasis remains debatable. The Collaborative Ocular Melanoma Study (COMS) group conducted a on more than 8,000 patients and found no difference in survival between men and women.[39] In contrast to the COMS report, Zloto and colleagues were able to observe a difference in survival in 723 UM patients and Rietschel and colleagues in 119 UM patients, in which men were more at risk for metastasis and developed metastasis faster than females.[40,41] Besides gender, also age at diagnosis is associated with survival. Patient diagnosed at a higher age tend to have a worse prognosis.[39] Moreover, patients diagnosed at a higher age usually also present with larger tumors.[42] Caucasian people are more at risk for developing UM, however according to a recent study which involved 8100 participants, ethnicity is not associated with the prognosis of UM.[43] Thus, although Caucasians are more at risk for developing UM, the risk for metastasis is not increased. On the other hand, patients with ocular melanosis have an increased risk for UM development and also a two-fold increased risk for developing metastasis.[44,45]

Tumor-related prognostic markers

Besides patient characteristics, also several tumor characteristics have been correlated to patient prognosis. The metastasis-rate varies for tumor location. Patients with iris melanoma have a five to ten-fold decreased risk of metastasis when compared to choroidal and ciliary body melanomas.[46,47] Patients with ciliary body melanoma or choroidal melanoma with ciliary body involvement (CBI) have the highest risk for metastasis when compared to posterior melanoma and iris melanoma.[46,47] Besides location, is has been shown that tumor diameter and thickness are both independently associated with survival, in which larger tumors associate with increased risk of metastasis.[29,47] Risk assessment for metastasis showed an increase in risk of 8% per millimeter extra in tumor diameter.[29] Local invasion which may occur via aqueous channels, ciliary arteries or nerves, vortex veins or the optic nerve may associate with prognosis.[48] Extraocular extension (EXE) can be identified using ultrasonography.[49] An increase in the size of the extension is associated with shorter survival.[42,50]

Tumor Node Metastasis (TNM) Classification

The tumor (T), node (N) and metastases (M) classification is a universally used classification based on primary tumor size and regional and systemic dissemination of the malignancy at the time of diagnosis, to prognosticate patients in risk groups. The first classification for uveal melanoma was described in the 7th edition of the *American Joint Committee on Cancer* (AJCC) *Cancer Staging Manual* in 2009.[51] For tumor stage (T) it includes tumor diameter, tumor thickness (prominence), ciliary body involvement (CBI) and extraocular extensions (EXE). Based on tumor size the UM are categorized in T1 – T4 (larger tumors have higher T categories) and subcategorized in (a) – (d) based on CBI and EXE. With the tumor category (T) in combination with the metastasis status (M), UM patients can be divided in four stages with an increasing risk of metastasis with increasing stage.[42,51,52] Patients with Stage IV are patients with confirmed diagnoses of metastasized disease at the time of diagnose. In contrast to histopathological and genetic prognostic markers, the TNM Staging classification lends the possibility for risk assessment without the need for tumor material, since tumor size and local infiltration (in the ciliary body or sclera) can be determined using ultrasonography.[42,51,52]

Histopathological prognostic markers

Whenever tumor material is available, UM can be investigated for several histopathological features. UM can be divided based on two cell types, which are spindle cells and epithelioid cells (Figure 4A and 4B). The presence of epithelioid cells in the UM are associated with a worse prognosis for the patient.[53,54] Also high mitotic activity, the presence of closed vascular loops (Figure 4C), inflammatory inflammation, tumor necrosis (Figure 4D) and degree of pigmentation are associated with metastasis.[53,54] However, a study of 1,527 enucleated eyes conducted by the COMS group revealed that these histopathological characteristics are not independent but associated with each other.[53] Tumors located in the peripheral choroid of the eye are in general larger, contain more epithelioid cells and contain more tumor necrosis. Moreover, epithelioid cells in UMs are associated with a higher degree of tumor necrosis, pigmentation and inflammation and large tumor size.[53] Based on the statistics it is hard to determine which feature precedes the other. It is most likely that tumors located more anterior might be diagnosed later since these tumors tend to cause less symptoms. Growing tumors without proper vascularization develop necrosis, which recruits

inflammatory cells. The hypoxia-induced necrosis can also recruit vascularization and epithelial-to-mesenchymal transition (EMT) factors that promote proliferation and local invasion.[55] This results in a higher metastatic risk.

With the increasing knowledge on genetics and the development of Next Generation Sequencing tools to explore tumor specimen, a shift towards genetic determinants of tumorigenesis and risk for metastasis was feasible.

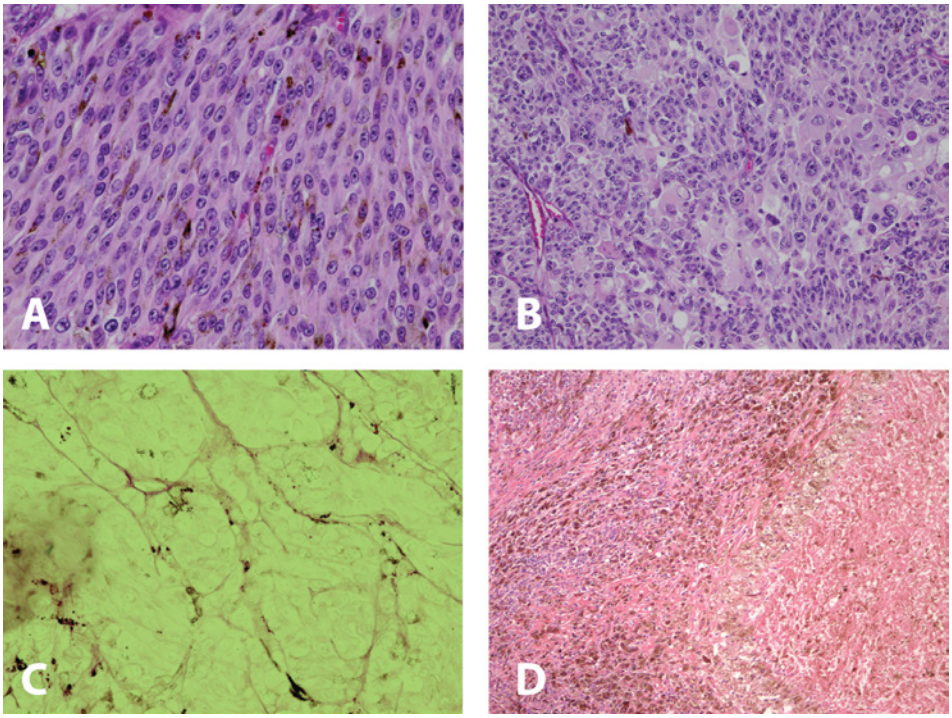

Figure 4. ***(A)*** *Heamatoxylin and eosin (HE) staining of a uveal melanoma sample (EOM-0921) with spindle cell type (200x).* ***(B)*** *HE staining of a sample with epithelioid cell type (200x).* ***(C)*** *Periodic acid–Schiff (PAS) staining showing closed vascular loops (400x).* ***(D)*** *HE staining showing tumor necrosis (25x).*

Chapter 1.3

Genetic prognostic markers

Chromosomes

Somatic cells in humans are diploid with 46 chromosomes, containing two parental copies of the 22 autosomale chromosomes (2 x 22) and two sex chromosomes which are either XX in women or XY in men. Cancer is a malignancy of human somatic cells that in general contain chromosomal aberrations either as the initiation of cancer or consequence of cancer. These chromosomal aberrations can be numerical (loss or gain of entire chromosomes) or structural e.g. translocations of chromosome parts to other chromosomes. Uveal melanoma is a malignancy characterized by several non-random recurring chromosomal aberrations.[56-58] 'Non-random recurring' means that the tumors in a proportion of the patients contain similar chromosomal aberrations. As every chromosome has two copies, chromosomal aberrations are also named copy number variations (CNVs).

Chromosome 3

Among these non-random recurring CNVs, the loss of the entire chromosome 3 was observed several decades ago in tumor material of UM patients. Loss of chromosome 3 (monosomy 3) is observed in nearly half of the UM, and is to date still the most strongly associated CNV with metastases.[56-58] In UM with monosomy 3, different regions of the tumor were analyzed for chromosome 3 to determine intra-tumor heterogeneity. This revealed that monosomy 3 UMs show loss of chromosome 3 in the entire tumor suggesting that UM with monosomy 3 are quite homogenous.[59] Besides monosomy 3, another chromosomal abnormality that can be observed is isodisomy 3.[60] In these tumors there are two identical copies of chromosome 3, thus resulting in a loss of heterozygosity (LOH). LOH of chromosome 3 is even more predictive for metastasis than monosomy 3.[60]

Chromosome 8q

Another copy number (CN) event is the gain of the long arm of chromosome 8. Gain of chromosome 8q is observed by either entire chromosome 8 gain, the formation of an isochromosome 8q or a partial amplification of the distal end of 8q.[56,61] The formation of an isochromosome 8q is mainly observed mutually with the loss of chromosome 3 (**Figure** 5),[62,63] in which the combination of these CN events in the UM are associated with the most rapid systemic progression of the disease.[64] Partial amplification of chromosome 8q, with the breakpoint at 8q21, is mainly observed in disomy 3 tumors.[61]

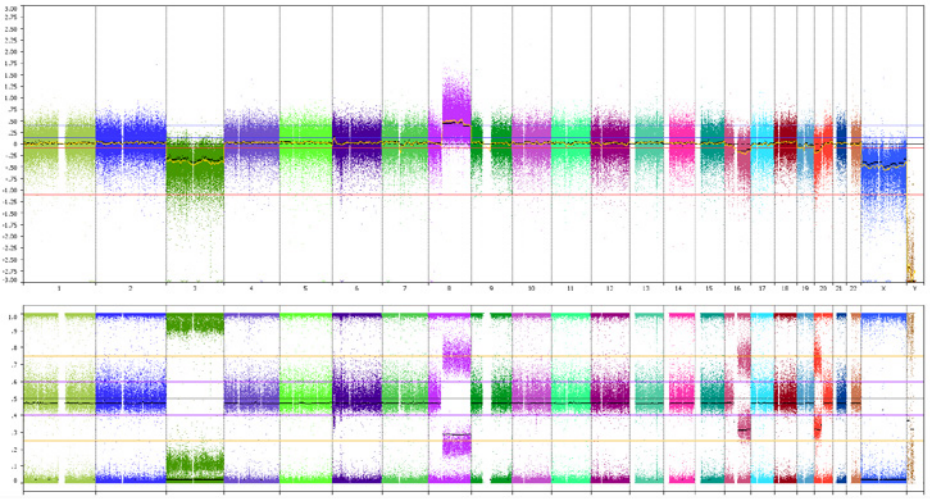

Figure 5. *A Single Nucleotide Polymorphism (SNP) array analyses of a uveal melanoma (EOM-0219). As observed in the upper picture (Log R ratio) this tumor has a loss of chromosome 3, loss of chromosome 8p and gain of chromosome 8q (indicative of isochromosome 8q)The lower picture represent the allelic imbalance displayed as the B-allele frequency.*

Chromosome 6p

Chromosome 6p gain is present in almost half of the UMs and usually observed in tumor samples without chromosome 3 loss.[56] Similar to chromosome 8q, chromosome 6p gain is observed either by an entire gain of chromosome 6, via the formation of an isochromosome 6p or an amplification of the distal part of chromosome 6p.[57,58,61,63,65] Unlike chromosome 8q, the different types of gain have not been associated with other chromosomal aberrations.

Other chromosomes

Other less frequent occurring chromosomal aberrations described in UM, are loss of chromosome 1p, 6q, 8p, and 16q.[54,56-58,61-63,66-70] Chromosome 1p loss is usually observed together with monosomy 3, in which monosomy with loss of chromosome 1p has a worse prognosis than monosomy without chromosome 1p loss.[67] Loss of chromosome 8p has been correlated with worse outcome in the survival.[71] However, these losses are frequently observed with isochromosomes 8q, thus making it likely that the loss of these chromosome arms are confounders to the isochromosome formation.[61] Chromosome 16q loss, observed mainly in tumors with loss of chromosome 3, has been proposed as a late event in tumorigenesis and is not associated with prognosis.[66,70]

Polyploidy

Besides aneuploidy, also polyploidy has been described in UM.[72-74] Polyploidy is a state in which the genome has three or more copies of each chromosome instead of the usual diploid state.[75,76] Polyploidy occurs in other malignancies as well, ranging from 11-54%.[75] Polyploidization in a cell can occur through three mechanisms: cell fusion, problems during cytokinesis/metaphase/anaphase or by endoreduplication.[75] In general, polyploidy in malignancies has been associated with worse prognosis compared to tumors with diploid cells.[75,76] It is thought that polyploidy causes treatment resistance since these cells are very adaptive.[76] Polyploidy in UM, measured with flowcytometry, has been described in 17-18% of the patients.[72-74] In UM, this higher DNA content was also associated with an increased risk of metastasis.[72,74]

Genes

Besides presence of chromosomal aberrations, mutated genes are also a typical characteristic of cancer. The type of mutation can be divided in germline and somatic mutations. Germline mutations are inherited from one or both of the parents. These mutations are present in all the cells of the affected individual and can give rise to cancer prone syndromes. An example is a *BRCA1* germline mutation in hereditary breast cancers.[77] Somatic mutations are acquired during the lifetime of an individual. Most somatic mutations are caused by environmental factors, such as smoking, alcohol and UV-light exposition. Cancer-associated genes can be divided in two major groups; oncogenes and tumor suppressor genes. Oncogenes are usually involved in cell growth. When mutated in cancer, these genes give a continuous activation of pathways promoting cell growth and thus have a gain-of-function effect in cancer.[77] Tumor suppressor genes on the other hand are usually involved in apoptosis, cell division and DNA-repair, preventing cell growth and instability. Since human cells contain two copies of each gene, both copies of tumor suppressor genes must be affected to accomplish the loss-of-function effect in cancer. Besides these gain and loss-of-function mutations also other mutations have been described with an altered-function effect.[77]

Also UMs harbor mutations in genes that are in involved in tumorigenesis. Although most of these mutations are somatic, germline mutations giving rise to the *BAP1*-syndrome have been described which is typically associated with malignant mesothelioma and uveal melanoma development. In this Chapter we will only focus on somatic

mutations, since these germline mutated genes only represent in a very small amount of patients.[78,79]

GNAQ, GNA11, CYSLTR2 and *PLCB4*

Sequencing of 24 potential oncogenes involved in the RAF/MEK/ERK pathway led to the discovery of a hotspot mutation in *GNAQ* (Guanine nucleotide binden protein, subunit q; chromosome 9q21.2).[80] This hotspot mutation targeting amino acid 209 (Q209) was confirmed in UM by other groups.[81,82] Within a year the hotspot Q209 mutation in *GNA11* (Gunanine nucleotide binding protein, subunit 11; chromosome 19p13.3), the homologue of *GNAQ*, was identified.[83] Besides mutation targeting Q209, recurring mutation targeting amino acid 183 (R183) were observed for both genes in UM.[83] Mutations in either gene occuring in approximately 90% of the UM, were independently or together not associated with survival.[82,84]

The majority of UM samples harbor *GNAQ*/*GNA11* mutation, however there is a small percentage of UM samples that lack a mutation in one of these two oncogenes. In some of these cases recurring mutations in *CYSLTR2* (Cysteinyl Leukotriene Receptor 2; chromosome 13q14.2) were found, targeting amino acid L129 in all.[85] $CysLT_2R$ is a G-protein Coupled Receptor (GPCR) upstream from Gαq. This recurring missense mutation causes activation of the same signaling pathways as *GNAQ* and *GNA11*.[85] Similar to *GNAQ*/*GNA11* mutations, *CYSLTR2* mutations were also found in blue nevi.[86] Another mutated gene found in *GNAQ*/*GNA11* wildtype UMs was *PLCB4* (Phospholipase C Beta 4; chromosome 20p12.3), targeting amino acid D630 in all described cases.[87] Also this gene is part of the signaling cascade of *GNAQ*/*GNA11*, acting as a canonical downstream target.[87]

Taken together with the occurrence of the same mutations in benign oculodermal laesions, this suggests that activating mutations in these oncogenes are the initial steps in tumorigenesis of UM.

BAP1

Whole-exome sequencing (WES) of two samples with a loss of chromosome 3 led to the discovery of inactivating mutations in the tumor suppressor gene *BAP1* (BRCA-associated protein 1; chromosome 3p21.1).[88] Additional analyses of 45 samples revealed that *BAP1* mutations occurred in ~40% of the patients and this was congruent with monosomy 3 status of the tumor.[88] Since *BAP1* usually harbors truncating mutations, the lack

of BAP1 expression can be tested with immunohistochemical staining (IHC).[89,90] Lack of BAP1 expression was almost congruent with *BAP1* mutations, thus proving BAP1 IHC to be a rapid and reliable alternative to sequencing all 17 coding exons of *BAP1*. Unlike *GNAQ*/*GNA11* mutations, *BAP1* status of the tumor was strongly correlated with survival.[88,90,91]

SF3B1

Additional WES of 18 primary UM, led to the discovery of an *SF3B1* (Splicing factor 3b, subunit 1; chromosome 2q33.1) missense mutation in exon 14 in two samples, targeting amino acid 625 (R625) in both.[92] *SF3B1* mutations also occurred in chronic lymphocytic leukemia (CLL) and myeolodysplastic syndrome (MDS) predominantly in exon 12 to 16, usually with other hotspot mutations.[93,94] In approximately 20% of UM samples, an *SF3B1* mutation was found targeting R625 in almost all cases, although rarely other mutations were also observed.[92,95,96] *SF3B1* mutations were strongly correlated to disomy 3 tumors.[92,95] *SF3B1*-mutated tumors are also associated with a better disease-free survival when compared to *SF3B1*-wildtype within five years after treatment,[95] however another study with a prolonged follow-up of ten years was not able to see this difference.[92] Moreover, when stratified for chromosome 3 status, we showed that UM with *SF3B1* mutations were correlated to late-onset metastasis.[97]

EIF1AX

Another recurring mutated gene in UM discovered with WES is *EIF1AX* (Eukaryotic translation initiation factor 1A, X-linked; chromosome Xp22.12).[96] Similar to *SF3B1* mutations, also *EIF1AX* mutations were strongly correlated with disomy 3 tumors.[91,96] *EIF1AX* mutations occur in approximately 20% of the UM cases, and were only found in the first 15 amino acid (exon 1 and partially exon 2).[96] Also similar to the *SF3B1* mutations, the *EIF1AX* mutations are gain of function mutations result in an intact albeit altered protein. Tumors harboring an *EIF1AX* mutation are associated with a better survival compared to tumors without *EIF1AX* mutations.[91,96,97]

Gene expression

Gene expression profiling (GEP) is commonly used in cancer research. The mRNA expression of several thousand genes are measured simultaneous to construct specific patterns that can be used to classify patients. Patients with UMs could be divided

in low-risk profiles (Class I) and high-risk profiles (Class II) based on RNA expression.[98-102] In large multi-center studies, GEP proved to be more accurate in predicting metastasis at three years of follow-up when compared to the TNM classification and chromosome 3 status of the tumor.[103,104] Although GEP proves to be an accurate predictor, Augsburger and colleagues described discordant GEP result in more than 10% of the cases in fine-needle aspiration biopsy (FNAB) extracted samples.[105] Another report showed that also non-melanoma tumors can be categorized in Class I or II, falsely classifying non-melanoma tumors as uveal melanomas.[106]

Metastasis is most strongly correlated to class II UMs, however also a small proportion of class I UMs eventually develops metastasis. Recently, *PRAME* (preferentially expressed antigen in melanoma) was identified as a marker for metastasis in class I UM, for which increased expression was associated with a high risk.[107,108]

MicroRNA

New players in the field of oncology are microRNAs (miRNAs). For several cancers it has already been shown that miRNAs can target oncogenes and tumor suppressor genes.[109] Compared to normal human cells, cancer cells generally have lower miRNA expression.[110]

Unsupervised hierarchical clustering revealed that UMs can be divided into two clusters based on miRNA expression, which overlapped with the GEP classes.[111] Overall, Class II UMs (high-risk) expressed less miRNAs compared to Class I UMs (low-risk).[111] Similarly, another study showed that more miRNAs were downregulated in metastasized UMs compared to non-metastasized UMs.[112]

Methylation

Hypermethylation of promotor sites of tumor suppressor genes is also a way to epigenetically silence gene expression.[113,114] Also for UM, methylation has been investigated intensively.

Several studies showed promotor methylation of *RASSF1A* (Ras Association Domain Family Member 1, chromosome 3p21.31) in 13-83% of UM cases and cell lines.[115-118] Furthermore, *in vitro* analyses revealed that ectopic RASSF1A expression in cell lines with promotor methylation of *RASSF1A* resulted in slower proliferation and more sensitivity to cisplatin.[115,119] Also *BAP1* was analyzed for methylation since it was hypothesized that this gene could also be silenced trough promotor methylation, however this was not the case.[120]

Chapter 1.4

Prognostic testing in patients with uveal melanoma

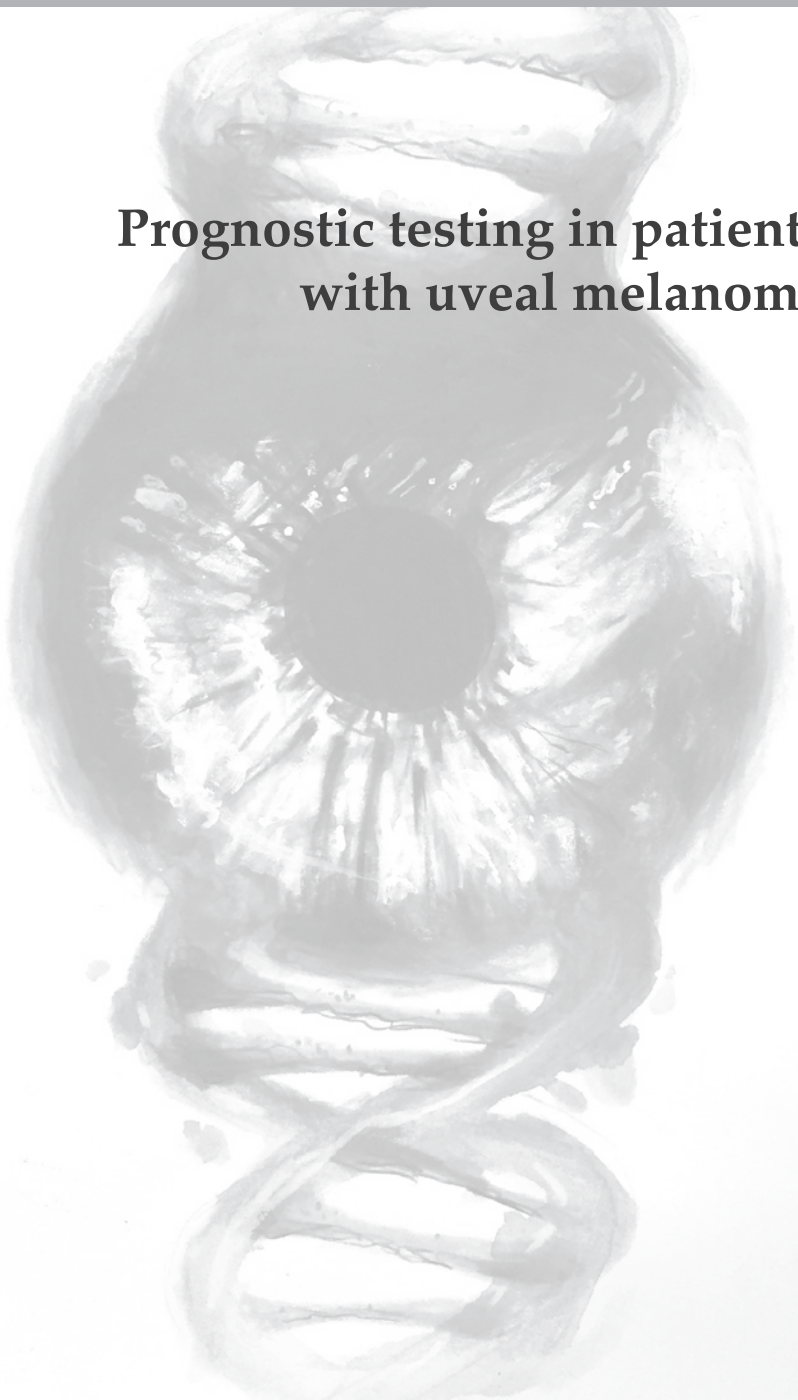

As described in this Chapter, we have seen that prognosis can be determined in many ways. The choice for different methods for prognostication depends largely on the available material and techniques.[121]

Clinical variables, as described by the AJCC classification, are currently the only prognostic classifiers when there is no tumor material available. However, many more options for prognostication are possible when tissue is available.

Several studies have been published in which the chromosome status, in particular chromosome 3 and 8q, minimizes the prognostic value of the AJCC classification.[122] Furthermore, the combination of AJCC classification and the chromosome status seem to be the most accurate predictor.[122,123] An online tool, combining multiple prognostic factors, is the Liverpool Uveal Melanoma Prognosticator Online (LUMPO).[124] This tool provides a patient specific risk for metastasis, taking into account the clinical and histopathological variables and chromosome 3 status, if available.[124]

Also for gene expression is has been shown that the GEP status together with tumor size are the most accurate prognostic predictors.[104,125] Also when material was obtained by FNAB, GEP proved to be more superior in prognostic testing than cytogenetics.[126]

For genetic analyses *BAP1* status is shown to be the most accurate predictor for metastasis, especially in combination with the *EIF1AX* mutation status.[90,91]

Future studies should be performed where all variables are included such as the clinical and histopathological variables, gene expression profiling, chromosome and mutational status. The Cancer Genome Atlas (TCGA) has recently made data available for 80 UMs including all of the before mentioned variables and more (available at https://cancergenome.nih.gov/). Studies using the TCGA data and other online-available data will hopefully provide more insight in the genetics of UM and also more insight in the prognostic value of all variables.

Chapter 1.5

Scope and outline of this thesis

With the development of novel techniques for genetic analyses, the genetic basis of uveal melanoma etiology has made a great progression. Next-generation sequencing led to the discovery of recurrent mutated genes such as *BAP1*, *SF3B1* and *EIF1AX*. The aim of this thesis was to investigate whether compared to AJCC classification or GEP analysis, these genetic changes would provide a better prognostic tool to classify patients with UM in high-risk and low-risk groups.

We set to analyze whether different mutated genes have their own prognosis and chromosomal patterns. In **Chapter 2.1** the prognostic value of *SF3B1* mutation in UM was analyzed. Following this, **Chapter 2.2** concerns the specific chromosomal aberrations and patterns associated with the recurrent mutated genes, *BAP1*, *SF3B1* and *EIF1AX*. In this Chapter somatic mutational signatures in UMs, a novel technique to associate mutational spectrum with several clinical features and cellular pathways, are also analyzed.

When metastasis occurs in UM patients, the metastases present themselves in a variety of ways. In **Chapter 2.3**, we set to analyze whether there is a clinical difference in metastasis presentation in patients with either *BAP1* or *SF3B1*-mutated UMs. For this purpose 100 scans of liver metastases of UM patients were collected and the genetic data of 68 UM patients. Furthermore, the prognostic value are described of polyploidy in UM and the association of polyploidy with the known mutated genes in UM (**Chapter 3.1**) and the occurrence of chromothripsis, another chromosomal anomaly in UM (**Chapter 3.2**)**. Chapter 3.3** describes a case-report of lipomatous changes in an UM.

Finally, in **Chapter 4** we discuss our results and the current literature on genetics in UM.

References

1. Singh, A.D., Turell, M.E. & Topham, A.K. Uveal melanoma: trends in incidence, treatment, and survival. *Ophthalmology* **118**, 1881-5 (2011).
2. Shields, C.L. *et al.* Iris melanoma: risk factors for metastasis in 169 consecutive patients. *Ophthalmology* **108**, 172-8 (2001).
3. Char, D.H. *et al.* Diagnostic modalities in choroidal melanoma. *Am J Ophthalmol* **89**, 223-30 (1980).
4. Damato, B. Developments in the management of uveal melanoma. *Clin Exp Ophthalmol* **32**, 639-47 (2004).
5. Guyer, D.R. *et al.* Digital indocyanine-green videoangiography of intraocular tumors. *Semin Ophthalmol* **8**, 224-9 (1993).
6. Krantz, B.A., Dave, N., Komatsubara, K.M., Marr, B.P. & Carvajal, R.D. Uveal melanoma: epidemiology, etiology, and treatment of primary disease. *Clin Ophthalmol* **11**, 279-289 (2017).
7. Bove, R. & Char, D.H. Nondiagnosed uveal melanomas. *Ophthalmology* **111**, 554-7 (2004).
8. Eskelin, S. & Kivela, T. Mode of presentation and time to treatment of uveal melanoma in Finland. *Br J Ophthalmol* **86**, 333-8 (2002).
9. Singh, A.D., Kalyani, P. & Topham, A. Estimating the risk of malignant transformation of a choroidal nevus. *Ophthalmology* **112**, 1784-9 (2005).
10. Sumich, P., Mitchell, P. & Wang, J.J. Choroidal nevi in a white population: the Blue Mountains Eye Study. *Arch Ophthalmol* **116**, 645-50 (1998).
11. Shields, C.L. *et al.* Combination of clinical factors predictive of growth of small choroidal melanocytic tumors. *Arch Ophthalmol* **118**, 360-4 (2000).
12. Shields, C.L. *et al.* Choroidal nevus transformation into melanoma: analysis of 2514 consecutive cases. *Arch Ophthalmol* **127**, 981-7 (2009).
13. Virgili, G. *et al.* Incidence of uveal melanoma in Europe. *Ophthalmology* **114**, 2309-15 (2007).
14. Gonder, J.R., Shields, J.A., Albert, D.M., Augsburger, J.J. & Lavin, P.T. Uveal malignant melanoma associated with ocular and oculodermal melanocytosis. *Ophthalmology* **89**, 953-60 (1982).
15. Singh, A.D. *et al.* Lifetime prevalence of uveal melanoma in white patients with oculo(dermal) melanocytosis. *Ophthalmology* **105**, 195-8 (1998).
16. Weis, E., Shah, C.P., Lajous, M., Shields, J.A. & Shields, C.L. The association of cutaneous and iris nevi with uveal melanoma: a meta-analysis. *Ophthalmology* **116**, 536-543 e2 (2009).
17. Weis, E., Shah, C.P., Lajous, M., Shields, J.A. & Shields, C.L. The association between host susceptibility factors and uveal melanoma: a meta-analysis. *Arch Ophthalmol* **124**, 54-60 (2006).
18. Shah, C.P., Weis, E., Lajous, M., Shields, J.A. & Shields, C.L. Intermittent and chronic ultraviolet light exposure and uveal melanoma: a meta-analysis. *Ophthalmology* **112**, 1599-607 (2005).
19. Shields, J.A.S., C.A. *Intraocular Tumors. An Atlas and Textbook*, (Lippincott Williams and Wilkins, Philadelphia, PA, USA, 2008).
20. Dunavoelgyi, R. *et al.* Local tumor control, visual acuity, and survival after hypofractionated stereotactic photon radiotherapy of choroidal melanoma in 212 patients treated between 1997 and 2007. *Int J Radiat Oncol Biol Phys* **81**, 199-205 (2011).
21. Gragoudas, E.S. Proton beam irradiation of uveal melanomas: the first 30 years. The Weisenfeld Lecture. *Invest Ophthalmol Vis Sci* **47**, 4666-73 (2006).
22. Kaiserman, N., Kaiserman, I., Hendler, K., Frenkel, S. & Pe'er, J. Ruthenium-106 plaque brachytherapy for thick posterior uveal melanomas. *Br J Ophthalmol* **93**, 1167-71 (2009).
23. Kaliki, S. & Shields, C.L. Uveal melanoma: relatively rare but deadly cancer. *Eye (Lond)* **31**, 241-257 (2017).
24. Kapoor, A., Beniwal, V., Beniwal, S., Mathur, H. & Kumar, H.S. Management of uveal tract melanoma: A comprehensive review. *J Egypt Natl Canc Inst* **28**, 65-72 (2016).
25. Melia, B.M. *et al.* Collaborative ocular melanoma study (COMS) randomized trial of I-125 brachytherapy for medium choroidal melanoma. I. Visual acuity after 3 years COMS report no. 16. *Ophthalmology* **108**, 348-66 (2001).
26. Chang, M.Y. & McCannel, T.A. Local treatment failure after globe-conserving therapy for choroidal melanoma. *Br J Ophthalmol* **97**, 804-11 (2013).
27. Fabian, I.D. *et al.* Secondary Enucleations for Uveal Melanoma: A 7-Year Retrospective Analysis.

Am J Ophthalmol **160**, 1104-1110 e1 (2015).
28. Eskelin, S., Pyrhonen, S., Summanen, P., Hahka-Kemppinen, M. & Kivela, T. Tumor doubling times in metastatic malignant melanoma of the uvea: tumor progression before and after treatment. *Ophthalmology* **107**, 1443-9 (2000).
29. Kujala, E., Makitie, T. & Kivela, T. Very long-term prognosis of patients with malignant uveal melanoma. *Invest Ophthalmol Vis Sci* **44**, 4651-9 (2003).
30. Zimmerman, L.E., McLean, I.W. & Foster, W.D. Does enucleation of the eye containing a malignant melanoma prevent or accelerate the dissemination of tumour cells. *Br J Ophthalmol* **62**, 420-5 (1978).
31. Bakalian, S. *et al.* Molecular pathways mediating liver metastasis in patients with uveal melanoma. *Clin Cancer Res* **14**, 951-6 (2008).
32. Augsburger, J.J., Correa, Z.M. & Shaikh, A.H. Effectiveness of treatments for metastatic uveal melanoma. *Am J Ophthalmol* **148**, 119-27 (2009).
33. Collaborative Ocular Melanoma Study, G. The COMS randomized trial of iodine 125 brachytherapy for choroidal melanoma: V. Twelve-year mortality rates and prognostic factors: COMS report No. 28. *Arch Ophthalmol* **124**, 1684-93 (2006).
34. Pereira, P.R. *et al.* Current and emerging treatment options for uveal melanoma. *Clin Ophthalmol* **7**, 1669-82 (2013).
35. Spagnolo, F. *et al.* Treatment of metastatic uveal melanoma with intravenous fotemustine. *Melanoma Res* **23**, 196-8 (2013).
36. Akyuz, M. *et al.* Laparoscopic management of liver metastases from uveal melanoma. *Surg Endosc* **30**, 2567-71 (2016).
37. Lin, S., Wan, D., Chen, H., Chen, K. & Zheng, S. Complete resection of isolated hepatic metastatic uveal melanoma with a notably long disease-free period: A case report and review of the literature. *Oncol Lett* **10**, 196-200 (2015).
38. Carvajal, R.D. *et al.* Metastatic disease from uveal melanoma: treatment options and future prospects. *Br J Ophthalmol* **101**, 38-44 (2017).
39. Shields, C.L., Kaliki, S., Furuta, M., Mashayekhi, A. & Shields, J.A. Clinical spectrum and prognosis of uveal melanoma based on age at presentation in 8,033 cases. *Retina* **32**, 1363-72 (2012).
40. Rietschel, P. *et al.* Variates of survival in metastatic uveal melanoma. *J Clin Oncol* **23**, 8076-80 (2005).
41. Zloto, O., Pe'er, J. & Frenkel, S. Gender differences in clinical presentation and prognosis of uveal melanoma. *Invest Ophthalmol Vis Sci* **54**, 652-6 (2013).
42. Shields, C.L. *et al.* American Joint Committee on Cancer Classification of Uveal Melanoma (Anatomic Stage) Predicts Prognosis in 7,731 Patients: The 2013 Zimmerman Lecture. *Ophthalmology* **122**, 1180-6 (2015).
43. Shields, C.L. *et al.* Prognosis of uveal melanoma based on race in 8100 patients: The 2015 Doyne Lecture. *Eye (Lond)* **29**, 1027-35 (2015).
44. Mashayekhi, A. *et al.* Metastasis from uveal melanoma associated with congenital ocular melanocytosis: a matched study. *Ophthalmology* **120**, 1465-8 (2013).
45. Shields, C.L. *et al.* Association of ocular and oculodermal melanocytosis with the rate of uveal melanoma metastasis: analysis of 7872 consecutive eyes. *JAMA Ophthalmol* **131**, 993-1003 (2013).
46. McLean, I.W., Foster, W.D. & Zimmerman, L.E. Uveal melanoma: location, size, cell type, and enucleation as risk factors in metastasis. *Hum Pathol* **13**, 123-32 (1982).
47. Shields, C.L. *et al.* Metastasis of uveal melanoma millimeter-by-millimeter in 8033 consecutive eyes. *Arch Ophthalmol* **127**, 989-98 (2009).
48. Coupland, S.E., Campbell, I. & Damato, B. Routes of extraocular extension of uveal melanoma: risk factors and influence on survival probability. *Ophthalmology* **115**, 1778-85 (2008).
49. Scott, I.U., Murray, T.G. & Hughes, J.R. Evaluation of imaging techniques for detection of extraocular extension of choroidal melanoma. *Arch Ophthalmol* **116**, 897-9 (1998).
50. van Beek, J.G. *et al.* The prognostic value of extraocular extension in relation to monosomy 3 and gain of chromosome 8q in uveal melanoma. *Invest Ophthalmol Vis Sci* **55**, 1284-91 (2014).
51. C.C., E.S.B.B.D.R.C. *AJCC Cancer Staging Manual. 7th edition*, (Springer, New York, 2010).
52. Force, A.O.O.T. International Validation of the American Joint Committee on Cancer's 7th Edition Classification of Uveal Melanoma. *JAMA Ophthalmol* **133**, 376-83 (2015).

53. Histopathologic characteristics of uveal melanomas in eyes enucleated from the Collaborative Ocular Melanoma Study. COMS report no. 6. *Am J Ophthalmol* **125**, 745-66 (1998).
54. Gill, H.S. & Char, D.H. Uveal melanoma prognostication: from lesion size and cell type to molecular class. *Can J Ophthalmol* **47**, 246-53 (2012).
55. Asnaghi, L. *et al.* EMT-associated factors promote invasive properties of uveal melanoma cells. *Mol Vis* **21**, 919-29 (2015).
56. Hoglund, M. *et al.* Dissecting karyotypic patterns in malignant melanomas: temporal clustering of losses and gains in melanoma karyotypic evolution. *Int J Cancer* **108**, 57-65 (2004).
57. Prescher, G., Bornfeld, N. & Becher, R. Nonrandom chromosomal abnormalities in primary uveal melanoma. *J Natl Cancer Inst* **82**, 1765-9 (1990).
58. Sisley, K. *et al.* Non-random abnormalities of chromosomes 3, 6, and 8 associated with posterior uveal melanoma. *Genes Chromosomes Cancer* **5**, 197-200 (1992).
59. Mensink, H.W. *et al.* Chromosome 3 intratumor heterogeneity in uveal melanoma. *Invest Ophthalmol Vis Sci* **50**, 500-4 (2009).
60. Onken, M.D. *et al.* Loss of heterozygosity of chromosome 3 detected with single nucleotide polymorphisms is superior to monosomy 3 for predicting metastasis in uveal melanoma. *Clin Cancer Res* **13**, 2923-7 (2007).
61. Trolet, J. *et al.* Genomic profiling and identification of high-risk uveal melanoma by array CGH analysis of primary tumors and liver metastases. *Invest Ophthalmol Vis Sci* **50**, 2572-80 (2009).
62. Ehlers, J.P., Worley, L., Onken, M.D. & Harbour, J.W. Integrative genomic analysis of aneuploidy in uveal melanoma. *Clin Cancer Res* **14**, 115-22 (2008).
63. Hughes, S. *et al.* Microarray comparative genomic hybridisation analysis of intraocular uveal melanomas identifies distinctive imbalances associated with loss of chromosome 3. *Br J Cancer* **93**, 1191-6 (2005).
64. van den Bosch, T. *et al.* Higher percentage of FISH-determined monosomy 3 and 8q amplification in uveal melanoma cells relate to poor patient prognosis. *Invest Ophthalmol Vis Sci* **53**, 2668-74 (2012).
65. Cassoux, N. *et al.* Genome-wide profiling is a clinically relevant and affordable prognostic test in posterior uveal melanoma. *Br J Ophthalmol* **98**, 769-74 (2014).
66. de Lange, M.J. *et al.* Heterogeneity revealed by integrated genomic analysis uncovers a molecular switch in malignant uveal melanoma. *Oncotarget* **6**, 37824-35 (2015).
67. Kilic, E. *et al.* Concurrent loss of chromosome arm 1p and chromosome 3 predicts a decreased disease-free survival in uveal melanoma patients. *Invest Ophthalmol Vis Sci* **46**, 2253-7 (2005).
68. van Engen-van Grunsven, A.C. *et al.* Whole-genome copy-number analysis identifies new leads for chromosomal aberrations involved in the oncogenesis and metastastic behavior of uveal melanomas. *Melanoma Res* **25**, 200-9 (2015).
69. Damato, B., Dopierala, J.A. & Coupland, S.E. Genotypic profiling of 452 choroidal melanomas with multiplex ligation-dependent probe amplification. *Clin Cancer Res* **16**, 6083-92 (2010).
70. Kilic, E. *et al.* Clinical and cytogenetic analyses in uveal melanoma. *Invest Ophthalmol Vis Sci* **47**, 3703-7 (2006).
71. Ewens, K.G. *et al.* Genomic profile of 320 uveal melanoma cases: chromosome 8p-loss and metastatic outcome. *Invest Ophthalmol Vis Sci* **54**, 5721-9 (2013).
72. Meecham, W.J. & Char, D.H. DNA content abnormalities and prognosis in uveal melanoma. *Arch Ophthalmol* **104**, 1626-9 (1986).
73. Mooy, C. *et al.* DNA flow cytometry in uveal melanoma: the effect of pre-enucleation irradiation. *Br J Ophthalmol* **79**, 174-7 (1995).
74. Toti, P. *et al.* DNA ploidy pattern in choroidal melanoma: correlation with survival. A flow cytometry study on archival material. *Br J Ophthalmol* **82**, 1433-7 (1998).
75. Davoli, T. & de Lange, T. The causes and consequences of polyploidy in normal development and cancer. *Annu Rev Cell Dev Biol* **27**, 585-610 (2011).
76. Dewhurst, S.M. *et al.* Tolerance of whole-genome doubling propagates chromosomal instability and accelerates cancer genome evolution. *Cancer Discov* **4**, 175-85 (2014).
77. Weinberg, R.A. *The Biology of Cancer, 2nd edition*, (Garland Science, Taylor and Francis Group, New York, 2014).
78. Martorano, L.M., Winkelmann, R.R., Cebulla, C.M., Abdel-Rahman, M.H. & Campbell, S.M.

Ocular melanoma and the BAP1 hereditary cancer syndrome: implications for the dermatologist. *Int J Dermatol* **53**, 657-63 (2014).
79. Rai, K., Pilarski, R., Cebulla, C.M. & Abdel-Rahman, M.H. Comprehensive review of BAP1 tumor predisposition syndrome with report of two new cases. *Clin Genet* **89**, 285-94 (2016).
80. Onken, M.D. *et al.* Oncogenic mutations in GNAQ occur early in uveal melanoma. *Invest Ophthalmol Vis Sci* **49**, 5230-4 (2008).
81. Van Raamsdonk, C.D. *et al.* Frequent somatic mutations of GNAQ in uveal melanoma and blue naevi. *Nature* **457**, 599-602 (2009).
82. Bauer, J. *et al.* Oncogenic GNAQ mutations are not correlated with disease-free survival in uveal melanoma. *Br J Cancer* **101**, 813-5 (2009).
83. Van Raamsdonk, C.D. *et al.* Mutations in GNA11 in uveal melanoma. *N Engl J Med* **363**, 2191-9 (2010).
84. Koopmans, A.E. *et al.* Patient survival in uveal melanoma is not affected by oncogenic mutations in GNAQ and GNA11. *Br J Cancer* **109**, 493-6 (2013).
85. Moore, A.R. *et al.* Recurrent activating mutations of G-protein-coupled receptor CYSLTR2 in uveal melanoma. *Nat Genet* **48**, 675-80 (2016).
86. Moller, I. *et al.* Activating cysteinyl leukotriene receptor 2 (CYSLTR2) mutations in blue nevi. *Mod Pathol* **30**, 350-356 (2017).
87. Johansson, P. *et al.* Deep sequencing of uveal melanoma identifies a recurrent mutation in PLCB4. *Oncotarget* **7**, 4624-31 (2016).
88. Harbour, J.W. *et al.* Frequent mutation of BAP1 in metastasizing uveal melanomas. *Science* **330**, 1410-3 (2010).
89. Kalirai, H., Dodson, A., Faqir, S., Damato, B.E. & Coupland, S.E. Lack of BAP1 protein expression in uveal melanoma is associated with increased metastatic risk and has utility in routine prognostic testing. *Br J Cancer* **111**, 1373-80 (2014).
90. Koopmans, A.E. *et al.* Clinical significance of immunohistochemistry for detection of BAP1 mutations in uveal melanoma. *Mod Pathol* **27**, 1321-30 (2014).
91. Ewens, K.G. *et al.* Chromosome 3 status combined with BAP1 and EIF1AX mutation profiles are associated with metastasis in uveal melanoma. *Invest Ophthalmol Vis Sci* **55**, 5160-7 (2014).
92. Harbour, J.W. *et al.* Recurrent mutations at codon 625 of the splicing factor SF3B1 in uveal melanoma. *Nat Genet* **45**, 133-5 (2013).
93. Patnaik, M.M. *et al.* SF3B1 mutations are prevalent in myelodysplastic syndromes with ring sideroblasts but do not hold independent prognostic value. *Blood* **119**, 569-72 (2012).
94. Rossi, D. *et al.* Mutations of the SF3B1 splicing factor in chronic lymphocytic leukemia: association with progression and fludarabine-refractoriness. *Blood* **118**, 6904-8 (2011).
95. Furney, S.J. *et al.* SF3B1 mutations are associated with alternative splicing in uveal melanoma. *Cancer Discov* **3**, 1122-9 (2013).
96. Martin, M. *et al.* Exome sequencing identifies recurrent somatic mutations in EIF1AX and SF3B1 in uveal melanoma with disomy 3. *Nat Genet* **45**, 933-6 (2013).
97. Yavuzyigitoglu, S. *et al.* Uveal Melanomas with SF3B1 Mutations: A Distinct Subclass Associated with Late-Onset Metastases. *Ophthalmology* **123**, 1118-28 (2016).
98. Onken, M.D., Worley, L.A., Davila, R.M., Char, D.H. & Harbour, J.W. Prognostic testing in uveal melanoma by transcriptomic profiling of fine needle biopsy specimens. *J Mol Diagn* **8**, 567-73 (2006).
99. Onken, M.D., Worley, L.A., Ehlers, J.P. & Harbour, J.W. Gene expression profiling in uveal melanoma reveals two molecular classes and predicts metastatic death. *Cancer Res* **64**, 7205-9 (2004).
100. Petrausch, U. *et al.* Significance of gene expression analysis in uveal melanoma in comparison to standard risk factors for risk assessment of subsequent metastases. *Eye (Lond)* **22**, 997-1007 (2008).
101. van Gils, W. *et al.* Gene expression profiling in uveal melanoma: two regions on 3p related to prognosis. *Invest Ophthalmol Vis Sci* **49**, 4254-62 (2008).
102. Worley, L.A. *et al.* Transcriptomic versus chromosomal prognostic markers and clinical outcome in uveal melanoma. *Clin Cancer Res* **13**, 1466-71 (2007).
103. Onken, M.D. *et al.* Collaborative Ocular Oncology Group report number 1: prospective validation of a multi-gene prognostic assay in uveal melanoma. *Ophthalmology* **119**, 1596-603 (2012).

104. Correa, Z.M. & Augsburger, J.J. Independent Prognostic Significance of Gene Expression Profile Class and Largest Basal Diameter of Posterior Uveal Melanomas. *Am J Ophthalmol* **162**, 20-27 e1 (2016).
105. Augsburger, J.J., Correa, Z.M. & Augsburger, B.D. Frequency and implications of discordant gene expression profile class in posterior uveal melanomas sampled by fine needle aspiration biopsy. *Am J Ophthalmol* **159**, 248-56 (2015).
106. Klufas, M.A. *et al.* Variable Results for Uveal Melanoma-Specific Gene Expression Profile Prognostic Test in Choroidal Metastasis. *JAMA Ophthalmol* **133**, 1073-6 (2015).
107. Field, M.G. *et al.* PRAME as an Independent Biomarker for Metastasis in Uveal Melanoma. *Clin Cancer Res* **22**, 1234-42 (2016).
108. Field, M.G. *et al.* Epigenetic reprogramming and aberrant expression of PRAME are associated with increased metastatic risk in Class 1 and Class 2 uveal melanomas. *Oncotarget* **7**, 59209-59219 (2016).
109. Esquela-Kerscher, A. & Slack, F.J. Oncomirs - microRNAs with a role in cancer. *Nat Rev Cancer* **6**, 259-69 (2006).
110. Gaur, A. *et al.* Characterization of microRNA expression levels and their biological correlates in human cancer cell lines. *Cancer Res* **67**, 2456-68 (2007).
111. Worley, L.A., Long, M.D., Onken, M.D. & Harbour, J.W. Micro-RNAs associated with metastasis in uveal melanoma identified by multiplexed microarray profiling. *Melanoma Res* **18**, 184-90 (2008).
112. Radhakrishnan, A., Badhrinarayanan, N., Biswas, J. & Krishnakumar, S. Analysis of chromosomal aberration (1, 3, and 8) and association of microRNAs in uveal melanoma. *Mol Vis* **15**, 2146-54 (2009).
113. Esteller, M., Corn, P.G., Baylin, S.B. & Herman, J.G. A gene hypermethylation profile of human cancer. *Cancer Res* **61**, 3225-9 (2001).
114. Momparler, R.L. & Bovenzi, V. DNA methylation and cancer. *J Cell Physiol* **183**, 145-54 (2000).
115. Calipel, A. *et al.* Status of RASSF1A in uveal melanocytes and melanoma cells. *Mol Cancer Res* **9**, 1187-98 (2011).
116. Maat, W. *et al.* Epigenetic inactivation of RASSF1a in uveal melanoma. *Invest Ophthalmol Vis Sci* **48**, 486-90 (2007).
117. Merhavi, E. *et al.* Promoter methylation status of multiple genes in uveal melanoma. *Invest Ophthalmol Vis Sci* **48**, 4403-6 (2007).
118. Moulin, A.P., Clement, G., Bosman, F.T., Zografos, L. & Benhattar, J. Methylation of CpG island promoters in uveal melanoma. *Br J Ophthalmol* **92**, 281-5 (2008).
119. Dratviman-Storobinsky, O. *et al.* The role of RASSF1A in uveal melanoma. *Invest Ophthalmol Vis Sci* **53**, 2611-9 (2012).
120. van de Nes, J.A. *et al.* Comparing the Prognostic Value of BAP1 Mutation Pattern, Chromosome 3 Status, and BAP1 Immunohistochemistry in Uveal Melanoma. *Am J Surg Pathol* **40**, 796-805 (2016).
121. Schopper, V.J. & Correa, Z.M. Clinical application of genetic testing for posterior uveal melanoma. *Int J Retina Vitreous* **2**, 4 (2016).
122. Bagger, M. *et al.* The prognostic effect of American Joint Committee on Cancer staging and genetic status in patients with choroidal and ciliary body melanoma. *Invest Ophthalmol Vis Sci* **56**, 438-44 (2014).
123. Dogrusoz, M. *et al.* The Prognostic Value of AJCC Staging in Uveal Melanoma Is Enhanced by Adding Chromosome 3 and 8q Status. *Invest Ophthalmol Vis Sci* **58**, 833-842 (2017).
124. DeParis, S.W. *et al.* External Validation of the Liverpool Uveal Melanoma Prognosticator Online. *Invest Ophthalmol Vis Sci* **57**, 6116-6122 (2016).
125. Walter, S.D. *et al.* Prognostic Implications of Tumor Diameter in Association With Gene Expression Profile for Uveal Melanoma. *JAMA Ophthalmol* **134**, 734-40 (2016).
126. Correa, Z.M. & Augsburger, J.J. Sufficiency of FNAB aspirates of posterior uveal melanoma for cytologic versus GEP classification in 159 patients, and relative prognostic significance of these classifications. *Graefes Arch Clin Exp Ophthalmol* **252**, 131-5 (2014).

Chapter 2

Patient stratification in Uveal Melanoma

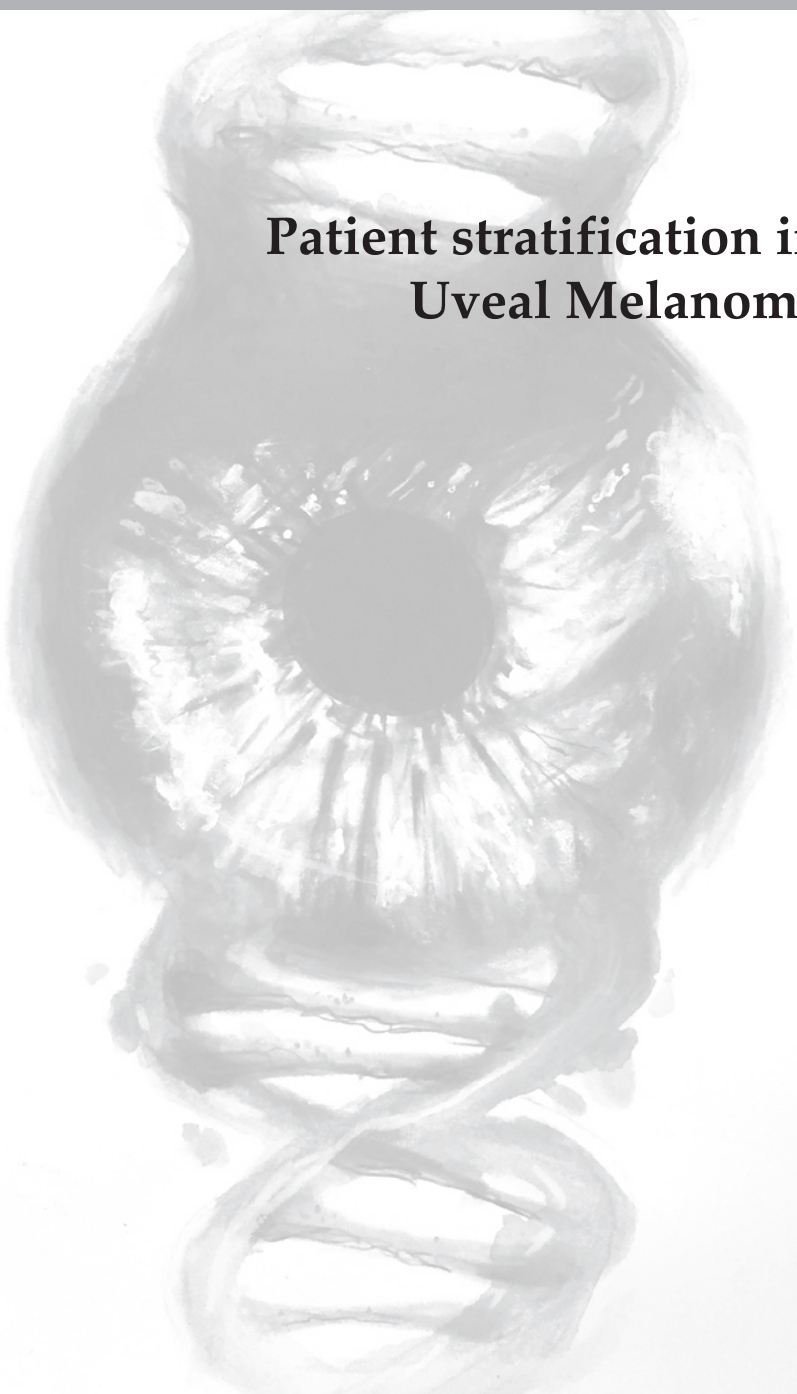

Chapter 2.1

Uveal melanomas with *SF3B1* mutations: a distinct subclass associated with late onset metastases

Serdar Yavuzyigitoglu,* Anna E. Koopmans,* Robert M. Verdijk, Jolanda Vaarwater, Bert Eussen, Alice van Bodegom, Dion Paridaens, Emine Kiliç, Annelies de Klein

* These authors contributed equally to this work.

Ophthalmology. 2016 May;123(5):1118-28. doi: 10.1016/j.ophtha.2016.01.023

Supplementary material for this manuscript are available at www.aaojournal.org

Abstract

Objective: To investigate the prevalence and prognostic value of *SF3B1* and *EIF1AX* mutations in uveal melanoma (UM) patients.

Design: Case series

Subjects: A cohort of 151 patients diagnosed and treated for UM.

Methods: *SF3B1* and *EIF1AX* mutations in primary tumors were investigated using whole-exome sequencing (n = 25) and Sanger sequencing (n = 151). For the detection of *BAP1* mutations a previously reported patient cohort of 90 patients was extended using *BAP1* sequencing or immunohistochemistry.

Main outcome measures: Status of *SF3B1*, *EIF1AX* and *BAP1* in tumors of patients were correlated to clinical, histopathological and genetic parameters. Survival analyses were performed for patients whose tumors had *SF3B1*, *EIF1AX* and *BAP1* mutations.

Results: Patients with tumors harboring *EIF1AX* mutations rarely developed metastases (2 out of 28 patients) and had overall a longer disease-free survival (DFS 190.1 versus 100.2 months, $P < 0.001$). Within the patient group with disomy 3 UM patients with an *SF3B1* mutation had an increased metastatic risk compared to those without an *SF3B1* mutation (DFS 132.8 versus 174.4 months, $P = 0.008$). Patients with such a mutation were more prone to develop late metastases (median 8.2 years, range 23-145 months). Patients with UM and loss of BAP1 expression had a significantly decreased survival (DFS 69.0 versus 147.9 months, $P < 0.001$). Conclusion: According to our data, patients with UM can be classified into three groups of which *EIF1AX* mutated tumors and tumors without *BAP1*, *SF3B1* and *EIF1AX* mutations associate with prolonged survival and low metastatic risk, *SF3B1* mutated tumors associate with late metastasis, and tumors with an aberrant BAP1 in tumors associate with an early metastatic risk and rapid decline in patients' disease free survival.

Introduction

Uveal melanoma (UM) is the most frequent primary tumor in the eye, with an estimated annual incidence between 4.3 and 8.6 cases per 1 million in the Western world.[1,2] This tumor is derived from melanocytes in the choroid, ciliary body or iris. Approximately 40% of patients demonstrate metastasis with a peak within 4 years after initial treatment, but metastatic disease has been observed even 15 years or longer after diagnosis. This suggests the presence of occult micrometastases at the time of primary treatment of the tumor since treatment of the primary UM is almost always successful without local recurrence.[3,4]

In addition to clinical features, such as the age of the patient and the tumor size, molecular and genetic markers are used to prognosticate UM patients with low- and high-risk profiles.[5-7] Chromosomal aberrations have been associated with metastatic disease in UM patients, of which loss of chromosome 3 (monosomy 3) is the most prominent.[7] Monosomy 3 is present in approximately half of the tumors and is associated strongly with poor survival.[7] In contrast, tumors with disomy 3 rarely metastasize within the first 3 years of follow-up.[7] A gain of chromosome 8q is associated independently with decreased survival, and this is even more profound in combination with the loss of chromosome 3.[8] In addition to chromosomal abnormalities, RNA expression also has been used to categorize UM patients in low-risk (class 1) and high-risk (class 2) categories with high accuracy.[9]

DNA sequencing led to the identification of recurrent affected genes in UM. Activating *GNAQ* and *GNA11* hotspot mutations were found in most cases of UM, but were not associated with prognosis.[10-12] Hemizygous mutations in the BRCA-associated protein 1 (*BAP1*) were found in most monosomy 3 tumors, resulting in an inactivation of the protein and loss of BAP1 expression.[6] Hence, *BAP1* mutations or no detectable BAP1 expression are associated with metastatic disease in UM patients.[13-15]

More recently, 2 other genes, *SF3B1* (splicing factor 3 subunit B1) and *EIF1AX* (eukaryotic translation initiation factor 1A) were reported to be mutated in UM patients.[13,16-19] *SF3B1* mutations, almost exclusively in amino acid 625 (R625 located in exon 14) can be found in 10% to 21% of UM.[16-18] Mutations in this gene have been associated with favorable prognostic features in UM patients, such as lower age at diagnosis and tumors with disomy 3, in contrast to patients with *BAP1*-mutated tumors.[16,18]

Survival analyses revealed that patients with *SF3B1*-mutated UM had a better survival compared to the *SF3B1* wild-type patients.[16] However, in another study with a longer follow-up, these survival differences between patients with *SF3B1*-mutant and *SF3B1* wild-type tumors did not reach significance.[18] In 16% to 19% of UM patients, *EIF1AX* mutations were observed mainly in disomy 3 tumors.[13,17,19] The patients with *EIF1AX* mutations had a better survival than those with *EIF1AX* wild-type tumors at 48 months of follow-up.[13]

The high prevalence of mutations in these genes and distinct survival patterns of UM patients urged us to investigate the prognostic value of these genes in a large cohort with long follow-up. We performed mutation analysis of *SF3B1* and *EIF1AX* in tumor DNA of 151 patients. *BAP1* mutation analysis and immunohistochemical detection of BAP1 loss in a subset of 74 tumors has been previously reported by our group,[15] and additional immunohistochemistry and mutation data were added. We correlated the mutational status with clinical, histopathologic and genetic parameters.

Methods

Study population

Tissue specimens were obtained from 151 UM patients. Patients with UM (n = 144) underwent primary enucleation between 1993 and 2013 at the Erasmus University Medical Centre or The Rotterdam Eye Hospital, the Netherlands. Seven patients primarily underwent irradiation of the UM, of whom 6 patients underwent secondary enucleation (median, 15 months; range 3-55) and 1 patient underwent biopsy examination 26 months after irradiation. Patient survival data were updated from the patients' charts. After enucleation, tumor material was obtained and partly snap frozen in liquid nitrogen, whereas the remaining tumor was embedded in paraffin. A histopathological diagnosis of melanoma was made by an experienced ophthalmic pathologist (R.M.V.) conforming to the Royal College of Pathologists guidelines (available at: www.rcpath.org/resourceLibrary/dataset-for-the-histopathological-reporting-of-uveal-melanoma--3rd-edition-.html). Patients with iris melanoma were excluded. The local ethics committee approved this study, and informed consent was obtained before to the intervention. This study was performed according to the guidelines of the Declaration of Helsinki.

DNA extraction and copy number analysis

DNA was extracted directly from fresh tumor tissue or frozen sections using the QIAmp DNA-mini kit (Qiagen, Hilden, Germany) according to the manufacturer's instructions. The tumors were processed for fluorescence in situ hybridization (FISH) and single nucleotide polymorphism(SNP) array analysis (HumanCytoSNP-12 v2.1 BeadChip and Illumina 610Q BeadChip, Illumina, San Diego, CA), as described previously.[15] Cutoff limits for deletion (>15% of the nuclei with 1 signal) or amplification (>10% of the nuclei with 3 or more signals) were adapted from the literature.[20] Tumors were examined for ploidy status with fluorescence in situ hybridization using control probes on chromosome 5q (chromosome 5q is usually not altered in UM). Polyploid tumors were excluded from the analyses because chromosomal abnormalities in these tumors require much more detailed analyses.

Whole-Exome sequencing

Uveal melanoma samples of 25 patients were subjected to whole-exome sequencing (WES). For 19 samples, SureSelect version 4 capture kit (Agilent Technologies, Santa Clara, CA) was used with 1 μg of genomic DNA, followed by sample preparation and

sequencing using the HiSeq 2000 system (Illumina). A CLC Cancer Research Workbench (QIAGEN, Redwood, CA) was used with default Burrows Wheeler aligner settings for the alignment against human reference genome build (hg19) to generate BAM files (*.bam). For the remaining 6 samples, the ACE Clinical Exome assay (Personalis Inc., Menlo Park, CA) was used on 1 to 3 μg genomic DNA. Sequencing (*.fastq) and alignment (*.bam) were generated and provided by Personlis, Inc. For all whole-exome sequencing samples, the BAM files were investigated manually for the regions of interest (*BAP1*, *SF3B1*, *EIF1AX*, *GNAQ*, and *GNA11*) using the Integrative Genomics Viewer version 2.3 (Broad Institute, Cambridge, MA). In general, all exons including the flanking regions (up to 25 base pairs) were covered at least 10 times and for exons with insufficient coverage, additional Sanger sequencing was carried out. Found variants were validated using Sanger sequencing.

Sanger sequencing

We sequenced exon 14 of *SF3B1* covering codon 625 (n = 151) with polymerase chain reaction (PCR). Additionally, we sequenced exon 12 to 16 of *SF3B1* in 106 samples that proved to be wild-type for codon 625. For *EIF1AX*, we amplified the 5'UTR with exon 1 and exon 2, including surrounding splice site sequences. The primers are shown in Supplementary Table 1. The PCR and Sanger sequencing protocols are available upon request. Sequences were aligned and compared with reference sequence hg19 from the Ensemble genome database (ENST00000335508 and ENST00000379607). De novo missense mutations found in the genes of interest were evaluated with PolyPhen-2 (http://genetics.bwh.harvard.edu/pph2/index.shtml) and SIFT (http://sift.jcvi.org/) for predictions (using default settings) to determine the possible functional impact and pathogenicity of the amino acid change. Mutations analysis of *GNAQ*, *GNA11* and *BAP1* was carried out as reported previously.[12,15]

cDNA sequencing

For cDNA sequencing, 5 samples were selected based on the mutation type in *EIF1AX*. As described previously,[21] 1 μg of RNA was extracted from fresh frozen tumor material and converted to cDNA with the iScript™ cDNA Synthesis Kit (Bio-Rad Laboratories, Veenendaal, the Netherlands). This cDNA was amplified and sequenced using the primers shown in Supplementary Table 1. Sequences were aligned and compared with the same reference sequence used for genomic mutation analyses.

Immunohistochemical staining

Immunohistochemistry was performed with an automated immunohistochemistry staining system (BenchMark Ultra; Ventana Medical Systems Inc., Tucson, AZ), as described previously.[15] For BAP1 staining, we used a mouse monoclonal antibody raised against amino acids 430 through 729 of human BAP1 (clone sc-28383, 1:50 dilution, Santa Cruz Biotechnology, Inc., Dallas, TX), for which liver, tonsil, breast tissue, and the retinal pigment epithelium were used as positive controls. All slides were cut at the time of staining. More details are provided in a previous paper.[15]

Statistical methods

Disease-free survival (DFS) was calculated from the date of enucleation to metastasis resulting from UM or last follow-up. Death resulting from another cause was censored. Survival curves were generated using the Kaplan-Meier method, and the difference between groups was compared with the log-rank test. The effect of continuous variables on DFS was assessed using the Cox proportional hazard analysis. Multivariate analysis was conducted with the Cox proportional hazard analysis using a forward stepwise method based on likelihood ratios. P values less than 0.05 were considered significant (SPSS software version 21.0; SPSS Inc., IBM, Armonk, NY). The Fisher exact and chi-square test were used to determine association between categorical variables. For continuous variables, we used the Mann-Whitney U test. To adjust for multiple testing with associations, a corrected P value less than 0.005 was considered significant.

Results

FISH or SNP data and DNA were available for 151 tumors. Eighteen tumors had a polyploid karyotype and therefore were excluded from further analysis. In the remaining cohort of 133 patient with a diploid tumor karyotype, FISH and SNP analysis revealed recurrent monosomy 3 (n = 57), loss of chromosome 1p (n = 36), and gain in chromosome 6p (n = 61) and chromosome 8q (n = 76; Table 1). In 7 cases of UM, a deletion of chromosome 3q was detected while the short arm of chromosome 3 showed 2 copies. The tumors were treated as disomy 3 tumors in further analysis based on published data.[22,23] The demographic and histopathologic patient and tumor characteristics are shown in Table 1. At the time of diagnosis, the median age of the patients (72 men and 61 women) was 61 years (range, 22–92 years). The mean largest tumor diameter and mean tumor height were 13.2 mm (range, 5–22 mm) and 7.9 mm (range, 1.5–22.0 mm), respectively. Mean follow-up time of the patients was 66.0 months (range, 0–209.1 months). Of the 133 patients, 52 (39.1%) demonstrated metastasis and 50 subsequently died. Twenty-four patients died of causes other than metastatic disease.

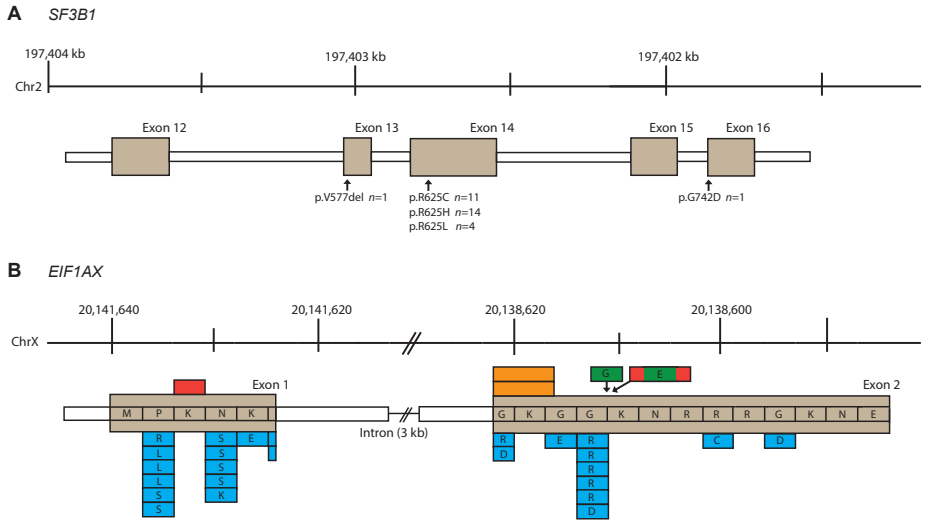

Figure 1. *Schematic overview of the mutations (insertions and deletions) found in the SF3B1 and EIF1AX genes. Exons 12 to 16 of SF3B1 are shown (**A**). Exon 1 and 2 of the EIF1AX gene are shown (B). The missense mutations are depicted in blue, deletions in red and insertions in green. The red block with a green segment represents a triplet nucleotide deletion resulting in the deletion of two amino acids and replacement with a glycine (p.Gly9_Lys10delinsGlu). Both splice site mutations (shown in orange) led to an alternative splice site resulting in a loss of the first six nucleotides of exon 2.*

SF3B1, EIF1AX and *BAP1* mutations

In total, 32 of the 133 tumor DNA samples (24.1%) harbored an *SF3B1* mutation, and all but 1 were located at amino acid or codon 625. These missense mutations resulted in the amino acid changes p.R625C in 12 samples, p.R625H in 15 samples, and p.R625L in 4 samples; all these amino acid changes were predicted to be probably damaging and deleterious by PholyPhen-2 and SIFT prediction software (Figure 1A; Supplementary Table 2). One UM (0.8%) had an *SF3B1* mutation in exon 16 (p.G742D), which was predicted to be probably damaging by PolyPhen-2 and to be tolerated by SIFT.

For *EIF1AX*, 28 of 133 tumors (21.1%) had a mutation in either exon 1 (n = 14) or exon 2 (n = 14). Details are shown in Figure 1B and Supplementary Table 2. These mutations included missense mutations (n = 23), in-frame deletions (n = 2), an in-frame insertion (n = 1), and mutations located at a splice site of the exon (n = 2) (Figure 1B). cDNA sequencing confirmed that tumors that harbored a splice site mutation use alternative splicing by eliminating the first six nucleotides of exon 2, resulting in an in-frame deletion of two amino acids (Supplementary Figure 1). PholyPhen-2 (either benign or probably damaging) and SIFT (either tolerated or deleterious) software predictions were in all samples probably damaging and deleterious for missense mutation in exon 2 and predicted either benign (PolyPhen-2) or tolerated (SIFT) if the missense mutation occurred in exon 1 (Supplementary Table 2).

In total, BAP1 immunohistochemistry was available for 126 tumors, of which 48 had a loss of expression of BAP1 and 78 did express BAP1 (Figure 2). In seven tumors, the BAP1 immunohistochemistry could not be performed because of the absence of tumor tissue. Mutation analyses data was obtained from a previous publication for 47 samples, of which 17 tumors harbored a mutation in *BAP1* and 28 were wild-type.[15] Additionally, we sequenced *BAP1* in 12 samples of which nine harbored a mutation in *BAP1* and three were wild-type for the coding exons. Of those 12 samples, we observed discrepancies between immunohistochemistry and mutational analyses in 6 tumors. One of these samples had no expression of BAP1, whereas the mutation analyses of the coding exons did not reveal a mutation. Five tumors harboring a *BAP1* mutation expressed BAP1 immunohistochemically, of which 4 were monosomy 3 tumors and in one case we observed 2 identical copies (isodisomy) of chromosome 3 (Figure 2). In 3 cases, the mutations were missense mutations (p.S10N, p.C91Y and p.A92V) and the 2 remaining cases contained nonsense mutations (p.Q36* and p.E406*). All three missense mutations were predicted probably damaging by PolyPhen-2 and deleterious by SIFT.

Table 1. Correlations between *SF3B1, EIF1AX* and BAP1 and other clinic-histopathological and genetic features.

	***n*=133**	Associations		
	mean (range)	*SF3B1*		
Variables	*n* (%)	**Mutated**	**Wild type**	**P-value**
Age, years (range)	61.0 (22-92)	54.1	64.0	**<0.001**[a]
Largest tumor diameter, mm (range)	13.2 (5 – 22)	13.8	13.1	0.219[a]
Tumor height, mm (range)	7.9 (1.5 – 22.0)	7.9	7.8	0.508[a]
Sex				
Male, *n* (%)	72 (54.1)	18	54	0.783[b]
Female, *n* (%)	61 (45.9)	14	47	
Involvement ciliary body, *n* (%)				
Present, *n* (%)	34 (25.6)	8	26	0.933[b]
Not present, *n* (%)	99 (74.4)	24	75	
Cell type, *n* (%)				
Spindle, *n* (%)	62 (46.6)	21	32	**0.001**[b]
Epithelioid/mixed, *n* (%)	71 (53.4)	11	69	
Extracellular matrix patterns				
Present, *n* (%)	58 (44.3)	5	53	**<0.001**[b]
Not present, *n* (%)	73 (54.9)	26	47	
Chromosome 3 [d]				
Loss, *n* (%)	57 (42.9)	0	57	**<0.001**[b]
Normal, *n* (%)	76 (57.1)	32	44	
Chromosome 8q				
Normal, *n* (%)	57 (42.9)	15	42	0.598[b]
Gain, *n* (%)	76 (57.1)	17	59	
BAP1 mutation				
Mutated, *n* (%)	26 (45.6)	0	26	**<0.001**[b]
Wild type, *n* (%)	31 (54.4)	17	14	
GNAQ mutation				
Mutated, *n* (%)	65 (49.2)	20	45	0.052[b]
Wild type, *n* (%)	67 (50.8)	11	56	
GNA11 mutation				
Mutated, *n* (%)	44 (44.7)	11	48	0.238 [b]
Wild type, *n* (%)	73 (55.3)	20	53	

P-values for the associations with continuous data were obtained by Mann-Whitney test (indicated with a), and for the categorical data by χ2-test (indicated with b) or Fisher's exact test (indicated with c). A P-value ≤ 0.005 was considered significant (shown in bold). Seven UM with partial deletion of chromosome 3q were included in the disomy 3 group (indicated with d).

	EIF1AX			BAP1		
	Mutated	**Wild type**	**P-value**	**No expression**	**Expression**	**P-value**
	61.7	61.6	0.895[a]	67.5	58.3	**0.001**[a]
	12.6	13.4	0.314[a]	14.0	13.0	0.101[a]
	8.9	7.6	0.187[a]	8.1	7.9	0.644[a]
	16	56	0.719[b]	22	47	0.114[b]
	12	49		26	31	
	4	30	0.124[b]	18	16	0.037[b]
	24	75		30	62	
	12	41	0.714[b]	7	42	**<0.001**[b]
	16	64		41	36	
	7	51	0.031[b]	34	24	**<0.001**[b]
	20	53		13	53	
	4	53	**0.001**[b]	45	9	**<0.001**[b]
	24	52		3	69	
	24	33	**<0.001**[b]	6	47	**<0.001**[b]
	4	72		42	31	
	1	25	0.016[c]	16	10	**<0.001[b]**
	9	22		2	29	
	17	48	0.171[b]	20	40	0.263[b]
	11	56		28	37	
	11	48	0.516[b]	26	32	0.16 [b]
	17	56		22	45	

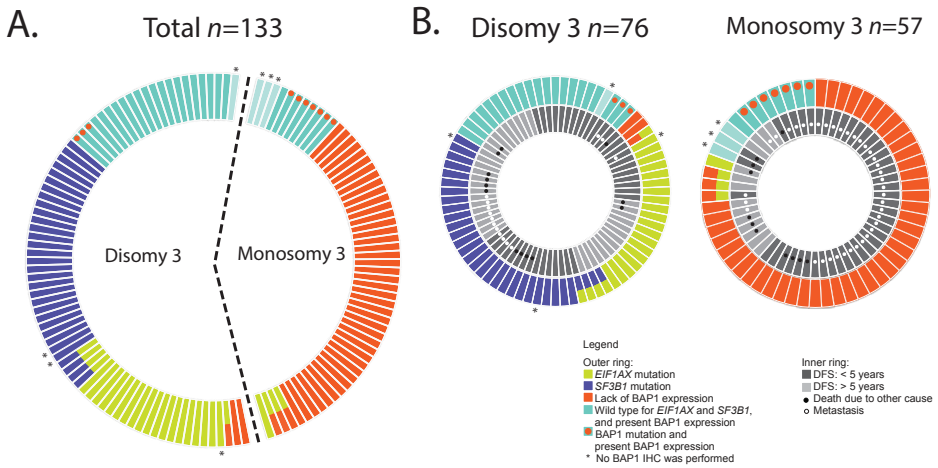

Figure 2. *Schematic overview of the uveal melanoma target genes. A doughnut chart was constructed for all samples (n = 133) regarding the mutation or expression status of uveal melanoma target genes EIF1AX, SF3B1 and BAP1 (**A**). The doughnut charts of disomy 3 and monosomy 3 tumors with the corresponding disease-free survival (DFS) with the survival status and presence of metastasis (**B**).*

Associations of *SF3B1*, *EIF1AX* and *BAP1* mutations

The occurrence of *SF3B1* and *EIF1AX* mutations was not mutually exclusive (P = 0.173), and 4 tumors (3.0%) harbored a mutation in both genes. *BAP1* mutations were mutually exclusive from *SF3B1* mutations and *EIF1AX* mutations ($P < 0.001$ and $P < 0.001$, respectively). Patients with an *SF3B1* mutation in the tumor were diagnosed at a younger age compared with *SF3B1* wild-type patients (mean age, 54.1 vs. 64.0 years; $P < 0.001$). *SF3B1* mutations were associated significantly with spindle-cell type ($P = 0.001$) and were associated inversely with extracellular matrix patterns ($P < 0.001$) and monosomy 3 ($P < 0.001$; Table 1). *EIF1AX* mutations were associated significantly with disomy 3 and disomy 8q in the overall cohort ($P = 0.001$ and $P < 0.001$, respectively; Table 1). Patients with no expression of BAP1 in the tumor were significantly older at diagnosis ($P < 0.001$). Lack of BAP1 expression also was associated significantly with the presence of epithelioid cells ($P < 0.001$), the presence of extracellular matrix patterns ($P < 0.001$), monosomy 3 ($P < 0.001$), and gain of chromosome 8q ($P < 0.001$; Table 1).

We divided the patients into groups based on the mutation status of the tumor. Patients with exclusive mutations in *SF3B1* or *EIF1AX* or no BAP1 expression in the tumor and tumors that do not harbor any of these mutations were considered separate groups. Twenty-two patients (16.5%) could not be categorized because of either an absence of

BAP1 status (n = 4), a lack of BAP1 expression with a co-occurring *EIF1AX* mutation (n = 4), co-occurrence of *SF3B1* and *EIF1AX* mutations (n = 4), or tumors with *BAP1* mutation however with the presence of BAP1 protein (n = 10) in the tumors.[13]

Differences in age at diagnoses between the separate groups showed that patients without BAP1 expression in the tumor were diagnosed at the oldest age (mean, 66.9 years), and patients with an *SF3B1* mutation at the youngest age (mean, 54.5 years; $P < 0.001$). Epithelioid cells were present most frequently in tumors without BAP1 expression (86%), less frequently in tumors with an *EIF1AX* mutation (60%), and least frequently in *SF3B1* mutated tumors and tumors without mutations in these 3 genes (36% and 32%, respectively; $P < 0.001$). Extracellular matrix patterns were observed most frequently in tumors without BAP1 expression (70%), followed by tumors without *BAP1, SF3B1* or *EIF1AX* mutations (42%), and least frequently in tumors with *SF3B1* or *EIF1AX* mutations (both 15%; $P < 0.001$). Chromosome 3 loss was observed in almost all tumors without BAP1 expression and present sporadically in *EIF1AX*-mutated tumors and tumors without these mutations. Chromosome 3 loss was completely absent in the *SF3B1*-mutated tumors (Figure 2). Chromosome 8q gain was present in almost all tumors without BAP1 expression (95%), more than half of the *SF3B1*-mutated tumors (54%) and was present less frequently in *EIF1AX*-mutated tumors and tumors without *BAP1, SF3B1* or *EIF1AX* mutations (10% and 21%, respectively; $P < 0.001$). Tumors had the largest diameter in patients without BAP1 expression in the tumor (mean, 14.1 mm) and in patients with *SF3B1*-mutated tumors (mean, 13.8 mm) when compared to patients with *EIF1AX*-mutated tumors or without a mutation (mean for both, 12.3 mm); however this did not reach significance ($P = 0.0.72$). Also, no difference was observed for tumor height, gender, involvement of the ciliary body, *GNAQ* and *GNA11* mutations between the patients in the separate groups (Table 2).

Table 2. Correlations between the BAP1, *SF3B1*, *EIF1AX* and no mutation groups and other clinic-histopathological and genetic features.

		Associations				
		BAP1	*SF3B1*	*EIF1AX*	No mutation	
Variables	***n*=111**	**No expression**	**Mutated**	**Mutated**		**P-value**
Age, years (range)	61.1 (22-92)	66.9	54.5	61.3	57.3	0.001
Largest tumor diameter, mm (range)	13.4 (5 – 22)	14.1	13.8	12.3	12.3	0.072
Tumor height, mm (range)	7.7 (1.5 – 22.0)	8.0	7.6	8.5	6.5	0.234
Sex						
Male, *n* (%)	59 (53.2)	20 (45%)	16 (57%)	12 (60%)	8 (42%)	0.621
Female, *n* (%)	52 (46.8)	24 (55%)	12 (43%)	8 (40%)	11 (58%)	
Involvement ciliary body						
Present, *n* (%)	32 (28.8)	18 (41%)	7 (25%)	3 (15%)	4 (21%)	0.124
Not present, *n* (%)	79 (71.2)	26 (59%)	21 (75%)	17 (85%)	15 (79%)	
Cell type						
Spindle, *n* (%)	45 (40.5)	6 (14%)	18 (64%)	8 (40%)	13 (68%)	<0.001
Epithelioid/mixed, *n* (%)	66 (59.8)	38 (86%)	10 (36%)	12 (60%)	6 (32%)	
Extracellular matrix patterns						
Present, *n* (%)	46 (41.4)	31 (70%)	4 (15%)	3 (15%)	8 (42%)	<0.001
Not present, *n* (%)	64 (57.7)	13 (30%)	23 (85%)	17 (85%)	11 (58%)	
Chromosome 3 [d]						
Loss, *n* (%)	44 (39.6)	42 (95%)	0 (0%)	1 (5%)	1 (6%)	<0.001
Normal, *n* (%)	67 (60.4)	2 (5%)	28 (100%)	19 (95%)	18 (94%)	
Chromosome 8q						
Normal, *n* (%)	48 (43.2)	2 (5%)	13 (46%)	18 (90%)	15 (79%)	<0.001
Gain, *n* (%)	63 (56.8)	42 (95%)	15 (54%)	2 (10%)	4 (21%)	
GNAQ mutation						
Mutated, *n* (%)	52 (47.3)	18 (41%)	16 (59%)	11 (55%)	7 (37%)	0.311
Wild type, *n* (%)	58 (52.7)	26 (59%)	11 (41%)	9 (45%)	12 (63%)	
GNA11 mutation						
Mutated, *n* (%)	52 (47.3)	24 (55%)	11 (41%)	9 (45%)	8 (42%)	0.650
Wild type, *n* (%)	58 (52.7)	20 (45%)	16 (59%)	11 (55%)	11 (58%)	

P-values for the associations with continuous data were obtained by One-way ANOVA test (indicated with [a]), and for the categorical data by χ^2-test (indicated with [b]). A P-value ≤ 0.005 was considered significant (shown in bold). Seven UM with partial deletion of chromosome 3q were included in the disomy 3 group (indicated with [d]).

Survival analysis

Tumors harboring *EIF1AX* mutations were associated significantly with a better metastatic-free survival (DFS, 190.5 [mutant] vs. 100.2 [wild type] months; $P < 0.001$; Figure 3A), whereas *SF3B1* mutations were not (DFS, 132.8 [mutant] vs. 120.9 [wild type] months; $P = 0.252$; Figure 3B; Table 3). Tumors with no BAP1 expression were associated with a worse survival (DFS, 69.0 [no expression] vs. 147.9 [with expression] months; $P < 0.001$). Univariate analyses of other single prognostic factors showed significant lower DFS for patients with larger tumor diameter ($P = 0.019$), the presence of epithelioid cells ($P = 0.007$), the presence of extracellular matrix patterns ($P = 0.001$), the loss of chromosome 3 ($P < 0.001$) and gain of chromosome 8q ($P < 0.001$) in the tumor compared with those without these features. Because *SF3B1* and *EIF1AX* mutations are associated with disomy 3,[13,16-19] we stratified for chromosome 3 status in the survival analysis to eliminate the impact of monosomy 3 on survival. In tumors with disomy 3 (n = 76), the presence of an *SF3B1* mutation (n = 32) was associated with a significantly worse prognosis and the development of late metastasis (DFS, 132.8 [mutant] versus 174.4 [wild type] months; P=0.008; Figure 3B; Table 3), whereas an *EIF1AX* mutation (n = 24) was associated with a better DFS survival ($P = 0.031$; Figure 3A; Table 3). Univariate analyses of other single prognostic factors showed a significantly lower DFS for patients with chromosome 8q gain ($P = 0.035$). No significant associations were observed for the other clinical parameters.

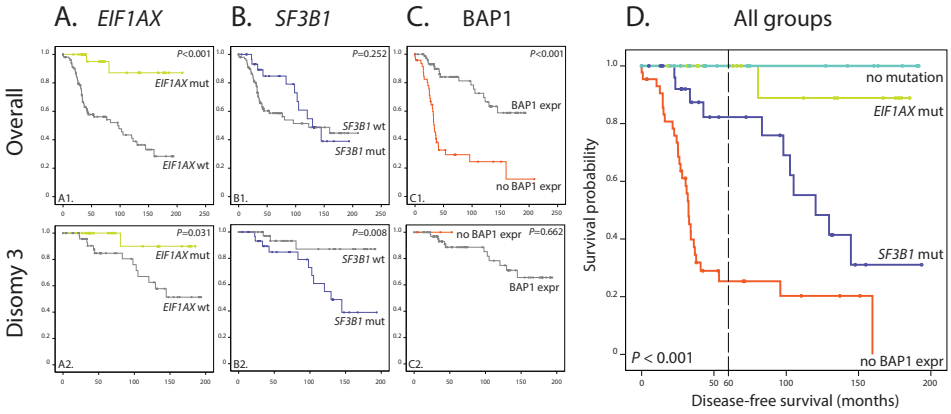

Figure 3. *Kaplan-Meier curves showing disease-free survival (DFS) for EIF1AX, SF3B1 and BAP1 status. In the overall group, the prognosis was better among uveal melanoma patients with an EIF1AX mutation (P < 0.001) (**A**). No difference in prognosis could be detected in patients with an SF3B1 mutation in the overall group (P = 0.252), however in the disomy 3 group, SF3B1 mutations were associated with worse survival (P = 0.008) (**B**). Tumors without BAP1 expression had a worse survival in the overall group (P < 0.001) (**C**). Survival curve for clustered based mutation status showed distinct survival patterns for each group (P < 0.001) (**D**).*

Table 3. Univariate and multivariate analysis of the uveal melanoma parameters in relation to patient survival

	Univariate analysis			Multivariate analysis		
	Mean	95% CI	P-value	HR	95% CI	P-value
Total group (*n* = 133)						
Largest tumor diameter (mean)	13.24	1.016-1.195[a]	**0.019**[c]	-	-	0.057[c]
Tumor height (mean)	7.85	0.995-1.117[a]	0.425[c]	-	-	-
Cell type						
Spindle (*n* = 53)	139.2	117-161[b]	**0.007**[d]	-	-	0.703[c]
Mixed/epithelioid (*n* = 80)	108.5	87-130[b]				
Closed vascular loops						
Present (*n* = 58)	96.3	71.9-120.7[b]	**0.001**[d]	-	-	0.172[c]
Absent (*n* = 73)	136.5	117.4-155.6[b]				
Chromosome 3						
Loss (*n* = 57)	73.4	52.0-94.8[b]	**<0.001**[d]	12.6	2.89-54.9	**0.001**[c]
Normal (*n* = 76)	155.1	138.2-172.1[b]				
Chromosome 8q						
Normal (*n* = 57)	173.6	153.6-193.7[b]	**<0.001**[d]	2.61	1.02-6.66	**0.045**[c]
Gain (*n* = 76)	82.8	64.4-101.1[b]				
BAP1 expression						
Yes (*n* = 68)	147.9	130.6-165.3[b]	**<0.001**[d]	-	-	0.849[c]
No (*n* = 58)	69.0	45.8-92.3[b]				
SF3B1						
Wild type (*n* = 101)	120.9	101.2-140.7[b]	0.252[d]	5.28	1.13-24.6	**0.034**[c]
Mutated (*n* = 32)	132.8	107.4-158.2[b]				
EIF1AX						
Wild type (*n* = 105)	100.2	83.7-116.7[b]	**<0.001**[d]	0.125	0.016-0.979[a]	**0.048**[c]
Mutated (*n* = 28)	190.5	166.2-214.8[b]				

CI: confidence interval; HR: hazard ratio. The 95% CI were calculated either for HR (indicated by [a]) or for survival in months (indicated by [b]). P-values for the univariate analyses were obtained by Log-rank test (indicated with [c]) and for the multivariate analysis by Cox regression analysis (indicated with [d]). A P-value ≤ 0.05 was considered significant (shown in bold). *BAP1* mutations were left out of the disomy 3 multivariate analyses due to the low number of tumors with a *BAP1* mutation.

		Univariate analysis			Multivariate analysis		
		Mean	95% CI	P-value	HR	95% CI	P-value
	Disomy 3 (*n* = 76)						
	Largest tumor diameter (mean)	13.02	0.904-1.212[a]	0.541[c]	-	-	-
	Tumor height (mean)	7.70	0.760-1.102[a]	0.349[c]	-	-	-
	Cell type						
	Spindle (*n* = 45)	150.3	128.8-171.8[b]	0.671[d]	-	-	-
	Mixed/epithelioid (*n* = 31)	158.8	132.5-185.1[b]				
	Closed vascular loops						
	Present (*n* = 17)	148.5	112.8-184.1[b]	0.808[d]	-	-	-
	Absent (*n* = 57)	155.0	135.6-174.6[b]				
	-	-	-		-	-	-
	-	-	-				
	Chromosome 8q						
	Normal (*n* = 49)	168.0	149.9-186.0[b]	**0.035[d]**	-	-	0.126[c]
	Gain (*n* = 27)	131.1	100.1-162.1[b]				
	-	-	-	-	-	-	-
	-	-	-	-			
	SF3B1						
	Wild type (*n* = 44)	174.4	155.9-193.0[b]	**0.008[d]**	4.764	1.325-17.12[a]	**0.017[c]**
	Mutated (*n* = 32)	132.8	107.4-158.2[b]				
	EIF1AX						
	Wild type (*n* = 52)	142.8	121.3-164.3[b]	**0.031[d]**	-	-	0.131[c]
	Mutated (*n* = 24)	174.8	155.3-194.3[b]				

A survival curve based on the groups (no BAP1 expression; *SF3B1* mutation; *EIF1AX* mutation; and no *BAP1*, *SF3B1* or *EIF1AX* mutation) revealed significantly different survival patterns between the groups ($P < 0.001$; Figure 3D). Five years after diagnosis (dotted vertical line in Figure 3D), patients without BAP1 expression in the tumor were at risk of developing metastases, whereas the other groups were not. However, after a longer survival period, the patients with an *SF3B1* mutation also demonstrated metastases. Patients with an *EIF1AX* mutation or no mutations in the target genes were at minimal risk of metastases developing.

Multivariate Cox regression analysis was performed for those variables that were associated significantly with survival in the univariate analyses to determine which of these parameters were independent prognostic factors for DFS. *SF3B1* was also included in the multivariate analyses because *SF3B1* also was predictive when corrected for chromosome 3. For the overall group, loss of chromosome 3 (hazard ratio [HR], 12.6; $P = 0.001$), *SF3B1* mutations (HR, 5.28; $P = 0.034$), chromosome 8q gain (HR, 2.61; $P = 0.045$) and *EIF1AX* mutations (HR, 0.125; $P = 0.,048$) were shown to be independent predictors for metastatic disease in UM patients (Table 3). In disomy 3 tumors, only *SF3B1* mutations (HR, 4.8; $P = 0.017$) were an independent predictor for metastases. In this subgroup, *EIF1AX* mutation status and chromosome 8q gain did not reach significance.

Discussion

Uveal melanoma is a rare ocular tumor with a high mortality. Currently, UM prognosis is based on dichotomous classifications, either by gene expression (class 1 vs. class 2),[9] chromosome status (monosomy 3 vs. disomy 3),[7,8] or protein expression (presence vs. absence of BAP1 expression),[13-15] in which a group of patients tends to be misclassified. In this study, we found evidence that UM patients have different risks for metastases based on the mutational status of *BAP1*, *SF3B1* and *EIF1AX*. As described by others, *BAP1* mutations in the tumor are associated with rapid metastasis and *EIF1AX* mutations with prolonged metastatic-free survival.[13-15,17] *SF3B1* mutations have an intermediate risk and are associated with late metastasis.

In the multivariate analyses we observed that chromosome 3 loss, *SF3B1* mutation, chromosome 8q gain and *EIF1AX* wild-type status were associated independently with metastatic disease. Contrary to previous work by our group and others, we did not find BAP1 immunohistochemistry results to be the strongest predictor of metastases of all variables.[6,13-15] However, this can be explained by the discrepancies between BAP1 staining and *BAP1* mutation analyses in the entire cohort. Ten tumors stained positive for BAP1, whereas mutation analyses did reveal a mutation in the tumors. Among these 10 patients, metastases developed in 8, as illustrated in Figure 2. Within a cohort of 133 patients, the impact on survival of these patients with metastasis is very high, and therefore can explain why BAP1 immunohistochemistry is not an independent prognostic predictor. However this does not mean that BAP1 immunohistochemistry is irrelevant. In fact, if we cluster *BAP1*-mutated tumors with tumors lacking BAP1 expression together, we observe that BAP1 status is the strongest predictor for metastases of all variables (statistics not shown). Furthermore, in 40 of the 52 patients with metastatic disease, we detected a *BAP1* mutation or, with immunohistochemistry, loss of BAP1 expression. Moreover, we found that 90% of these patients in whom metastases developed demonstrated this within 5 years after diagnosis. *BAP1* is a tumor suppressor gene that is involved in various cancers.[24] Functionally, BAP1 is involved repair of DNA damage, most notably double-strand breaks, through deubiquitination and chromatin remodeling.[25] DNA-damage repair insufficiency leads to genomic instability, and thus enhancement of the cancer pathogenicity.[26] Patients with tumors with *BAP1* mutations account for the majority of metastasizing UM in our cohort; nevertheless, there remains a subgroup of patients who demonstrate metastasis, mainly beyond 5 years after primary treatment, who do not harbor *BAP1* mutations.

Previous studies demonstrated that *SF3B1* mutation in UM associated with good prognostic features and that UM tumors with these mutations rarely metastasize.[16-18] In this study, we confirmed the association of *SF3B1* with known favorable prognostic features in the overall cohort. Ewens et al.[13] reported a series of 63 UM patients with metastasis (cases) and 53 patients without metastasis (controls) in which *SF3B1* mutations did not influence the metastatic behavior of UM. In that study, the cutoff point for follow-up was set at 48 months. In the Kaplan-Meier survival curve of the overall group in our study, we also observed a better survival for patients with *SF3B1*-mutated tumors versus wild-type during the first years after diagnosis (**Figure** 3B). However, when the follow-up is longer, as shown in **Figure** 3B, the decline in survival for UM patients with *SF3B1* mutations in their tumors began at a later stage. A similar survival curve was created by Harbour et al,[18] whose study showed that *SF3B1* mutations seem to predispose for favorable outcome, but this did not reach significance with a follow-up of 10 years. The most likely explanation is that, as in the series of Ewens et al, some of the nonmetastatic patients with an *SF3B1* mutation in their tumor will demonstrate metastasis when the follow-up is prolonged. In our cohort, we demonstrated that in patients with an *SF3B1* mutation, metastasis occurred in general (in 64%) more than 5 years after diagnosis, with a median of approximately 8.2 years (range, 23-145 months). This emphasizes the importance of a long follow-up time in prognostic UM studies.

To eliminate the impact of monosomy 3 tumors, we stratified for chromosome 3 status in the survival analysis. In this subset of 76 disomy 3 tumors from the present study we demonstrated that patients with disomy 3 tumors and *SF3B1* mutations have a 5-fold increased risk of metastatic disease occurring at a longer follow-up time, thus contradicting the current literature on the prognostic value of SF3B1 in UM.[13,16-18] This highlights the fact that patients with an *SF3B1* mutation are a distinct subclass among UM patients with an increased risk of metastatic disease. Fourteen disomy 3 patients demonstrated metastasis, of whom 11 harbored an *SF3B1* mutation in the tumor, explaining 79% (11/14) of metastatic cases of disomy 3 patients. Two other disomy 3 patients who demonstrated metastases harbored *BAP1* mutations. Although these tumors stained positively for BAP1 using immuhistochemistry, we detected a homozygous *BAP1* missense mutation (p.A92V) in 1 patient and 2 N-terminal missense mutations (p.Y173C & p.P88del) in the other patient, indicating that these 2 patients belong to the *BAP1*-mutated subgroup. These 2 metastases were diagnosed at 34 and 44 months after initial treatment, which fits in the metastatic rate of monosomy

3 patients with *BAP1* mutations and seems earlier compared with metastases from patients with *SF3B1* mutations. However, we need to validate the effect of these missense mutations with functional assays before we can draw absolute conclusions.

SF3B1 mutations are described in other malignancies such as chronic lymphocytic leukemia and myelodysplastic syndrome.[27,28] SF3B1 is essential in pre-mRNA splicing,[29] and is hypothesized to be involved in cancer through alternative splicing of target genes, which may play a role in tumorigenesis.[16] More recently, SF3B1 has been described to be involved in DNA-damage repair as well,[30,31] which may explain the unfavorable prognosis through a potential role in pathways similar to BAP1.

EIF1AX mutations are also associated with favorable prognostic features and are correlated with prolonged survival,[13,17,19] which we confirm in this study. Even when stratified for chromosome 3 status, patients with *EIF1AX* mutations have a significantly better DFS than patients without *EIF1AX* mutations (Figure 3A). One can debate whether an *EIF1AX* mutation on its own is correlated with better survival or whether the lack of *BAP1* and *SF3B1* mutations is the reason for a better survival; first, most missense mutations in *EIF1AX* are predicted by the PolyPhen-2 and SIFT software to be either benign or tolerated. Secondly, similar survival has been observed between patients who do not harbor mutations in *BAP1*, *SF3B1* and *EIF1AX* in the tumor (wild-type) versus patients with only *EIF1AX* mutations in the tumor (Figure 3D). EIF1AX is involved in mRNA translation through its essential role in start codon recognition of the target mRNA.[32] Overexpression of EIF1AX has been described to promote protein synthesis and cell proliferation, which may explain its role in cancer.[33]

As observed in the overall survival curves, the impact of the large proportion of *BAP1*-mutated tumors has an enormous effect on survival (Figure 3) and can cause erroneous interpretations for the disomy 3 patients. After eliminating that group, we observed that patients with *SF3B1* mutations are also at risk for metastasis, in particular late-onset metastasis.

All but 1 of the investigated tumors were obtained after enucleation, an intervention that is performed mainly in patients with large tumors. None of the mutations were associated significantly with tumor size (Table 2). Whether an enlarged tumor size increases the risk for metastases is unclear; it has been reported that by calculating tumor doubling time, tumors can disseminate up to 5 years before treatment.[4] The

mutational spectrum for smaller tumors may differ from larger tumors, although we cannot draw any conclusions based on our data. In a previous study, monosomy 3 was described in half of the patients who underwent secondary enucleation after fractionated stereotactic radiotherapy as a treatment of the primary UM (which was small to medium-sized).[34] In our current cohort, we also observed monosomy 3 in approximately half of the patients, suggesting a similar spectrum of genetic abnormalities between medium sized and large tumors.

The discrepancies between the BAP1 staining and the *BAP1* mutation status, as mentioned before in this discussion, also must be addressed. BAP1 staining is a rapidly applicable technique to determine BAP1 inactivation; however, we still observe tumors that express BAP1 immunohistochemically while harboring a mutation. We therefore suggest *BAP1* mutation analyses in all tumors with loss of chromosome 3 (or isodisomy 3) in combination with BAP1 expression because alternative regulation of BAP1 expression in these tumors still might contribute to metastasis.

In conclusion, we showed that patients with aberrant *BAP1* tumors correlate with a rapid decline in survival, patients with *SF3B1* mutations with late-onset metastasis, and patients with *EIF1AX* mutations or no mutations in the *BAP1*, *SF3B1* and *EIF1AX* genes have a prolonged survival. These results suggest that there are more than 2 classes in UM; however, validation of our findings using an independent data set is needed to confirm this new classification.

References

1. Singh AD, Turell ME, Topham AK. Uveal melanoma: trendsin incidence, treatment, and survival. Ophthalmology2011;118:1881–5.
2. Virgili G, Gatta G, Ciccolallo L, et al. Incidence of uvealmelanoma in Europe. Ophthalmology 2007;114:2309–15.
3. Zimmerman LE, McLean IW, Foster WD. Does enucleation ofthe eye containing a malignant melanoma prevent or acceleratethe dissemination of tumour cells. Br J Ophthalmol 1978;62:420–5.
4. Eskelin S, Pyrhonen S, Summanen P, et al. Tumor doublingtimes in metastatic malignant melanoma of the uvea: tumorprogression before and after treatment. Ophthalmology2000;107:1443–9.
5. Gill HS, Char DH. Uveal melanoma prognostication: fromlesion size and cell type to molecular class. Can J Ophthalmol2012;47:246–53.
6. Harbour JW, Onken MD, Roberson ED, et al. Frequent mutationof BAP1 in metastasizing uveal melanomas. Science2010;330:1410–3.
7. Prescher G, Bornfeld N, Hirche H, et al. Prognostic implicationsof monosomy 3 in uveal melanoma. Lancet 1996;347:1222–5.
8. Sisley K, Rennie IG, Parsons MA, et al. Abnormalities ofchromosomes 3 and 8 in posterior uveal melanoma correlatewith prognosis. Genes Chromosomes Cancer 1997;19:22–8.
9. Onken MD, Worley LA, Ehlers JP, Harbour JW. Gene expressionprofiling in uveal melanoma reveals two molecular classesand predicts metastatic death. Cancer Res 2004;64:7205–9.
10. Van Raamsdonk CD, Bezrookove V, Green G, et al. Frequentsomatic mutations of GNAQ in uveal melanoma and bluenaevi. Nature 2009;457:599–602.
11. Van Raamsdonk CD, Griewank KG, Crosby MB, et al. Mutationsin GNA11 in uveal melanoma. N Engl J Med 2010;363:2191–9.
12. Koopmans AE, Vaarwater J, Paridaens D, et al. Patient survivalin uveal melanoma is not affected by oncogenic mutationsin GNAQ and GNA11. Br J Cancer 2013;109:493–6.
13. Ewens KG, Kanetsky PA, Richards-Yutz J, et al. Chromosome3 status combined with BAP1 and EIF1AX mutation profilesare associated with metastasis in uveal melanoma. InvestOphthalmol Vis Sci 2014;55:5160–7.
14. Kalirai H, Dodson A, Faqir S, et al. Lack of BAP1 proteinexpression in uveal melanoma is associated with increasedmetastatic risk and has utility in routine prognostic testing. Br JCancer 2014;111:1373–80.
15. Koopmans AE, Verdijk RM, Brouwer RW, et al. Clinicalsignificance of immunohistochemistry for detection of BAP1mutations in uveal melanoma. Mod Pathol 2014;27:1321–30.
16. Furney SJ, Pedersen M, Gentien D, et al. SF3B1 mutations areassociated with alternative splicing in uveal melanoma. CancerDiscov 2013;3:1122–9.
17. Martin M, Masshofer L, Temming P, et al. Exome sequencingidentifies recurrent somatic mutations in EIF1AX and SF3B1 inuveal melanoma with disomy 3. Nat Genet 2013;45:933–6.
18. Harbour JW, Roberson ED, Anbunathan H, et al. Recurrentmutations at codon 625 of the splicing factor SF3B1 in uvealmelanoma. Nat Genet 2013;45:133–5.
19. Dono M, Angelini G, Cecconi M, et al. Mutation frequenciesof GNAQ, GNA11, BAP1, SF3B1, EIF1AX and TERT in uvealmelanoma: detection of an activating mutation in the TERTgene promoter in a single case of uveal melanoma. Br J Cancer2014;110:1058–65.
20. Vandekken H, Pizzolo JG, Reuter VE, Melamed MR. Cytogeneticanalysis of human solid tumors by in situ hybridizationwith a set of 12 chromosome-specific DNA probes. CytogenetCell Genet 1990;54:103–7.
21. van Gils W, Lodder EM, Mensink HW, et al. Gene expressionprofiling in uveal melanoma: two regions on 3p related toprognosis. Invest Ophthalmol Vis Sci 2008;49:4254–62.
22. Abdel-Rahman MH, Christopher BN, Faramawi MF, et al.Frequency, molecular pathology and potential clinical significanceof partial chromosome 3 aberrations in uveal melanoma.Modern Pathology 2011;24:954–62.
23. Thomas S, Putter C, Weber S, et al. Prognostic significance ofchromosome 3 alterations determined by microsatellite analysisin uveal melanoma: a long-term follow-up study. Br JCancer

2012;106:1171–6.
24. Carbone M, Yang HN, Pass HI, et al. BAP1 and cancer. NatRev Cancer 2013;13:153–9.
25. Yu H, Pak H, Hammond-Martel I, et al. Tumor suppressor anddeubiquitinase BAP1 promotes DNA double-strand breakrepair. Proc Natl Acad Sci U S A 2014;111:285–90.
26. Khanna KK, Jackson SP. DNA double-strand breaks:signaling, repair and the cancer connection. Nat Genetics2001;27:247–54.
27. Patnaik MM, Lasho TL, Hodnefield JM, et al. SF3B1 mutationsare prevalent in myelodysplastic syndromes with ringsideroblasts but do not hold independent prognostic value.Blood 2012;119:569–72.
28. Rossi D, Bruscaggin A, Spina V, et al. Mutations of the SF3B1splicing factor in chronic lymphocytic leukemia: associationwith progression and fludarabine-refractoriness. Blood2011;118:6904–8.
29. Golas MM, Sander B, Will CL, et al. Molecular architecture ofthe multiprotein splicing factor SF3b. Science 2003;300:980–4.
30. te Raa GD, Derks IAM, Navrkalova V, et al. The impact ofSF3B1 mutations in CLL on the DNA-damage response.Leukemia 2015;29:1133–42.
31. Eldering E, te Raa D, Derks I, et al. Sf3b1 mutations in Cll areassociated with a defective DNA damage response. Haematologica2014;99:315–6.
32. Chaudhuri J, Si K, Maitra U. Function of eukaryotic translationinitiation factor 1A (eIF1A) (formerly called eIF-4C) ininitiation of protein synthesis. J Biol Chem 1997;272:7883–91.
33. Yu CP, Luo CC, Qu B, et al. Molecular network includingeIF1AX, RPS7, and 14-3-3 gamma regulates protein translationand cell proliferation in bovine mammary epithelialcells. Arch Biochem Biophys 2014;564:142–55.
34. van den Bosch T, Vaarwater J, Verdijk R, et al. Risk factorsassociated with secondary enucleation after fractionated stereotacticradiotherapy in uveal melanoma. Acta Ophthalmol2015;93:555–60.

Chapter 2.2

Molecular classification of uveal melanoma subtypes using integrative mutational and whole-genome copy number analysis.

Serdar Yavuzyigitoglu,* Wojtek Drabarek,* Kyra N. Smit, Askar Obulkasim, Natasha M. van Poppelen, Anna E. Koopmans, Jolanda Vaarwater, Tom Brands, Bert Eussen, Hendrikus J. Dubbink, Job van Riet, Harmen J.G. van de Werken, Berna Beverloo, Robert M. Verdijk, Naus, Dion Paridaens, Emine Kilic, and Annelies de Klein

* These authors contributed equally to this work.

Partially published as

S. Yavuzyigitoglu*, Wojtek Drabarek*, Kyra N. Smit, Natasha van Poppelen, Anna E. Koopmans, Jolanda Vaarwater, Tom Brands, Bert Eussen, Hendrikus J. Dubbink, Job van Riet, Harmen J.G van de Werken, Berna Beverloo, Robert M. Verdijk, Nicole Naus, Dion Paridaens, Emine Kilic and Annelies de Klein. Correlation of Gene Mutation Status with Copy Number Profile in Uveal Melanoma. *Ophthalmology. 2017 Apr;124(4):573-575.*

Abstract

Purpose: Classification of structural and numerical chromosomal changes to elucidate the observed metastatic risk difference in uveal melanoma (UM) patients with mutually exclusive *BAP1*, *SF3B1* and *EIF1AX* mutations.

Design: Case series.

Participants: 280 UM patients from the Rotterdam Ocular Melanoma Study (ROMS) cohort.

Methods: Unsupervised hierarchical clustering of genome-wide single nucleotide polymorphism (SNP) array data was used to identify molecular subclasses with distinct chromosomal patterns. Conventional karyograms were analyzed for the number and type of copy number variations (CNVs) and correlated with the different mutational statuses of UM. Results were validated using data from The Cancer Genome Atlas (TCGA).

Main Outcome Measures: Identification of specific chromosomal profiles corresponding to the mutational status of UM patients. To determine whether specific anomalies such as isochromosomes or structural variants are associated to the different molecular subclasses.

Results: Unsupervised clustering identified five clusters with distinct copy number aberrations patterns, each of them was mainly comprised of UMs with a specific mutated gene. *BAP1*, *SF3B1* or *EIF1AX*-mutated UMs contained distinctive and specific chromosomal patterns. We show that BAP1 negative UMs have the largest CNVs in size and *SF3B1*-mutated UMs harbored the most CNV events. Whereas *EIF1AX*-mutated UMs were characterized by the lack of CNVs. Isochromosomes occurred almost exclusively in BAP1 negative UMs. Somatic mutation signature analyses generated different signatures for the clusters harboring mutations in either *BAP1*, *SF3B1* or *EIF1AX*.

Conclusion: UMs harboring mutations in *BAP1*, *SF3B1* or *EIF1AX* have distinct chromosomal aberration patterns that mainly differ by the affected chromosomes, the absolute number of CNVs and the type of CNVs. Mutations in these genes are strongly associated with distinct molecular subclasses. This highlights and reflects the biological difference between UMs on a genetic level.

Introduction

Uveal melanoma (UM) is a rare malignancy, characterized by non-random chromosomal aberrations and recurrent mutated genes. Despite successful treatment of the primary tumor, half of the patients develop clinically detectable metastases within five years after diagnosis.[1]

Copy number variations (CNVs) and chromosomal changes have been investigated extensively in tumors of UM patients. Classification using a combination of chromosome 3 and chromosome 8q CNVs indicated that UM patients can be categorized into at least four groups with each a different metastatic risk.[2-4] Loss of chromosome 3 (monosomy 3), observed in half of the patients, is strongly associated with early metastatic disease.[5] Monosomy 3 is often observed in combination with gain of chromosome 8q and this combination gives the worst prognosis for UM patients compared to solely monosomy 3 or chromosome 8q gain.[2-4, 6] Disomy 3 is usually a favorable feature in UM patients, with a low metastatic disease risk.[3-6] However, disomy 3 with chromosome 8q gain is an indicator for intermediate risk of metastatic disease. Gain of chromosome 6p was found to correlate with a favorable prognosis in UM patients and is almost exclusively observed in patients with disomy 3 UM.[3, 4, 7]

Besides these chromosomal changes, recurrent mutations in tumor suppressor and oncogenes have been described. *GNAQ* and *GNA11* encode for guanine nucleotide-binding protein G subunit alpha (Gα) and the activating mutations of codons p.R183 and p.Q209 occur in over 90% of the UM.[8-11] Tumors without *GNAQ*/*GNA11* mutations often contain activating hotspot mutations in *PLCB4* (phospholipase C, beta 4) or *CYSLTR2* (cysteinyl leukotriene receptor 2).[12, 13] PLCB4 is a downstream effector of Gα whereas $CysLT_2R$ is located upstream in the Gα pathway.[12, 13] Since Gα mutations were not associated with survival it was hypothesized that these mutations are an initial step in tumorigenesis.[9]

Half of the UMs display monosomy 3 in which the remaining allelic copy of the *BAP1* (BRCA-associated protein 1) gene, situated at chromosome 3, is inactivated leading to early metastatic disease.[14-16] Somatic mutations in *SF3B1* (splicing factor 3, subunit 1) and *EIF1AX* (eukaryotic initiation factor 1A, X-linked) are almost exclusively observed in disomy 3 tumors.[17, 18] The N-terminal part of *EIF1AX* is changed by an in frame mutation of the first 15-20 amino acids of this protein in 20 % of UM patients, and

these patients seldom develop metastases.[18, 19] *SF3B1* mutations are seen in 20-25% of UM patients and target mostly codon p.R625.[8, 17, 19, 20] Although UM patients harboring somatic *SF3B1* mutations appear to have a favorable prognosis compared to patients with *BAP1* mutations,[20] a longer follow-up study showed that also *SF3B1*-mutated UM patients will eventually developed metastases.[19] Mutations in *BAP1*, *SF3B1* and *EIF1AX* occur almost mutually exclusive, and associate with distinct survival patterns suggesting that these somatic changes appear to mark different tumor subtypes within UM patients.[19, 21]

BAP1 and *SF3B1* are both involved in DNA damage repair pathways.[22, 23] It is therefore likely that mutations in these genes will give rise to chromosomal aberrations. The aim of this study was to integrate the chromosomal and mutational characteristics of UMs. We demonstrate that CNV patterns in UM correlate with these different mutated subtypes of UM. Using data from genome-wide profiling and traditional karyotyping we show that the type and combination of chromosomal aberrations are distinct for *BAP1*, *SF3B1* and *EIF1AX*-mutated UM. This highlights the genetic diversity of UMs and is a further step towards the elucidation of affected cellular pathways determining the prognosis of UM patients.

Methods

Study population

Patients were selected from the Rotterdam Ocular Melanoma Study group (ROMS) database based on the availability of whole-genome single nucleotide polymorphism (SNP) array analysis and karyotyping. Patients with iris melanoma or patients who underwent primary tumor irradiation were excluded. In total, 280 patients were included in this study. All patients underwent primary enucleation (n = 278) or received a biopsy (n = 2) between 1993 and 2015 at the Erasmus University Medical Center or the Rotterdam Eye Hospital, the Netherlands. SNP array data of the primary UM was available for 217 patients and karyotyping of the tumor was available for 119 patients. For 56 patients, SNP array data as well as cytogenetic data was available. An overview of patient and tumor characteristics is provided in Table 1. Patient's follow-up data was updated until March 2016. Informed consent was obtained from all patients. This study was approved by the local ethics committee and performed according to the guidelines of the Declaration of Helsinki.

Mutational status

After enucleation or biopsy, the tumor was divided in three parts and either snap-frozen in liquid nitrogen, embedded in paraffin or used for culturing and DNA extraction. DNA was extracted from fresh or frozen tumor tissue using the QIAmp DNA-mini kit (Qiagen, Hilden, Germany) according to the manufacturer's instructions as described previously.[19]

Mutation analyses of *GNAQ*, *GNA11*, *BAP1*, *SF3B1* and *EIF1AX* were performed using Sanger sequencing and targeted sequencing on the ION Torrent Personal Genome Machine (Life Technologies, Carlsbad, CA, USA) as described before.[19, 24] BAP1 protein expression was analyzed in most cases using immunohistochemistry (IHC), and in 101 cases also Sanger sequencing was used to confirm mutations in the coding exons of *BAP1*.[16, 24] We sequenced exon 14 of *SF3B1* and exon 1 and 2 with flanking regions up to 25 base pairs into the intron of *EIF1AX*. Based on the presence of mutations, the subgroups were defined into four major groups namely (1) *BAP1*$^{\mathbf{neg}}$: patients with BAP1 negative tumors (thus no BAP1 protein expression using IHC or a hemizygous *BAP1* mutation), (2) *SF3B1*$^{\mathbf{mut}}$*: SF3B1*-mutated tumors and (3) *EIF1AX*$^{\mathbf{mut}}$: *EIF1AX*-mutated tumors. Tumors which stained BAP1 positive and contained no *SF3B1* or *EIF1AX* mutations were grouped together and were called the (4) No Recurrent Mutations

(NRM) group. This group was further split into NRM^{LOH+} and NRM^{LOH-} subgroups based on the loss of heterozygosity (LOH) status of *BAP1*. We postulated that UMs with LOH of *BAP1* (allelic imbalance) might still harbor *BAP1* mutations despite the detection of BAP1 protein expression.

Table 1. *Clinical information of the ROMS cohort.*

Variable (n = 277)		n / median / mean
Gender		
Female		133
Male		144
Age at diagnosis	Median; range	62.4 years (22 – 95 years)
Largest tumor diameter	Mean; 95% CI	13.0 mm (12.5 – 13.4 mm)
Tumor thickness	Mean; 95% CI	7.4 mm (7.0 – 7.9)
TNM category		
1		41
2		79
3		127
4		22
Cell type		
Spindle		115
Mixed		113
Epithelioid		44
Ciliary body involvement		
No		201
Yes		71
Extracellular matrix patterns		
Absent		142
Present		125
Extraocular extensions		
Absent		200
Present		34

SNP array analyses

Two hundred nanograms of DNA input was used for whole-genome copy number analyses by SNP arrays. Three patients were excluded during SNP data processing since these samples only mapped approximately 65 % of the SNPs, whereas the threshold for adequate analyses was set at >90 % mapped SNPs. For the entire set, four types of Illumina Human SNP array platforms were used according to the manufacturers

guidelines: 18 UMs were analyzed using the CytoSNP-12 v2.0 BeadChip; 58 UMs were analyzed using theCytoSNP-12 v2.1; 46 UMs were analyzed using OmniExpress-12 v1 and 92 UMs were analyzed using CytoSNP-850K BeadChips (Bead Studio Illumina, San Diego, CA, USA). Nexus Copy Number 8.0 (BioDiscovery, Inc., El Segundo, CA, USA) was used to calculate the total percentage aneuploidy of the entire genome, the total copy number (CN) events and for visualization of the whole-genome SNP array data. For these calculations, the chromosomal aberrations of the sex chromosomes were left out of the analysis to prevent gender-based bias. Pairwise Wilcoxon test was used to compare the medians between the different groups. Holm's correction was used to correct for multiple testing. The statistical analyses was conducted using the R statistical package version 3.3.0.

Unsupervised hierarchal clustering

As mentioned earlier, data were generated on four different platforms, each has different number of SNPs. To combine samples across the four platforms, we only retained the 215,138 overlapped SNPs (Supplementary Figure 1). Thus, the dataset used for downstream analysis is of size 214 (samples) x 215,138 (features). To remove germline specific aberrations, tumor profiles in each platform underwent correction using the data from ten normal samples tented in that platform. The R-package NoWaves was used for this end.[25] Segmentation analysis was performed on the corrected data, which subsequently used to calculate the called data using R-package CGHcall.[26] The segmented and called data were combined to generate the regioned data, which has far more less features than the former two. Finally, hierarchical clustering analysis was performed using the dedicated R-package WECCA on the regioned data.[27] All analyses have been performed using the R statistical environment, version 3.3.1.

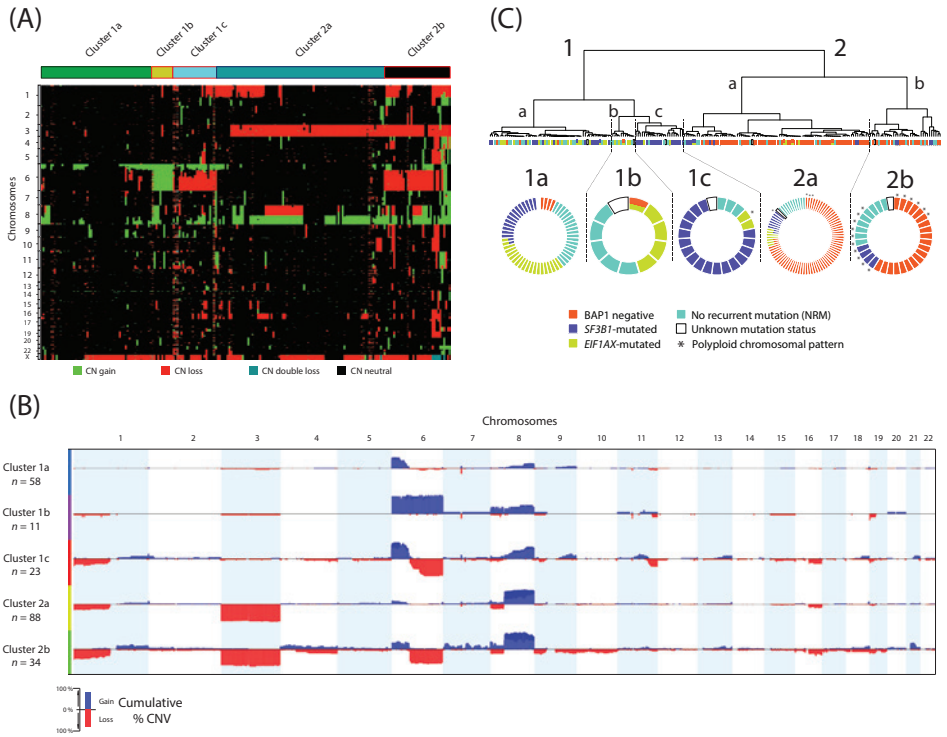

Figure 1. (A) Heatmap for the copy number variations (CNVs) constructed with unsupervised hierarchical clustering.(B) Chromosomal patterns for the five clusters constructed by unsupervised hierarchical clustering.(C) Doughnut charts for every cluster showing the distribution of the mutation status.

Karyotyping

For cytogenetic analyses, metaphases were obtained after short term tissue culture as described previously and were carried out according to the ISCN guidelines.[28, 29] In five cases, besides conventional karyotyping, spectral karyotyping (SKY) was performed to define the affected regions more accurately. These five cases were described in detail previously.[29, 30] Cytogenetic data from conventional karyotyping was available for 119 cases. The superiority of conventional cytogenetic analyses over SNP arrays is illustrated by the possibility to observe the origin and complexity of the chromosomal anomaly in a single cell, and the identity of the structural variants. Each sample was analyzed for the presence of isochromosomes and the amount of structural variants (translocations and subchromosomal CNVs). The mutational status was known in 70 patients (discovery set). Statistical analyses to determine differences between the groups was performed using the pairwise Fisher's exact test. Holm's correction was used to correct for multi-

ple testing. Of the 70 UMs, six cases revealed completely normal karyotypes, whereas the SNP array and direct FISH data showed chromosomal aberrations indicating that after short-term culture only normal cells were analyzed. These six cases were therefore excluded from the analyses. The 49 cases with an unknown mutational status were used as a validation cohort for the karyotype analyses.

The Cancer Genome Atlas (TCGA) database

For the SNP array analyses, a validation cohort of UM data (n = 80) was obtained from the National Institute of Health TCGA server. Level 3 SNP array data (normalized segmented copy number data), Level 2 Whole Exome Sequencing derived data (Broad Institute curated somatic mutation calling) and Level 3 RNA-seq V2 data (normalized expression) were used for analyses. We screened whole-exome data for mutations in the UM genes. The segmented SNP array data was visualized using Nexus Copy Number 8.0. The percentage of aneuploidy was calculated the same as for the SNP arrays in the ROMS cohort.

Signatures of Somatic Mutations Analysis

Mutation Annotation Format (MAF) files of UM Whole Exome Sequencing(WES) data generated by The Cancer Genome Atlas (TCGA) consortium was downloaded from the National Cancer Institute GDC portal (https://gdc-portal.nci.nih.gov/). For each somatic variant, its trinucleotide context was derived using the human reference genome (build hg19) and enumerated into a mutational spectrum matrix Mij (i = 96; number of trinucleotide contexts ;j = number of samples or groups of samples) using the SomaticSignatures R packages version 2.8.4 from Bioconductor version 3.3.[31, 32] The consensus mutational signatures, established by Alexandrov et. al, (matrix Sij; i = 96; number of trinucleotide motifs ;j = number of signatures) were downloaded from COSMIC (http://cancer.sanger.ac.uk/cancergenome/assets/signatures_probabilities.txt).[33] Per group, a constrained linear combination of the 21 validated mutational signatures from Alexandrov et al. was constructed which reconstructs the group-specific mutational spectrum, using non-negative least squares regression implemented in the R package pracma version 1.9.3 (retrieved from https://cran.r-project.org/package=pracma). Samples were grouped based on mutually exclusive *BAP1*, *SF3B1* and *EIF1AX* mutations (n =48). Relative contributions of Alexandrov's validated signatures per group are depicted in Figure 5. Signatures with less than one percent average contribution over all groups were combined as "others". The statistical analyses was conducted using the R statistical package version 3.3.0.

Results

Association of the clusters with mutational status

From the ROMS cohort, we selected patients for which SNP array data was available. Unsupervised hierarchical clustering (HC) was performed to examine whether the SNP array data could predict the mutational status. For this, the SNP arrays of 214 UM patients were analyzed using HC. For 209 patients the mutational status (BAP1 IHC and mutations in *BAP1*, *SF3B1* or *EIF1AX*) of the UM was known.

HC analyses unraveled five clusters, which are mainly driven by CNVs on chromosomes 1, 3, 6 and 8 (Figure 1A). The first major branching of the HC tree (cluster 1 versus cluster 2) divided disomy 3 and monosomy 3 UMs (Supplementary Figure 2A). For Cluster 1 and 2, also chromosome 8q CNV had a high importance score in discriminating between Cluster 1 and 2. Strikingly, the centromeric part of chromosome 8q had a higher importance score than the distal part of chromosome 8q. Within the two major clusters, we defined five sub-clusters.

The most discriminating CNV in the three sub-clusters in the left branch of the HC tree are characterized by CNVs in chromosome 6q (Supplementary Figure 2B and Figure 1C). Samples in Cluster 1a have no CNVs on chromosome 6q, whereas Cluster 1b was characterized by chromosome 6q gain and Cluster 1c is composed of patients with chromosome 6q loss in the UM. Chromosome 6q was also the most discriminating CNV between Cluster 2a and 2b (Supplementary Figure 2D).

Cluster 1a contained samples with only small CNVs or no CNVs at all (Figure 1B). Two-third of the samples in this cluster were *EIF1AX*^{mut} UMs or belonged to the NRM group (Figure 1C). Fourteen UMs had a partial chromosome 8q gain, of which none were *EIF1AX*^{mut} but 12 of the 14 cluster 1a UMs with partial chromosome 8q gain harbored an *SF3B1*-mutation. Interestingly, also four BAP1^{neg} UM cases clustered in this group, probably because these tumors lacked typical aberrations such as monosomy 3 and chromosome 8q gain.

Cluster 1b was characterized by a gain of an entire chromosome 6, which was solely observed in *EIF1AX*^{mut} and NRM UMs (Figure 1C). Only two UMs in another cluster (Cluster 2b) harbored an entire chromosome 6 gain. Moreover, these two UMs displayed a polyploid genome with many CNVs stretching entire chromosomes. This

suggests that chromosome 6 gain without polyploidy is predictive of *EIF1AX*-mutated tumors or UM without a recurrent mutation.

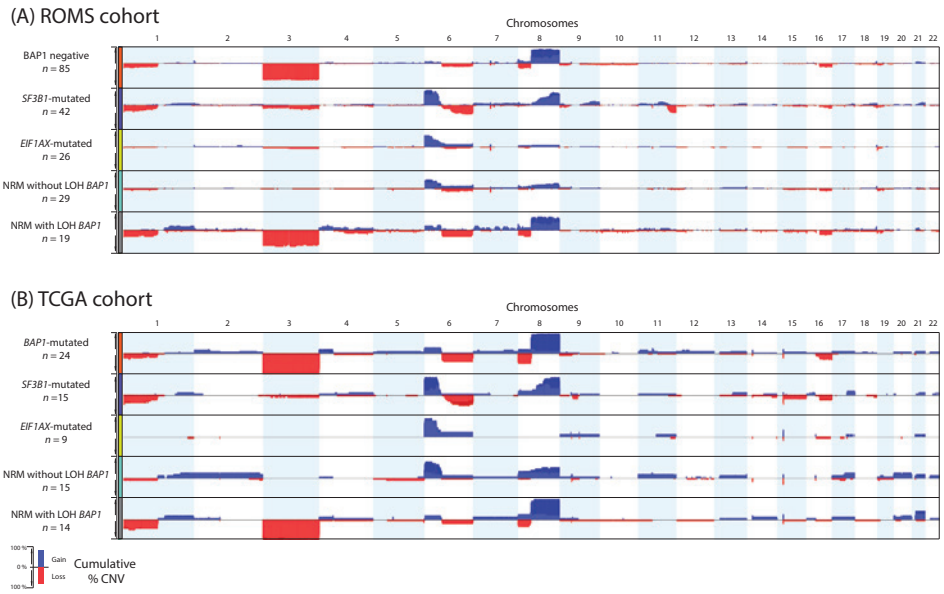

Figure 2. Summary CNV plots for the mutations specific groups of uveal melanomas (UMs) in the Rotterdam Ocular Melanoma Study (ROMS) (A) and The Cancer Genome Atlas (TCGA) (B) cohort. The chromosomes are depicted on the x-axis. The Y-axis shows the cumulative percentage of copy number variation per group. Dark blue indicates gain of chromosome and red indicated loss of chromosome. The sex-chromosomes are excluded.

Cluster 1c was characterized by gains in chromosome 6p and 8q, loss in chromosome 6q (Figure 1B) and enriched for *SF3B1*^{mut} (77 %; Figure 1C).

As displayed in Figure 1C, Clusters 2a and 2b were enriched for BAP1^{neg} UMs (70 %). Other samples in Cluster 2 consisted of five *SF3B1*^{mut} and seven NRM UMs (10%) that could be explained by polyploidy. As described previously, polyploid UM are highly aneuploid and contain a relative loss of chromosome 3 in all cases, which may cause the clustering in Cluster 2.[24] Eight other UMs in cluster 2 had a disomy 3. These cases have chromosome 1p loss without chromosome 6q loss. The remaining sixteen cases consisted of three *SF3B1*^{mut}, two *EIF1AX*^{mut} and eleven NRM UMs with LOH of *BAP1*. As these UMs displayed similar chromosomal patterns as *BAP1* deficient UMs, it is likely that these tumors might harbor cryptic *BAP1* mutations or have epigenetic silencing of the *BAP1* We observed that the clusters are indicative of the samples'

mutation status. BAP1^{neg} UMs mainly clustered based on monosomy 3. UMs with *EIF1AX* mutations or no detectable recurrent mutations tightly clustered together by either a very limited number of CNVs or the presence of chromosome 6 gain. *SF3B1*^{mut} UMs cluster together based on recurring CNVs of chromosome 6p, 6q and 8q. These analyses indicate that the UM tumor cells that are BAP1^{neg}, *SF3B1*^{mut} or *EIF1AX*^{mut} do have distinct chromosomal patterns.

Mutation-specific chromosomal changes

To validate this hypothesis, we performed supervised clustering. Cases were grouped based on the mutation status and analyzed for mutation-specific recurring CNVs (n = 209). Cases with double mutations - *BAP1* & *EIF1AX* (n = 4) or *SF3B1* & *EIF1AX* (n = 4) - were analyzed separately. To validate our findings in an independent cohort, we analyzed the publicly available UM data from TCGA (n = 80). A flowchart of the cases in both cohorts are illustrated in Supplementary Figures 3A and 3B.

BAP1^{neg} tumors (n = 85) were characterized by loss of chromosome 3 (95 %) and gain of the entire long (q)-arm of chromosome 8 (85 %) as illustrated in Figure 2A. Gain of chromosome 8q was often accompanied by loss of chromosome 8p (31 % of the cases). Loss of chromosome 1p, 6q and 16q was also observed frequently (25 %, 20 % and 20 % of the cases, respectively). *BAP1*-mutated UM (n = 24) in the TCGA dataset had similar results with loss of chromosome 1p (25 %), chromosome 3 (100 %), chromosome 6q (42 %), chromosome 8p (50 %) and chromosome 16q (29 %). Gain of chromosome 8q was observed in 96 % of the cases.

SF3B1^{mut} tumors (n = 42) were characterized by gain of chromosome 6p (86 %) and 8q (74 %), and loss of chromosome 6q (55 %) and 11q (48 %) (Figure 2A). In addition, loss of chromosome 1p (36 %) and gain of chromosome 9q (24 %) were present in *SF3B1*^{mut} tumors. Compared to BAP1^{neg} tumors, structural variants (SVs) within *SF3B1*^{mut} tumors were observed more frequently. BAP1^{neg} tumors harbored a gain of the entire chromosome 8q whereas *SF3B1*^{mut} UM were characterized by either a gain of chromosome 8q23qter or chromosome 8q13qter. Other SVs with gain or deletion of the distal ends of chromosomes were chromosome 6p12.3pter gain, chromosome 6q16.1qter loss, and chromosome 11q22qter loss. Although chromosome 1p loss occurred by deletion of the distal part of chromosome 1p, no clear recurring breakpoint could be observed. *SF3B1*^{mut} UM (n = 15) in the TCGA dataset also showed gain of chromosome 6p (86

%) with the breakpoint in chromosome band 6p12.3 and gain of chromosome 8q (86 %) at breakpoint 8q13.3 and 8q23.2. Chromosome 1p loss was observed in 43 % and chromosome 6q in 58 % usually with a breakpoint at chromosome band 6q16.1. The SVs with the recurring breakpoints in our set and that of TCGA were similar. There was only a clear difference observed for chromosome 11q deletions, which were practically absent in *SF3B1*^{mut} UM in the TCGA dataset.

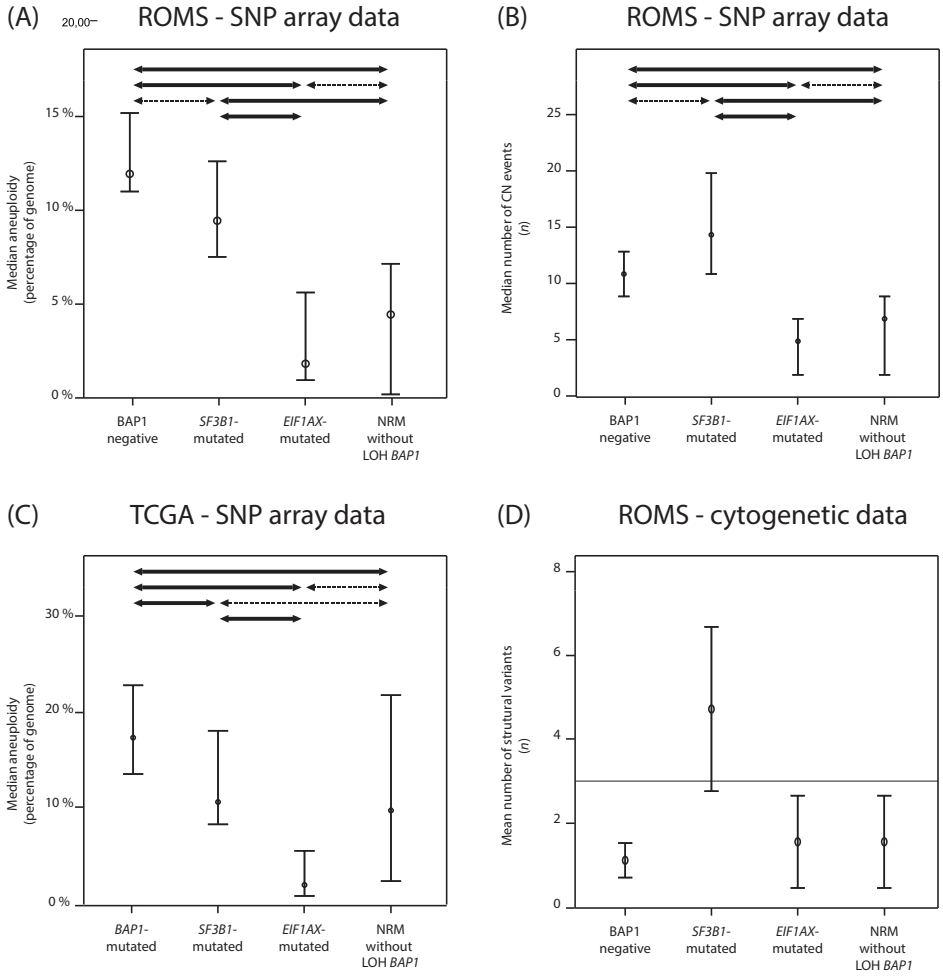

Figure 3. Statistical comparisons of the percentage of aneuploidy between the major groups (A) and the total number of copy number (CN) events (B) in the Rotterdam Ocular Melanoma Study (ROMS) cohort. (C) Comparison of the percentage of aneuploidy in The Cancer Genome Atlas (TCGA) cohort between the major groups. (D) Comparison of the number of structural variants obtained from cytogenetic data of the ROMS cohort between the major groups. The continuous lines between the groups are statistically significant differences ($P < 0.05$) between the groups. The dashed line depicts no significant difference between the groups.

For *EIF1AX*^{mut} tumors ($n = 26$) only gain of chromosome 6 or 6p was recurrent (65 %). Mostly a gain of chromosome 6p21.33pter was observed, which is a more distal region on chromosome 6 compared to that of *SF3B1*^{mut} tumors. Likewise, in the TCGA dataset, we observed a breakpoint mainly at chromosome band 6p21.1 in *EIF1AX*^{mut} UM with chromosome 6/chromosome 6p gain (89 %).

Tumors that were *SF3B1* and *EIF1AX* wildtype and stained BAP1 positive (NRM; $n = 48$) were subdivided based on LOH of *BAP1*, to prevent falsely NRM classified UMs. Nineteen UMs harbored LOH of *BAP1* (NRM^{LOH+}). The remaining 29 UMs were heterozygous for *BAP1* (NRM^{LOH-}).

NRM^{LOH-} tumors were enriched for gain of chromosome 6p (52 %) and 8q (31 %), and loss of chromosome 6q (17 %). Moreover, ten of the 29 patients with NRM^{LOH-} UMs lacked any large CNV (>1Mb) in the tumor. In the TCGA dataset no mutation in *BAP1*, *SF3B1* and *EIF1AX* were reported in 29 UMs. Fourteen of these UMs were classified as NRM^{LOH+} and fifteen as NRM^{LOH-}. The NRM^{LOH-} UMs - similar to the ROMS data - were characterized by partial chromosome 6p (80%) and chromosome 8 gain (33%).

As for the NRM^{LOH+} UMs, these cases were enriched for monosomy 3 and chromosome 8q gain with 8p loss and also chromosome 6p gain with 6q loss, very similar to BAP1^{neg} UMs in our cohort. For most cases in our cohort with LOH of *BAP1*, the coding exons were sequenced. In ten of the sixteen UMs, a mutation was observed despite the presence of protein expression. This positive BAP1 expression can largely be explained by the fact that four of the mutations were missense mutations and three were frameshift mutations at the C-terminus. For the remaining three mutations, which consisted of one nonsense mutation and two splice site mutations, Western blotting should be performed to explain the positive BAP1 IHC. Six UMs were wildtype for *BAP1*, however, four of these samples were polyploid and contained an isodisomic chromosome 3 pair, which explains the LOH of *BAP1*.[24] Similarly, UMs in the TCGA dataset that were wildtype for *BAP1*, *SF3B1* and *EIF1AX*, but with LOH of *BAP1*, harbored the same

chromosomal aberrations as *BAP1*-mutated UMs suggesting that UMs with LOH of *BAP1*, still might harbor mutations which are not detected by WES.

Minor groups were defined by co-occurring mutations in *BAP1*, *SF3B1* and *EIF1AX*. Our cohort lacked any BAP1 negative UMs with *SF3B1* mutations, whereas the TCGA dataset did not contain *BAP1* and *EIF1AX* co-mutations. Since the numbers per minor groups were too small, we could not draw conclusions based on recurring CNVs (Supplementary Figure 4).

All together, these analyses revealed that *BAP1*, *SF3B1* and *EIF1AX*-mutated UMs harbor specific chromosomal patterns. A similar association of specific mutations with chromosomal anomalies was seen in the independent cohort. More specific *BAP1* deficient UMs harbored entire chromosome or chromosome arm CNVs, whereas *SF3B1*^{mut} UMs harbored partial chromosome arm CNVs.

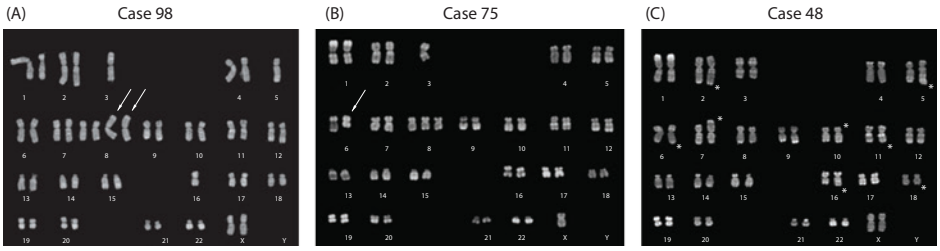

Figure 4. Cytogenetic data (reverse banded karyograms) illustrating the distinct chromosomal changes in the *BAP1* or *SF3B1*-mutated uveal melanoma (UM). A: Karyogram of a typical BAP1 negative UM (Case 98) shows monosomy 3 with 2x isochromosome 8q. B: Karyogram of an atypical BAP1 negative UM (Case 75) with monosomy 3, an isochromosome 6p and gain of chromosome 8. C: Karyogram of a typical *SF3B1*-mutated UM (Case 48) displaying multiple structural anomalies[29]. Arrow indicates isochromosomes. Asterisk indicates structural chromosomal changes.

Aneuploidy in *BAP1*, *SF3B1* and *EIF1AX*-mutated UM

Since we observed that BAP1^{neg} UMs contain entire chromosome or chromosome arm CNVs, and *SF3B1*^{mut} UMs smaller partial chromosome CNVs, we hypothesized that BAP1^{neg} UMs contain more aneuploidy. The total amount of aneuploidy of the genome (percentage) per tumor and the total number of CN events per tumor were calculated. Sex chromosomes were excluded to prevent gender-bias. Also, polyploid UMs were excluded to prevent biases since polyploid UMs are known to have multiple CNVs.[24]

The median percentage of aneuploidy in BAP1^{neg} tumors was 11.8 % of the genome and the median CN event was 11 events as measured by Nexus Copy Number software (Figure 3A and 3B). The median percentage of aneuploidy in *SF3B1*^{mut} tumors was 9.3 % of the genome and the median CN events was 14.5 events. BAP1^{neg} tumors are more aneuploidy than *SF3B1*^{mut} tumors ($P = 0.024$) however had less CN events than *SF3B1*^{mut} tumors ($P = 0.074$), although the latter did not reach significance.

The median percentage of aneuploidy in *EIF1AX*^{mut} tumors was 1.7 % of the genome and the median CN events was 5 events. *EIF1AX*^{mut} tumors had significantly less CN variations of the genome than BAP1^{neg} tumors and *SF3B1*^{mut} ($P < 0.001$ for both) and also less CN events ($P < 0.001$ for both). The median percentage of aneuploidy in NRM^{LOH-} tumors was 4.3 % of the genome and the median CN events was 7 events. Aneuploidy of the genome was lower than in BAP1^{neg} and *SF3B1*^{mut} UM ($P < 0.001$ and $P = 0.001$, respectively) but not significantly different from *EIF1AX*^{mut} UM ($P = 0.846$). BAP1^{neg} and *SF3B1*^{mut} UM had more CN events than NRM^{LOH-} UM ($P = 0.011$ and $P = 0.001$, respectively).

To validate these findings, the TCGA data was also analyzed for aneuploidy. Comparison between the numbers of CN events could not be performed as the curated TCGA SNP-array data contained segmented data, in which one CN event was annotated as several fragments. In the TCGA dataset, the median percentage aneuploidy of the entire genome was 17.2 % in *BAP1*^{mut} UM; 10.6 % in *SF3B1*^{mut} UM; 2.1 % in *EIF1AX*^{mut} UM; and 9.8 % in NRM^{LOH-} UM as illustrated in Figure 3C. *BAP1*^{mut} UMs had more aneuploidy than *SF3B1*^{mut} and *EIF1AX*^{mut} UMs ($P = 0.002$ and $P < 0.001$, respectively), whereas *EIF1AX*^{mut} UMs had less aneuploidy compared to the other groups ($P = 0.001$ for *SF3B1*^{mut} and $P = 0.052$ for NRM^{LOH-}). Although the percentages aneuploidy were higher in the TCGA dataset, the results were still comparable to our cohort. *BAP1*^{mut} UM harbored the largest CNVs, followed by *SF3B1*^{mut} UM and NRM^{LOH-}. *EIF1AX*^{mut} UM were characterized by lack of CNVs.

These findings show that *BAP1*^{mut} UMs contain larger CNVs of entire chromosome and chromosome arms, whereas *SF3B1*^{mut} UMs are characterized by a greater frequency of smaller CNVs events. *EIF1AX*^{mut} UMs on the other hand are characterized by the lack of CNVs.

Conventional karyotyping shows different type of chromosomal anomalies

To investigate whether the type of aneuploidy differs between the distinct groups, isochromosome formation and chromosomal structural variants (CSVs) were analyzed in UM cases for which karyotyping and mutation status were available. The discovery set consisted of 64 karyotypes. The cases in which the mutation status was not known, were used as a validation cohort (validation set; $n = 49$).

Isochromosomes were observed in 74 % of the BAP1^{neg} tumors ($n = 25/34$), of which 19 had an isochromosome 8q. Two tumors also harbored an isochromosome 6p besides 8q, and one tumor harbored an isochromosome 1q and 8q. Two tumors only had an isochromosome 6p and one harbored an isochromosome 2q. In the *SF3B1*^{mut} ($n = 12$) and *EIF1AX*^{mut} ($n = 6$) UMs, no isochromosomes were observed. One sample harbored an *SF3B1* and an *EIF1AX* mutation. This tumor also did not have any isochromosomes. In the tumors that were classified NRM ($n = 11$), four had an isochromosome. For these four UMs, the coding exons of *BAP1* were analyzed for the presence of any mutations. Two tumors had a mutation in *BAP1*, whereas the other two did not contain any mutations in the coding exons of *BAP1*. Moreover, the latter two also displayed a polyploid genome.

Of all cases with isochromosomes 93% were BAP1 negative tumors and the rest were polyploid NRM UMs. Isochromosomes were completely absent in UMs harboring *SF3B1* and/or *EIF1AX* mutations (Chi-square; $P < 0.001$).

Besides isochromosomes, we also investigated CSVs. Translocations or partial chromosome arm CNVs were categorized as CSVs. The mean number of CSVs was 1.06 variants per tumor in BAP1^{neg} UM, 4.67 in *SF3B1*^{mut} UM and 1.5 in *EIF1AX*^{mut} UM. The median CSVs in the NRM tumors was also 1.5 variants per tumor. Although cases were limited, *SF3B1*^{mut} UMs associated strongly with more than three CSVs per tumor compared to BAP1^{neg} ($P = 0.002$; Figure 3D). Moreover, 70% of the UMs with more than 3 CSVs harbored *SF3B1* mutations.

To validate the hypothesis that isochromosomes mainly occur in the tumors with a *BAP1* deficiency, and that multiple CSVs (more than three) occur mainly in *SF3B1*^{mut} tumors we selected cases from the cytogenetic karyotyped cohort in which the mutational status was not known (Supplementary Table 1). Since isochromosome 8q with

monosomy 3 strongly associated with BAP1^{neg} UMs, we only selected those cases with isochromosome formation of other chromosomes besides chromosome 8q. To analyze whether isochromosome formation in general is associated with deficient BAP1 these cases were tested for BAP1 expression with IHC. Tumors that had more than three CSVs were additionally stained for BAP1 and tested for the presence of *SF3B1* mutations.

In the validation set, nine UMs had an isochromosome other than or besides isochromosome 8q (Supplementary Table 1). From these nine UMs, two samples were not available for BAP1 IHC. Five of the remaining seven tumors were negative for BAP1, whereas two did express BAP1. One tumor was sequenced for *BAP1* since BAP1 IHC could not be performed in this sample. This tumor harbored a nonsense mutation at p.Q253. Interestingly, the samples from the discovery set and validation set which contained isochromosomes with BAP1 expression but without *BAP1* mutations suggests that similar pathways are involved that give rise to this specific type of aneuploidy. For the validation of multiple CSVs, seven UMs displayed more than three CSVs. For two cases, no material was available for mutational analyses. Of the remaining five tumors, four harbored a hotspot p.R625 *SF3B1* mutation.

These analyses showed that the majority of UMs with isochromosomes besides chromosome 8q are *BAP1* deficient and that UMs with multiple CSVs are mainly *SF3B1*-mutated (Figure 4). Strikingly, the same chromosomes are affected in *BAP1* deficient UMs and *SF3B1*-mutated UMs by either isochromosome formation or CSVs. This highlights a biological difference between these UMs, suggesting that different pathways might be involved that give rise to the same CNV event.

Mutational signatures

To get insight into the biological processes that generate the mutations in UM, we compared the somatic mutational signatures in UM with somatic mutational signatures as described by Alexandrov et al.[33] In this landmark study, they constructed 21 validated signatures based on single nucleotide mutations and its trinucleotide context. These signatures can be directly connected to the DNA damage and repair pathways among other processes and risk factors in cancer.[33, 34] We constructed somatic mutational spectra using the TCGA WES dataset, as our ROMS cohort did not contain tumor-normal matched WES data. The total number of somatic single nucleotide mutations detected

in the WES data ranged from 8 to 28 mutations per patient, with one outlier that harbored 578 mutations. Since the numbers of mutations per sample are limited we grouped the samples according to their mutational status of *BAP1*, *SF3B1* and *EIF1AX* and estimated the contribution of each signature to the three mutational spectra.

In general, all three groups displayed similar mutational spectra due to enrichment of specific somatic mutations in their trinucleotide context (Supplementary Figure 5). These specific mutations can be explained by the recurrent UM mutations that code for amino acid changes in the UM recurrent genes. *BAP1*-mutated were enriched for CTG>CAG mutations, which were mainly *GNA11* p.Q209L amino acid changes. When compared to the other groups, BAP1^{neg} IHC and *GNA11* p.Q209L amino acid changes co-occurred more often. Similarly *SF3B1*^{mut} tumors harbored more often *GNAQ* p.Q209P amino acid changes. *SF3B1*^{mut} UMs were also enriched for ACG>ATG and CCG>CTG mutations, which could be explained by the recurring hotspot mutations in *SF3B1*. UMs with solely *SF3B1*^{mut} harbored in 87 % (13/15) a p.R625H or p.R625C amino acids changes in *SF3B1*. *EIF1AX*^{mut} UMs had more often ACC>ATC mutations which could be explained by the recurring p.G6D, p.G9D and p.G15D amino acid changes in *EIF1AX*.

The relative contribution of the mutational signatures were identified for the groups with *BAP1*, *SF3B1* and *EIF1AX* mutations, respectively (Figure 5). Both Signature 1 and 5 are clock-like signatures and reflect the high median age when the enucleation of the primary UM tumor is commonly conducted.[33] Notably, in *SF3B1*^{mut} UMs Signature 5 was not detected and as reported before, patients with *SF3B1*^{mut} UMs are in general younger than patients with *BAP1*-mutated UMs.[19] Signature 16 contributed only to the signature of the *BAP1*-mutated UMs. Although the etiology is unknown, Signature 16 has been found in liver cancer, the organ that is affected in almost all metastasized patients with *BAP1* mutations. More than in the other groups, Signature 3 was found in *SF3B1*^{mut} UMs. Strikingly, Signature 3 has been strongly associated to *BRCA1* and *BRCA2* mutations. Therefore, the proposed etiology is defective DNA double-strand break-repair by homologous recombination. This might explain the multiple CSVs found in *SF3B1*mut UMs. A large proportion of *BAP1* mutations and to a lesser extent the *SF3B1*^{mut} were explained by Signature 6 and 15. Both signatures are usually observed together and are associated with DNA mismatch repair. In the *EIF1AX*^{mut} UMs only, both Signature 15 and the clock-like Signature 5, contributed substantially to their mutational phenotype. Moreover, a small number of mutations

are explained by Signature 4 , a mutational signature that is associated with smoking. However, Signature 7 that is associated with UV damage and is prominent in cutaneous melanoma was not detected in these samples.

The somatic signatures analysis revealed that different pathways may be involved in the initiation and progression of UMs, which is reflected by different single nucleotide mutations within their trinucleotide context. All UMs groups contained signatures involved in DNA mismatch repair, whereas defective homologous repair was most prominent in *SF3B1*^{mut} UMs and was not detected in *EIF1AX*^{mut} UMs. Validation could not be performed since other independent cohorts with mutational signature analyses did not contain samples from each mutational group.[13, 20]

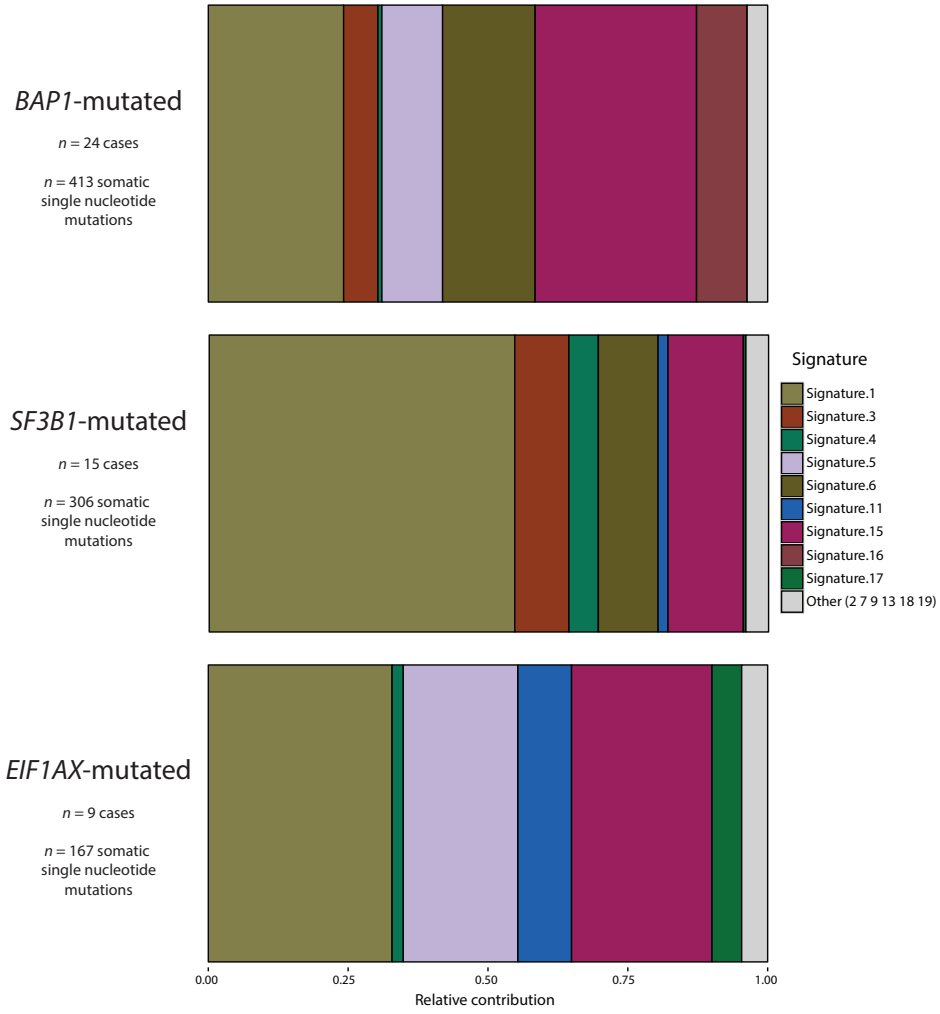

Figure 5. Relative contribution of mutational signatures detected in Whole Exome Sequencing data from TCGA uveal melanoma cohort. The signatures[33] are stratified by recurrent mutated genes *BAP1, SF3B1* and *EIF1AX* in uveal melanoma indicated with number of cases and number of total somatic single nucleotide mutations (*n*).

Discussion

Uveal melanoma is a malignancy characterized by non-random recurring chromosomal aberrations and recurrent mutated genes. Previous studies have shown that patients with either *BAP1*, *SF3B1* or *EIF1AX* mutations in their tumor have a diverse risk of metastatic disease.[19, 21] In this study, we show that UMs with different mutated genes also have a distinct chromosomal patterns with different types of chromosomal aberrations.

By unsupervised hierarchical clustering, UMs with the same mutated gene clustered predominantly together (Figure 1). The two major clusters were separated based on monosomy 3 and disomy 3 together with chromosome 8q. Disomy 3 was observed with partial chromosome 8q gain whereas monosomy 3 was more frequently observed with gain of entire chromosome 8q. Trolet et al. also described this difference in chromosome 8q gain based on chromosome 3.[4] Similar to our analyses, Trolet et al. found two major clusters based on chromosome 3. Within their disomy 3 cluster, one of the two sub-clusters was characterized by chromosome 6p gain, as our cluster 1a. The other disomy 3 cluster was characterized by 6p gain with 6q loss and 8q gain as observed in our cluster 1c. The breakpoint of chromosome 8q in disomy 3 UMs was at chromosome band 8q21, also comparable to our findings (Figure 2).[4] In contrast to others, the sub-clustering in monosomy 3 UMs was based on chromosome 6q and not chromosome 8q.[4, 35] In the hierarchical clustering chromosome 6q was represented more often (Figure 1A), and this weighed more than chromosome 8q gain. Although this sub-clustering based on chromosome 6q seems to be technical rather than biological, it still provided clusters which were homogenous and correlated to the mutational status of the UM. Polyploidy was the major cause of misplacement in other clusters, and should therefore always be checked in case of UM prognosticating based on the chromosomal aberrations.

Since the unsupervised hierarchal clustering showed clear correlations between chromosomal patterns and mutational status, we performed supervised clustering with the known mutational status. In this current study, different techniques were used to analyze the *BAP1* status. In our ROMS cohort, we used predominantly BAP1 IHC whereas in the TCGA cohort, *BAP1* was analyzed by WES. This should not make a difference in comparing both groups, as we and others have shown a strong association between the lack of BAP1 IHC staining and the presence of *BAP1* mutations.[16,

[36] When comparing both groups all affected chromosomes were the same, however the absolute numbers CNVs of these chromosomes were more frequent in the TCGA set. As shown in Figure 1A and 1B, some BAP1^{neg} UMs harbored no CNVs in the entire genome, which can explain the decreased cumulative frequency of CNVs in the ROMS cohort. BAP1^{neg} tumors are associated with the loss of chromosome 3 and gain of chromosome 8q, which has been described by our group and others.[14-16, 36-38] Also chromosome 1p loss, 6q gain, 8p loss and 16q occurred frequently. These CNVs have been correlated to monosomy 3 UMs before. [3-6, 35, 39, 40] Surprisingly, also chromosome 6p gain was observed in both datasets, as chromosome 6p gain is inversely associated to monosomy 3.[5, 7, 39, 41] Moreover, when investigated with cytogenetic data, these chromosome 6p gains were due to isochromosome 6p formation.

SF3B1 mutations, on the other hand, have been associated to chromosome 6p gain.[17-19] In the clustered overview, other CNVs were also observed such as chromosome 1p loss, 6q loss, 8p loss, 8q gain and 11q loss. In general, CNV frequencies were similar in those in the TCGA cohort, except for chromosome 11q loss which was almost completely absent in the TCGA data. Unfortunately, the unprocessed TCGA SNP array data was not available to be processed exactly as our SNP arrays. Thus, we cannot exclude that perhaps e.g. different threshold settings for segmentation or the content of the SNP array could explain this difference for chromosome 11q CNVs. Strikingly, in case of *SF3B1*^{mut} UMs, recurrent chromosome breakpoints were observed, in contrast to BAP1^{neg} UMs, which almost exclusively had entire chromosomes or chromosome arm CNVs. Translocations with recurring breakpoints in combination with disomy 3 are described more often,[42, 43] however, never associated with *SF3B1* mutations.

For *EIF1AX*^{mut} UM, the characteristic feature of the CNVs was the overall lack of CNVs or only partial chromosome 6p or entire chromosome 6 gain. Similar to *EIF1AX*^{mut} UMs, also NRM^{LOH-} UMs harbored these CNVs. This suggests that these type of UMs are relatively stable, which could be a protective factor in the metastatic process.

UMs that were BAP1 positive and wildtype for *SF3B1* and *EIF1AX* were treated as a heterogeneous group. Moreover, NRM UMs with LOH of *BAP1* harbored the same CNVs as BAP1^{neg} UMs, and NRM UMs without LOH of *BAP1* were more similar to *EIF1AX*^{mut} UMs. As expected subsequential analyses of *BAP1* for the NRM^{LOH+} UMs revealed mutations in most of them. Also for the TCGA data, cases without *BAP1* mutations with LOH were excluded. RNA expression was analyzed in these samples,

and this showed a low RNA expression similar to UMs with *BAP1* mutations (data not shown). We expect that these UMs might harbor *BAP1* mutations which are not easily detected by Whole Exome Sequencing.[36]

Besides the chromosomal patterns, also the aneuploidy and number of CN events per tumor were analyzed for each group. This revealed that *BAP1* deficient UMs harbored the largest CNVs, whereas *SF3B1*^{mut} UMs harbored the highest number of CN events, suggesting that different pathways are involved causing these genome rearrangements.

This was confirmed by analyzing conventional cytogenetic data. Monosomy 3 has been correlated to isochromosome 8q before, and we confirmed this in our study.[6, 39, 41] Besides isochromosome 8q, we also observed other isochromosomes in *BAP1* deficient UMs. This finding warrants future studies to investigate whether BAP1^{neg} UM cells have a deficiency in pathways involving the separation of chromosomes during metaphase.

By analyzing the cytogenetic data, we confirmed that *SF3B1*^{mut} UMs have in absolute numbers the most CN events. These CN events consisted of CNVs such as translocations and partial chromosome losses. *SF3B1* and *BAP1* are both involved in DNA double-strand break damage response.[22, 23] Since, the non-homologous end-joining repair pathways play a large role in chromosomal translocation,[44] it is likely that *SF3B-1*^{mut} UMs make use of these pathways. This would be of interest in the treatment of metastasized UMs, since deficiencies in DNA double-strand break repair can serve as a targetable therapy in malignancies.[45]

Somatic mutational signatures in other malignancies showed to be strongly associated with several cellular pathways and risk factors in cancer.[33] In WES data of UMs only a limited number of mutations were observed.[13, 20] Since single UMs did not contain more than 30 somatic mutations, we therefore analyzed UMs with the same mutated gene (*BAP1*, *SF3B1* and *EIF1AX*) as a cumulative group. Using the Whole Genome Sequencing (WGS) data would have been more appropriate . Unfortunately, WGS performed by Furney et al. and Johansson et al. did not contain enough *SF3B1*^{mut} UMs to compare the *BAP1*-mutated and *EIF1AX*^{mut} UMs. With the somatic mutational signature analyses of the WES data we showed that Signature 3 - which is associated with a homologous recombination deficiency - was more prominent in the signature

of *SF3B1*^{mut} UMs. Comparison between the signatures as constructed by Johansson et al. showed overlap for Signature 1, 3, 5 and 16 for *BAP1*-mutated UMs. Somatic mutational signatures can be studied more robustly in a larger cohort of patients with UMs and with using WGS data.

In conclusion, we show that patients with UM can be divided in molecular subclasses based on chromosomal patterns, and above all these groups correspond to the *BAP1*, *SF3B1* and *EIF1AX* mutational status. More importantly, we previously reported that the survival in patients with UM can be stratified based on mutation status. Here we have shown that each group is characterized by recurring CNVs. Also, these three subtypes of UMs harbor different type of chromosomal aberrations indicating that different pathways are involved in the etiology of UM development and progression towards metastatic disease. The exact nature of these pathways and the genes involved, remain elusive but will be important to develop the most optimal targeted therapy solution for the individual UM patients.

References

1. Kujala E, Makitie T, Kivela T. Very long-term prognosis of patients with malignant uveal melanoma. Invest Ophthalmol Vis Sci 2003;44:4651-9.
2. Cassoux N, Rodrigues MJ, Plancher C, et al. Genome-wide profiling is a clinically relevant and affordable prognostic test in posterior uveal melanoma. Br J Ophthalmol 2014;98:769-74.
3. Damato B, Dopierala JA, Coupland SE. Genotypic profiling of 452 choroidal melanomas with multiplex ligation-dependent probe amplification. Clin Cancer Res 2010;16:6083-92.
4. Trolet J, Hupe P, Huon I, et al. Genomic profiling and identification of high-risk uveal melanoma by array CGH analysis of primary tumors and liver metastases. Invest Ophthalmol Vis Sci 2009;50:2572-80.
5. Prescher G, Bornfeld N, Hirche H, et al. Prognostic implications of monosomy 3 in uveal melanoma. Lancet 1996;347:1222-5.
6. White VA, Chambers JD, Courtright PD, et al. Correlation of cytogenetic abnormalities with the outcome of patients with uveal melanoma. Cancer 1998;83:354-9.
7. Prescher G, Bornfeld N, Becher R. Nonrandom chromosomal abnormalities in primary uveal melanoma. J Natl Cancer Inst 1990;82:1765-9.
8. Dono M, Angelini G, Cecconi M, et al. Mutation frequencies of *GNAQ*, *GNA11*, *BAP1*, *SF3B1*, *EIF1AX* and *TERT* in uveal melanoma: detection of an activating mutation in the *TERT* gene promoter in a single case of uveal melanoma. Br J Cancer 2014;110:1058-65.
9. Koopmans AE, Vaarwater J, Paridaens D, et al. Patient survival in uveal melanoma is not affected by oncogenic mutations in *GNAQ* and *GNA11*. Br J Cancer 2013;109:493-6.
10. Van Raamsdonk CD, Bezrookove V, Green G, et al. Frequent somatic mutations of *GNAQ* in uveal melanoma and blue naevi. Nature 2009;457:599-602.
11. Van Raamsdonk CD, Griewank KG, Crosby MB, et al. Mutations in *GNA11* in uveal melanoma. N Engl J Med 2010;363:2191-9.
12. Moore AR, Ceraudo E, Sher JJ, et al. Recurrent activating mutations of G-protein-coupled receptor *CYSLTR2* in uveal melanoma. Nat Genet 2016. *In press*.
13. Johansson P, Aoude LG, Wadt K, et al. Deep sequencing of uveal melanoma identifies a recurrent mutation in PLCB4. Oncotarget 2016;7:4624-31.
14. Harbour JW, Onken MD, Roberson ED, et al. Frequent mutation of *BAP1* in metastasizing uveal melanomas. Science 2010;330:1410-3.
15. Kalirai H, Dodson A, Faqir S, et al. Lack of BAP1 protein expression in uveal melanoma is associated with increased metastatic risk and has utility in routine prognostic testing. Br J Cancer 2014;111:1373-80.
16. Koopmans AE, Verdijk RM, Brouwer RW, et al. Clinical significance of immunohistochemistry for detection of *BAP1* mutations in uveal melanoma. Mod Pathol 2014;27:1321-30.
17. Harbour JW, Roberson ED, Anbunathan H, et al. Recurrent mutations at codon 625 of the splicing factor *SF3B1* in uveal melanoma. Nat Genet 2013;45:133-5.
18. Martin M, Masshofer L, Temming P, et al. Exome sequencing identifies recurrent somatic mutations in *EIF1AX* and *SF3B1* in uveal melanoma with disomy 3. Nat Genet 2013;45:933-6.
19. Yavuzyigitoglu S, Koopmans AE, Verdijk RM, et al. Uveal Melanomas with *SF3B1* Mutations: A Distinct Subclass Associated with Late-Onset Metastases. Ophthalmology 2016;123:1118-28.
20. Furney SJ, Pedersen M, Gentien D, et al. *SF3B1* mutations are associated with alternative splicing in uveal melanoma. Cancer Discov 2013;3:1122-9.
21. Decatur CL, Ong E, Garg N, et al. Driver Mutations in Uveal Melanoma: Associations With Gene Expression Profile and Patient Outcomes. JAMA Ophthalmol 2016. *In press*.
22. Te Raa GD, Derks IA, Navrkalova V, et al. The impact of *SF3B1* mutations in CLL on the DNA-damage response. Leukemia 2015;29:1133-42.
23. Yu H, Pak H, Hammond-Martel I, et al. Tumor suppressor and deubiquitinase BAP1 promotes DNA double-strand break repair. Proc Natl Acad Sci U S A 2014;111:285-90.
24. Yavuzyigitoglu S, Mensink HW, Smit KN, et al. Metastatic Disease in Polyploid Uveal Melanoma Patients Is Associated With *BAP1* Mutations. Invest Ophthalmol Vis Sci 2016;57:2232-9.
25. van de Wiel MA, Brosens R, Eilers PH, et al. Smoothing waves in array CGH tumor profiles.

Bioinformatics 2009;25:1099-104.
26. van de Wiel MA, Kim KI, Vosse SJ, et al. CGHcall: calling aberrations for array CGH tumor profiles. Bioinformatics 2007;23:892-4.
27. Van Wieringen WN, Van De Wiel MA, Ylstra B. Weighted clustering of called array CGH data. Biostatistics 2008;9:484-500.
28. ISCN (2016): An International System of Human Cytogenetic Nomenclature. Basel: S. Karger, 2016.
29. Naus NC, van Drunen E, de Klein A, et al. Characterization of complex chromosomal abnormalities in uveal melanoma by fluorescence in situ hybridization, spectral karyotyping, and comparative genomic hybridization. Genes Chromosomes Cancer 2001;30:267-73.
30. Kilic E, van Gils W, Lodder E, et al. Clinical and cytogenetic analyses in uveal melanoma. Invest Ophthalmol Vis Sci 2006;47:3703-7.
31. Gehring JS, Fischer B, Lawrence M, Huber W. SomaticSignatures: inferring mutational signatures from single-nucleotide variants. Bioinformatics 2015;31:3673-5.
32. Gentleman RC, Carey VJ, Bates DM, et al. Bioconductor: open software development for computational biology and bioinformatics. Genome Biol 2004;5:R80.
33. Alexandrov LB, Nik-Zainal S, Wedge DC, et al. Signatures of mutational processes in human cancer. Nature 2013;500:415-21.
34. Nik-Zainal S, Alexandrov LB, Wedge DC, et al. Mutational processes molding the genomes of 21 breast cancers. Cell 2012;149:979-93.
35. de Lange MJ, van Pelt SI, Versluis M, et al. Heterogeneity revealed by integrated genomic analysis uncovers a molecular switch in malignant uveal melanoma. Oncotarget 2015;6:37824-35.
36. van de Nes JA, Nelles J, Kreis S, et al. Comparing the Prognostic Value of *BAP1* Mutation Pattern, Chromosome 3 Status, and BAP1 Immunohistochemistry in Uveal Melanoma. Am J Surg Pathol 2016;40:796-805.
37. Ewens KG, Kanetsky PA, Richards-Yutz J, et al. Chromosome 3 status combined with *BAP1* and *EIF1AX* mutation profiles are associated with metastasis in uveal melanoma. Invest Ophthalmol Vis Sci 2014;55:5160-7.
38. van Essen TH, van Pelt SI, Versluis M, et al. Prognostic parameters in uveal melanoma and their association with BAP1 expression. Br J Ophthalmol 2014;98:1738-43.
39. Aalto Y, Eriksson L, Seregard S, et al. Concomitant loss of chromosome 3 and whole arm losses and gains of chromosome 1, 6, or 8 in metastasizing primary uveal melanoma. Invest Ophthalmol Vis Sci 2001;42:313-7.
40. Kilic E, Naus NC, van Gils W, et al. Concurrent loss of chromosome arm 1p and chromosome 3 predicts a decreased disease-free survival in uveal melanoma patients. Invest Ophthalmol Vis Sci 2005;46:2253-7.
41. Prescher G, Bornfeld N, Friedrichs W, et al. Cytogenetics of twelve cases of uveal melanoma and patterns of nonrandom anomalies and isochromosome formation. Cancer Genet Cytogenet 1995;80:40-6.
42. Hoglund M, Gisselsson D, Hansen GB, et al. Dissecting karyotypic patterns in malignant melanomas: temporal clustering of losses and gains in melanoma karyotypic evolution. Int J Cancer 2004;108:57-65.
43. Sisley K, Tattersall N, Dyson M, et al. Multiplex fluorescence in situ hybridization identifies novel rearrangements of chromosomes 6, 15, and 18 in primary uveal melanoma. Exp Eye Res 2006;83:554-9.
44. Bohlander SK, Kakadia PM. DNA Repair and Chromosomal Translocations. Recent Results Cancer Res 2015;200:1-37.
45. Srivastava M, Raghavan SC. DNA double-strand break repair inhibitors as cancer therapeutics. Chem Biol 2015;22:17-29.

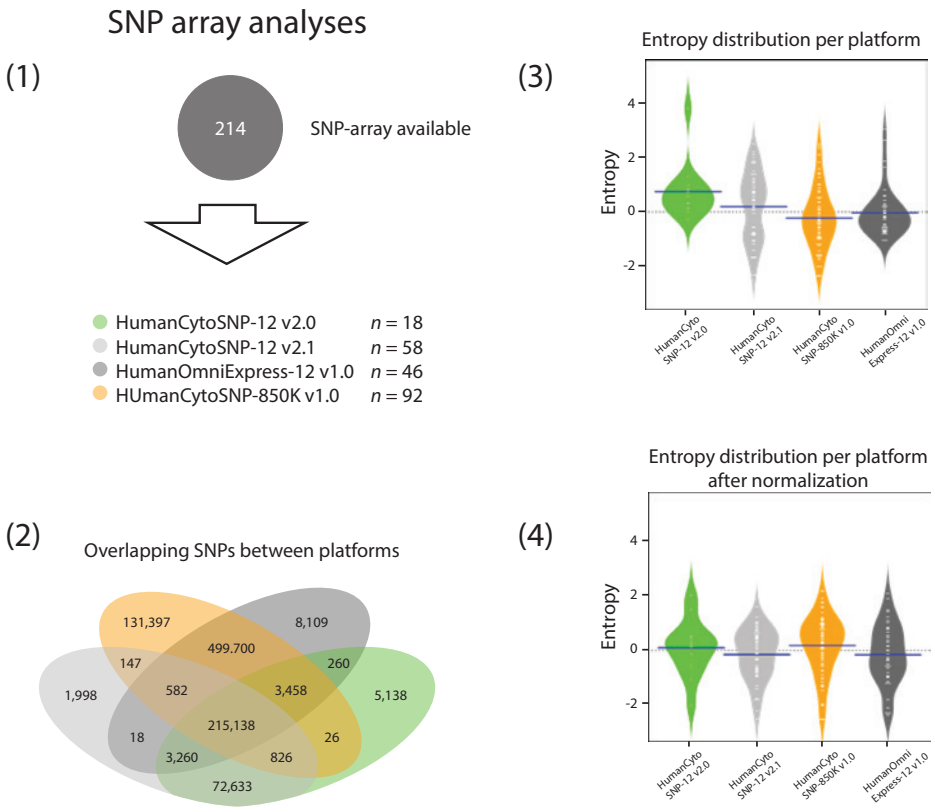

Supplementary Figure 1. Overview of the single nucleotide polymorphism (SNP) array analyses used for hierarchical clustering. (1) The distribution of the four SNP array types which were used in the analyses. (2) Venn-diagram depicting the overlap in SNPs. (3) The distribution of all samples clustered by the array type measured in entropy count. (3) The distribution of entropy after normalization of the data.

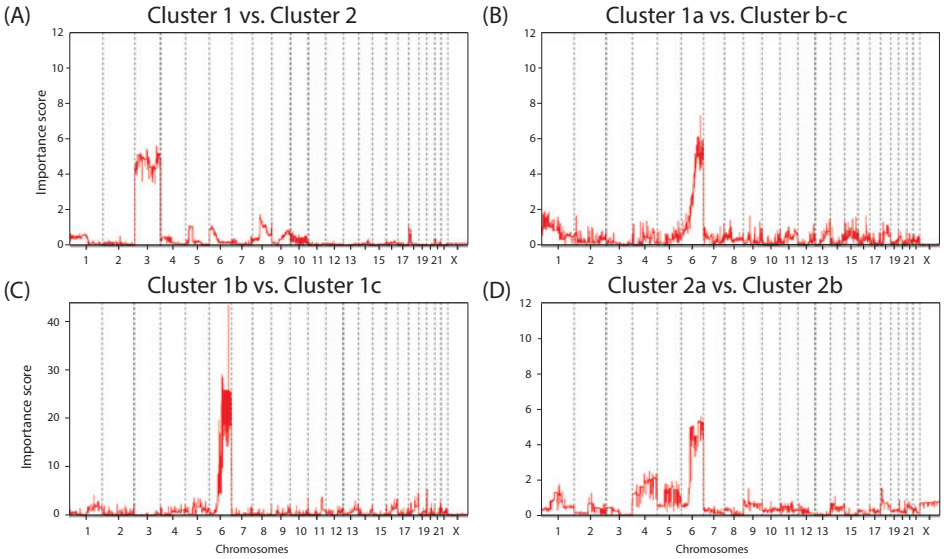

Supplementary Figure 2. Graphs depicting discriminating copy number (CN) variations between clusters. A higher importance score corresponds to a higher discriminating value of copy number variations (CNV) between clusters. (A-D) Graphs for the several cluster comparisons.

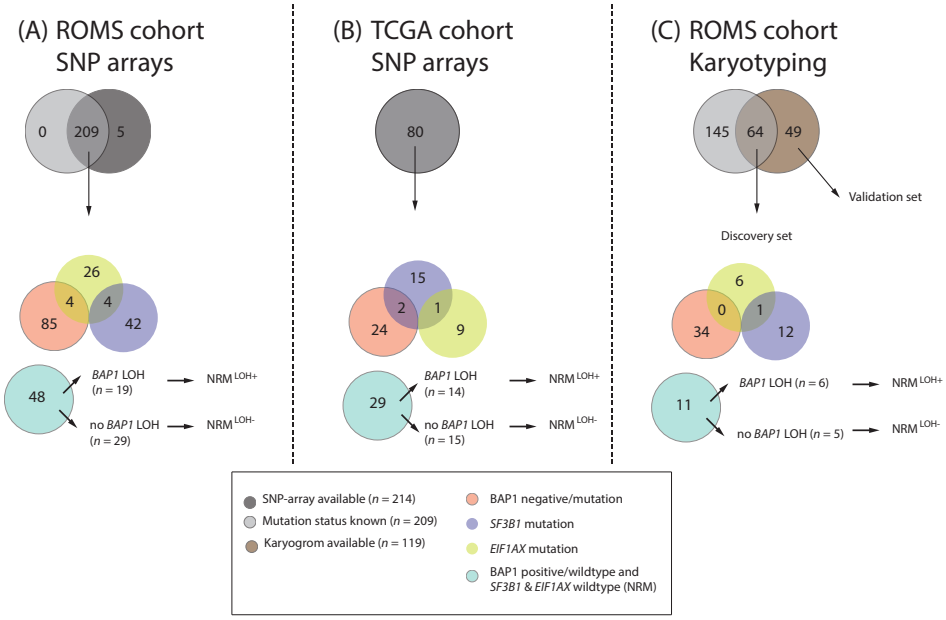

Supplementary Figure 3. Venn-diagrams depicting the distribution of several mutational groups used in the different analyses. A: ROMS Uveal Melanoma (UM) cohort samples stratified for the presence of specific mutations used for SNP array clustering. B: idem for the Cancer Genome Atlas (TCGA) samples. C: ROMS UM samples used for cytogenetic stratification.

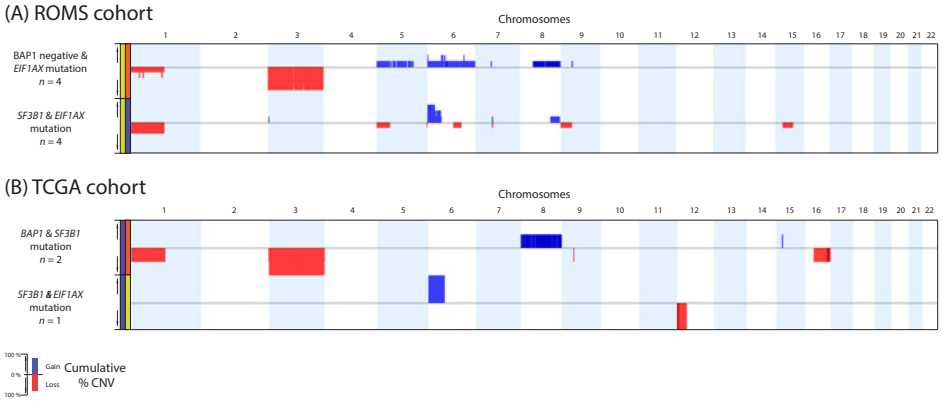

Supplementary Figure 4. Summary plots for the different minor groups of uveal melanomas (UMs). The chromosomes are depicted on the x-axis. The Y-axis shows the cumulative percentage of copy number variation per group. Dark blue indicates gain of chromosome and red indicated loss of chromosome. The sex-chromosomes are excluded.

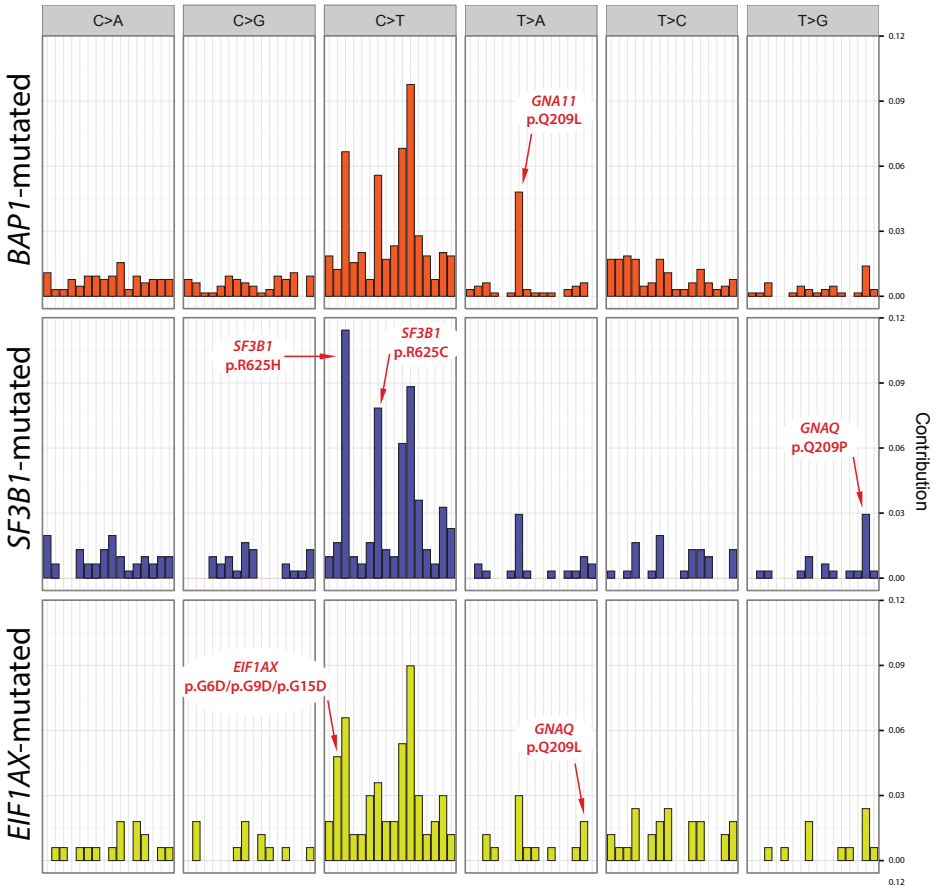

Supplementary Figure 5. Specific somatic mutations in their trinucleotide context obtained from Whole Exome Sequencing (WES) in *BAP1*-mutated (n=24), *SF3B1*-mutated (n=15)and *EIF1AX*-mutated (n=9) uveal melanomas (UMs) in the TCGA dataset.

Supplementary Table 1. Mutation analysis of samples from the validation set. UM cases with isochromosomes (top rows) or multiple chromosomal structural variants (CSVs) were tested.

Case #	Isochromosome(s)	BAP1 IHC	*BAP1*	*SF3B1*	*EIF1AX*
Cases with isochromosome(s)					
14	1q	positive	wildtype	wildtype	wildtype
20	6p, 8q	n.a.	p.Q253*	wildtype	wildtype
107	6p	negative	n.a.	n.a.	n.a.
110	6p, 8q	n.a.	n.a.	n.a.	n.a.
111	1q, 4q	negative	n.a.	n.a.	n.a.
124	5q, 6p, 22q	positive	wildtype	wildtype	wildtype
131	6p	negative	n.a.	n.a.	n.a.
132	6p, 8q	negative	n.a.	n.a.	n.a.
142	1q, 8q	negative	n.a.	n.a.	n.a.
Cases with more than three SVs					
92	none	positive	wildtype	p.R625H	wildtype
93	none	positive	n.a.	wildtype	wildtype
112	none	positive	n.a.	n.a.	n.a.
125	none	positive	n.a.	n.a.	n.a.
138	none	positive	wildtype	p.R625H	wildtype
143	none	positive	wildtype	p.R625H	wildtype
148	none	positive	wildtype	p.R625H	wildtype

n.a. = not available

Chapter 2.3

Metastatic disease in Uveal Melanoma patients in relation to tumor profile

Serdar Yavuzyigitoglu, Michael C.Y. Tang, Miguel Jansen, Kaspar Geul, Roy S. Dwarkasing, Natasha M. van Poppelen, Jolanda Vaarwater, Wojtek Drabarek, Robert M. Verdijk, Dion Paridaens, Nicole C. Naus, Annelies de Klein and Emine Kilic

Manuscript in preparation

Abstract

Purpose: This study reports the role played by the mutation status of the primary tumor in relation to hepatic tumor profiles found in metastasized uveal melanoma (UM).

Methods and materials: From 1983 until 2017, metastatic UM samples and radiological images were obtained from 100 patients treated at the Erasmus Medical Center Rotterdam or the Rotterdam Eye Hospital. Radiological images were derived from either computed tomography or magnetic resonance imaging. Mutation status was determined using immunohistochemistry, Sanger sequencing or ION Torrent. Analyses were performed using Pearson's chi-square test and Fischer's exact test for correlations. Log-rank test (Kaplan-Meier) was used for survival analyses.

Results: The mutation status of the primary tumor was not correlated with any hepatic tumor profiles (P = 0.296). Both the disease-free survival (DFS) and metastasized survival (MS) differed significantly from each of the tumor profiles (respectively, P = 0.032, P = 0.036). An overall trend was found for a shorter DFS and MS when livers harbored more lesions. However, only a significantly shorter DFS was found for the >10 lesion group compared to <10 lesions (P = 0.011). As well as a significantly different MS for the comparisons between: <5 lesions against >5 lesions and <10 lesions against >10 lesions (respectively, P = 0.027, P = 0.045).

Conclusion: Our study shows that there is an inverse correlation of the number of metastasis with the metastasized survival, indicating separate growth patterns. We also revealed that despite the lack of association between metastasis with the mutation status, loss of chromosome 8p was observed more frequently in livers containing more lesions.

Introduction

Uveal Melanoma (UM) is the most common intra-ocular malignancy in the Western World with an incidence of 5-6 per million per year.[1,2] UM derive from the melanocytes in the uveal tract which consists of the choroid, ciliary body and iris.[3] Treatment of the UM consists of radiotherapy, brachytherapy or enucleation. However in spite of excellent local tumor control, UM has a strong propensity to metastasize in up to 50% of the patients within 15 years after diagnosis.[4] Localization of these metastases can occur in the liver, pulmonary parenchyma, bone and skin. However, the liver is affected in more than 90% of the cases.[4]

UM are characterized by nonrandom cytogenetic aberrations and recurrent mutated genes that are associated with the patients' prognosis. The onset of metastatic UM is closely related to the presence of somatic mutations in the UM genes: *BAP1*, *SF3B1* and *EIF1AX*.[5] *BAP1*-mutated UM being classified as high risk with early metastases, *SF3B1*-mutated UM as intermediate risk with late-onset metastases and *EIF1AX*-mutated UM as low risk for metastases.[5] As for chromosomal changes, loss of chromosome 3 is most strongly correlated to metastatic disease together with the gain of chromosome 8q.[6,7] Other chromosomal aberrations that are associated with the worse prognosis include loss of chromosome 1p, 6q and 8p.[6,7] Chromosome 6p gain is associated with a favorable prognosis.[6,7]

The genetics of primary UM have been investigated intensively, however not much is known about the UM metastases (UM^{meta}). The liver is typically affected in metastasized UM, thus biopsies are not taken regularly to confirm the diagnosis of metastasis since findings on Computed Tomography (CT) scans and Magnetic Resonance Imaging (MRI) techniques suffice to make the diagnosis. Meir and colleagues investigated the expression of primary UM compared to matching metastases and showed that the expression of 193 genes differed between the primary and metastasized UM.[8] Moreover, the expression of the liver metastasis resembled normal liver tissue, although it was histopathologically shown that the investigated metastasis material did not contain liver tissue.[8] Looking at chromosomal aberrations in UM^{meta}, Trolet and colleagues showed that the majority of UM^{meta} harbor monosomy 3 with chromosome 8q gain.[7] However a smaller proportion of these tumors are disomy 3 with a gain of the terminal end of chromosome 8q.[7] As for the UM genes, loss of BAP1 expression and *BAP1* mutations were also shown to be frequently present in the majority of UM^{me-}

[ta].[9-11]*SF3B1* mutations in UM_{meta} were described in 40% in one study (2/5 UM^{meta}) and 4% in another study (1/26 UM^{meta}).[9,10]

Hepatic metastases can vary in size and pattern, from solitary lesions to a more disseminated or miliary pattern.[12] In this current study we set to analyze the difference in survival for the metastasis profiles and correlate these to clinical and genetic parameters of the primary UM.

Methods

Patient inclusion

All UM patients who were diagnosed with UM between 1983 and 2017 at the Erasmus University Medical Center and the Rotterdam Eye Hospital (Rotterdam, The Netherlands) were reviewed for metastatic disease. Iris melanoma were not included due to their aberrant metastatic behavior and different genetic etiology.[13] This study was performed retrospectively, in which we selected patients for whom CT or MRI images of the metastatic liver were available for analyses. This study was performed according to the tenets of the Declaration of Helsinki and after informed consent. The study was also approved by a local ethics committee.

Analyses of metastasis imaging

Classification of CT or MRI images were based on the total amount of hepatic metastases, resulting in the following groups: single nodular lesion, between two and five lesions, between six and ten lesions and more than ten lesions. Sub-analyses were performed on the group more than ten lesions, which we divided in more than ten large (>50 μm) lesions versus a miliary pattern (innumerable lesions of <50 μm). The first known and available CT or MRI images that confirmed hepatic metastases were used for analysis. Only CT and MRI images dating from 2003 and onwards were analyzed, because there were no digital images available before 2003. Also patients whom lacked available CT or MRI images, however still had well documented records of these images were included. Measurements of the CT or MRI images were taken manually with built-in measuring tools to determine the dimensions of hepatic metastases.

Material and mutation analyses

Whenever a patient was enucleated or a biopsy was taken, primary tumor material was available for genetic analyses. The mutation status of *GNAQ*, *GNA11*, *BAP1*, *SF3B1* and *EIF1AX* was determined using a combination of BAP1 immunohistochemistry (IHC), Sanger sequencing or sequencing using the ION Torrent Personal Genome Machine (Life Technologies, Carlsbad, CA, USA) as described before.[14] Single nucleotide polymorphism (SNP) arrays (Illumina HumanCytoSNP-12 v2.1 BeadChip and Illumina 610Q BeadChip; Illumina, San Diego, CA, USA) were used for detection of chromosomal aberrations. Nexus Copy Number 8.0 (BioDiscovery, Inc., El Segundo, CA, USA) was used to visualize the chromosomal patterns.

Statistical analysis

The disease-free survival (DFS) is defined as the first date of treatment till the development of metastatic UM. Survival with metastatic disease was not computed due to the difference in patient treatment after diagnosis of metastasis. Deaths due to other causes were censored. The survival analysis was generated using the Kaplan-Meier method and made use of the Log-Rank test to find differences between the groups for categorical variables. Cox proportional analyses were used for survival analyses of continuous variables. Multivariate analyses were performed using the Cox proportional regression analyses. Pearson's chi-square test or Fisher's exact test was used to test categorical groups with independent variables. Analysis of variance (ANOVA) was used to compare the means of multiple groups, while Fischer's least significant difference was used for post hoc testing. *P* values of 0.05 or less were considered significant. SPSS (version 24.0, IBM, Armonk, NY, USA) was used for all statistical analyses.

Results

A total of 197 patients with UM^{meta} were identified. The liver was affected in 191 patients (97%) and extra-hepatic metastases were found in 74 patients (38%) including six patients without hepatic UM metastases. CT or MRI images of the liver metastases were available for 77 patients. Another 21 patients were included which lacked available CT or MRI images, however still had well documented records of these images (including the number of metastases). Two patients with existing radiological records were excluded from analysis due to a lack of details concerning the number of metastatic lesions. The resulting 98 patients were included in the analyses.

From the included UM patients (n = 98; Table 1) a total of 64 underwent primary enucleation and 33 received stereotactic radiation therapy (SRT) of which nine underwent secondary enucleation due to local complications. One patient did not receive primary treatment. This patient was diagnosed with metastasis at the time of diagnoses and wished not to receive treatment of the primary tumor. Clinical, histopathological and genetic characteristics of the study population are summarized in Table 1. The study population comprised of 48 males and 50 females with a median age of 64 years at diagnoses of the primary UM (range, 37 - 87 years). The median DFS was 26.5 months (range, 0 - 159.6 months) and median survival with metastatic disease was 6.1 months (range, 0 – 42.3 months). Mutation status was known for 68 patients; 58 with loss of BAP1 expression, eight with an *SF3B1* mutation and one patient with an *EIF1AX* mutation in the primary UM. One patient was classified as 'No Recurrent Mutation' (NRM) since the tumor did not harbor a mutation in *BAP1*, *SF3B1*, or *BAP1*. For 30 patients the mutation status was unknown, due to lack of material of the primary tumor. Patients treated with SRT amassed the greatest share with 24 of the 30 unknown mutations. Six patients did not have hepatic metastasis, and as such they were not included in the analyses. The UM of these six patients comprised of: two UM with *BAP1* mutations and lack of BAP1 expression, two UM with positive BAP1 staining with disomy 3 (*SF3B1* and *EIF1AX* status unknown) and two patients with untested genetic status due to a lack of material.

Correlation with clinical and genetic features

Classification of CT or MRI images were based on the total amount of hepatic metastases, this resulted in the following groups: single nodular lesion (Figure 1A), between two and five lesions (Figure 1B), between six and ten lesions (Figure 1C) and more than ten lesions (Figure 1D).

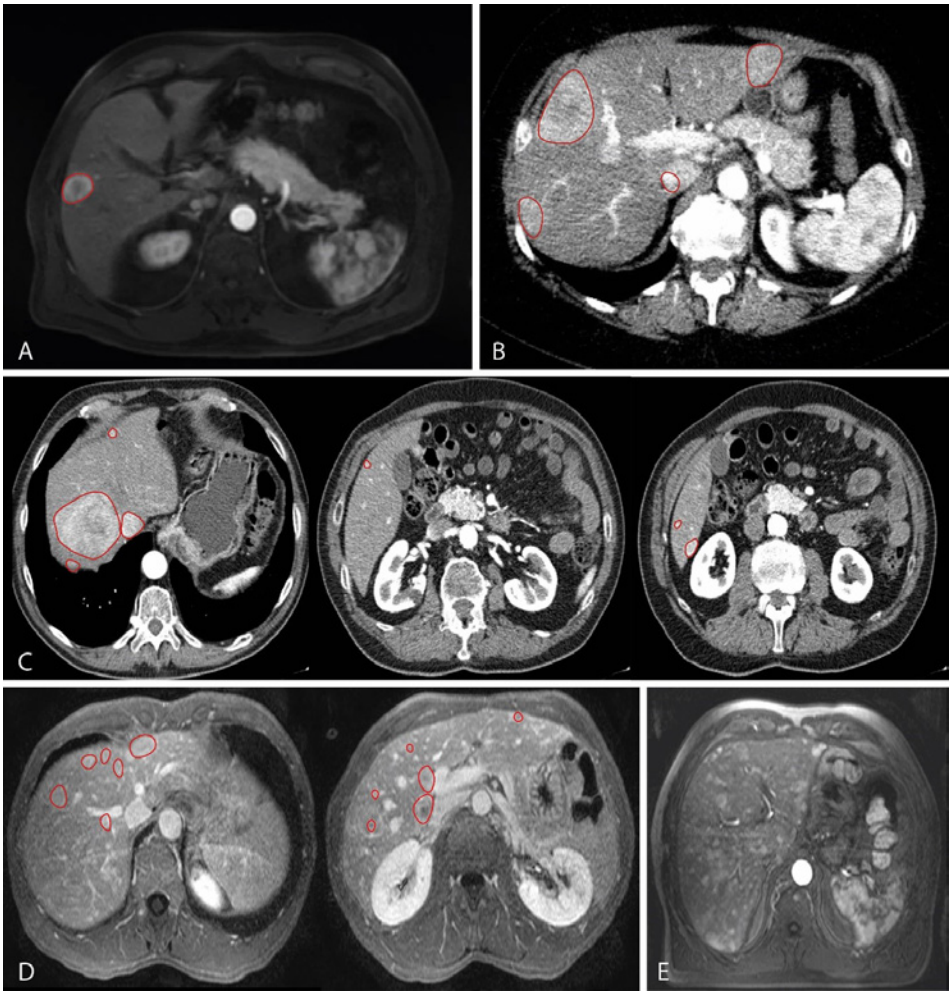

Figure 1. MRI images representing the classification based on the number of lesions found in metastatic UM in the liver, which have been contrasted by red markings. **A,** T1 weighted MRI with contrast showing a single nodular lesion in the liver. **B,** T2 weighted MRI with contrast showing four lesions. **C,** T2 weighted MRI sequence with contrast showing a total of seven lesions. Images from left to right correspond respectively from cranial to caudal localization. **D,** T2 weighted MRI sequence with contrast showing a total of twelve lesions. Images from left to right correspond respectively from cranial to caudal localization. **E,** T2 weighted MRI with contrast showing innumerable widespread small lesions throughout all liver segments. No red markings are present due to the number of lesions.

The age at diagnoses was the eldest in patients who developed solitary hepatic metastases, however a significant difference was not observed ($P = 0.738$). Mean largest basal diameter also did not differ between the metastases groups ($P = 0728$). A trend could be observed for tumor height of the primary UM, for which a larger tumor height of the

primary UM were to give more metastases, however no significance could be reached (P = 0.841). Also gender was equally divided between the groups (P = 0.776). BAP1 IHC, *SF3B1* and *EIF1AX* mutation status were not found to be significantly associated with any of the four different tumor profiles. (P = 0.976, P = 0.594 and P = 0.221, respectively). Although not significant, in patients with solitary lesions none of the primary tumors harbored *GNAQ* mutation whereas five of the six harbored a *GNA11* mutation. *GNAQ* and *GNA11* were divided equally for the other metastasis profiles (Table 1). We also looked at whether the presence of extrahepatic lesions was correlated to the number of hepatic metastases, however this was not the case (P = 0.875).

Table 1. Correlation between the number of metastatic lesions and Other Clinical, Histopathological, and Genetic Features

Variables	Metastasis profiles (number of metastases)				
	1 lesion (n = 14)	2-5 lesions (n = 28)	6-10 lesions (n = 15)	>10 lesions (n = 41)	P-value
Mean age (95% CI), yrs	64.6 (59-70)	61.8 (57-66)	64.3 (58-71)	64.4 (61-68)	0.738 *
Mean largest basal diameter (range), mm	10.0 (7-13)	10.3 (8-12)	8.1 (4-12)	9.4 (7-12)	0.728 *
Mean tumor height (range), mm	4.0 (2-6)	4.7 (3-6)	4.5 (2-7)	5.2 (3-7)	0.841 *
Gender, no. (%)					
Male	6 (12.5)	12 (25.0)	8 (14.0)	22 (45.8)	0.776 †
Female	8 (16.0)	16 (32.0)	7 (16.7)	19 (38.0)	
BAP1 IHC, no. (%)					
Negative	8 (14.5)	17 (30.9)	7 (12.7)	23 (41.8)	0.976 †
Positive	2 (16.7)	4 (33.3)	1 (8.3)	5 (41.7)	
SF3B1, no. (%)					
Wildtype	5 (20.0)	8 (32.0)	3 (12.0)	9 (36.0)	0.594 †
Mutated	2 (20.0)	5 (50.0)	0 (0.0)	3 (30.0)	
EIF1AX, no. (%)					
Wildtype	6 (16.7)	13 (36.1)	5 (13.9)	12 (33.3)	0.221 †
Mutated	1 (100)	0 (0.0	0 (0.0)	0 (0.0)	
GNAQ, no. (%)					
Wildtype	6 (26.1)	8 (34.8)	3 (13.0)	6 (26.1)	0.217 †
Mutated	0 (0.0)	6 (42.9)	3 (21.4)	5 (35.7)	
GNA11, no. (%)					
Wildtype	1 (5.9)	9 (52.9)	1 (5.9)	6 (35.3)	0.181 †
Mutated	5 (27.8)	5 (27.8)	3 (16.7)	5 (27.8)	
Extrahepatic lesions, no.	4/14	9/28	5/15	10/41	0.875 †

*One-way analysis of variance (ANOVA).
†Pearson's chi-square test.

We also analyzed the cumulative copy number variation (CNV) for each of the tumor profiles to look for potential differences (Figure 2). Majority of the known chromosomal aberrations were observed in each group, such as monosomy 3 and chromosome 8q gain. However, loss of chromosome 8p did not occur in the single lesion group, while it occurred more frequently in livers harboring more than one lesion, especially more than five lesions (~50%).

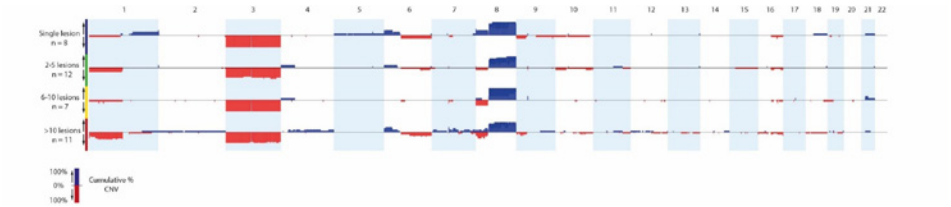

Figure 2. Summary plot showing chromosomal patterns in the different tumor profiles of UM. Chromosomes are depicted on the x-axis. The y-axis shows the cumulative percentage of copy number variation for each group. Blue indicates gain of chromosome and red indicates loss of chromosome. Sex chromosomes are excluded. Results are filtered to exclude gains and losses smaller than 1000 kB.

Survival analyses

Survival analyses were performed for time of diagnosis until metastasis (DFS). We observed a difference for DFS when comparing all groups (P = 0.032; Figure 3A). This showed a shorter DFS with increasing number of hepatic metastases. We also analyzed using thresholds rather than separate groups. These were set on one solitary lesion versus more than one (1 vs. >1); five or less versus more than five (≤5 vs. >5); ten or less versus more than ten lesions (≤10 vs. >10). This was not significantly different for the former two comparisons (P = 0.093 and P = 0.076, respectively; Figure 3B and Figure 3C), however did reach significance for ≤10 vs. >10 metastases (P = 0.011) in favor of patients with ≤10 lesions. For the UM^{meta} with more than ten lesions we observed two patterns, namely livers containing more than ten large nodules (>50 μm; Figure 3D) and a miliary pattern containing innumerable small lesions (<50 μm; Figure 3E). Comparing both groups did not show a significant difference in DFS (P = 0.922; Figure 3E).

We then analyzed whether a miliary metastatic pattern was of influence stratified for the mutation status. For patients without BAP1 expression in the primary UM, there was no difference in DFS between patients whom developed miliary metastases and those whom did not (P = 0.435). For *SF3B1*-mutated UM, although not significant (P = 0.075), the two cases with miliary metastases both metastasized within five years after

diagnoses, whereas in those without miliary metastases only two of the six patients presented with metastatic disease within five years after diagnosis.

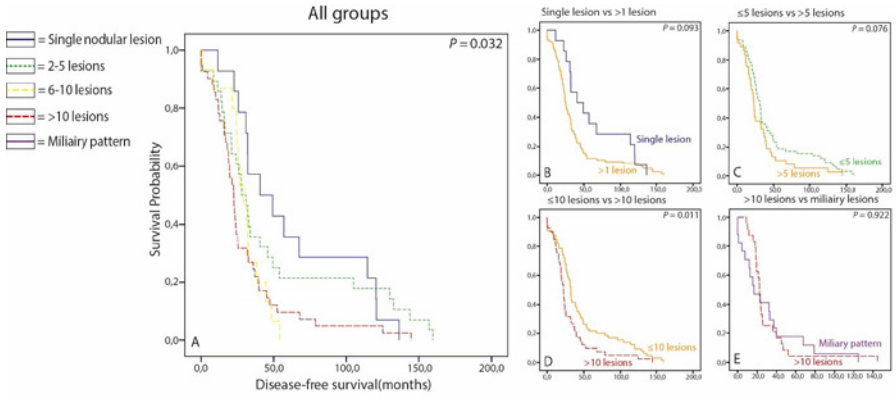

Figure 3. Kaplan-Meier curves showing the disease-free survival of the four classified tumor profiles as well as of multiple comparisons. **A,** The DFS differs significantly between the groups ($P = 0.032$). **B,** The DFS is trending in favor of the single lesions group, but it is not significantly different ($P = 0.093$). **C,** The DFS for the less than five lesions group is not significantly longer ($P = 0.076$). **D,** The more than ten lesions group has a significant shorter DFS compared to the less than ten lesion group ($P = 0.011$). **E,** Comparison of the more than ten lesions group and miliary pattern does not differ significantly ($P = 0.992$).

Since the metastatic patterns were predictive of DFS we also performed multi-variate analyses. From the univariate analyses (Table 2) only the *GNA11* mutation status ($P = 0.041$) and metastasis profiles ($P = 0.032$) were shown to associate with the DFS. In the multi-variate analyses only *GNA11* mutation in the primary UM was an independent predictor of DFS in patients with metastasized UM with a hazard ratio of 2.05 ($P = 0.047$).

Table 2. Univariate and Multivariate Analyses for patient with Metastasized Uveal Melanoma

	Univariate		Multivariate		
Covariate	95% CI	P Value	HR	95% CI	P Value
Irradiation					
Yes	22.7-39.8	0.060*			
No	34.3-55.4				
Gender					
Female	31.4-55.1	0.208*			
Male	26.9-45.8				
Age at diagnosis		0.516†			
Largest tumor diameter		0.471†			
Tumor height		0.196			
Extra-hepatic					
With	27.7-55.4	0.560*			
Without	30.0-48.3				
BAP1 IHC					
Positive	46.7-100.1	0.065*			
Negative	27.5-46.9				
GNAQ					
Wildtype	24.7-52.2	0.125*			
Mutated	28.4-81.5				
GNA11					
Wildtype	36.3-80.7	**0.041***	2.05	1.009-4.171	**0.047†**
Mutated	19.8-50.5				
Mutation status					
$BAP1^{neg}$	27.6-46.2	0.096*			
$SF3B1^{mut}$	40.6-114.1				
$EIF1AX^{mut}$	120.6				
NRM	13.7				
Metastasis profile					
1 lesion	39.1-84.0	**0.032***	-	-	0.120†
2-5 lesions	30.7-67.6				
6-10 lesions	22.5-36.6				
>10 lesions	20.8-38.9				

*Log-Rank
†Cox proportional regression analyses
Confidence interval (CI); 95% CI of survival (*) or hazard ratio (†)

Discussion

UM is the most common intra-ocular malignancy of the adult eye with a strong propensity to metastasize to the liver. A great deal of progress has been made in finding prognostic genetic markers in UM, however less is known about the hepatic metastasis in UM. Although a limited number of publications regarding this topic have appeared, none of them have focused specifically on the relation between the genetics of the primary UM and the pattern of metastases. In this current study we found that regardless of the mutation status of the primary UM, the metastases in these patients display the same metastatic profile. However chromosome 8p loss was absent in UM which give single solitary metastasis and more frequently found in UM^{meta} with more lesions, especially more than five lesions.

Interestingly enough, the DFS also differed between the groups. Although the sample size was not large enough to show a significant difference, the single nodular lesion group showed a trend towards a longer DFS compared to groups with more lesions. If the assumption was made that hepatic metastases grow in one linear fashion, single nodular UM^{meta} should have a shorter DFS than UM^{meta} with multiple lesions. However this was not the case, making it very likely that UM^{meta} with single nodular lesions have a slower growth and are distinct from UM^{meta} with multiple lesion. Histopathological findings showed that UM^{meta} indeed exhibit two types of growth patterns in the liver.[15,16] An infiltrative growth pattern which usually presents as many small (size <50 μm) lesions, also named lobular or replacement pattern. Another growth pattern called the nodular growth, which contain less but larger lesions (> 50 μm).[16] This nodular growth is also described as portal and pushing pattern. Both growth patterns have distinct anatomical locations, and also mixtures of both growth patterns in one affected liver are described.[17] Similar to our different metastatic patterns found with imaging, the difference in DFS is also shown for the histopathologically different growth patterns, in which the mean average doubling time of the infiltrative UM^{meta} is significantly less than that of the nodular UM^{meta}.[18]

We hypothesized that the different types of lesions would correspond to the mutation status of the primary UM since we previously reported that *BAP1*^{mut} UMs display rapid metastases and *SF3B1*^{mut} UMs display mostly late-onset metastases.[5] Strikingly this was not the case. It is thus very interesting that, irrespective of the mutation status, UM^{meta} with *BAP1*^{mut} and *SF3B1*^{mut} can show both growth patterns. However,

we did observe that the two patients with miliary metastases and an *SF3B1*^{mut} in the primary UM, both had early-onset metastases. This difference was not that clear for *BAP1*^{mut} UM. It remains debatable whether this metastatic spread is purely by change or whether there is a genetic predisposition of the primary UM.

Similar to our findings, another study also reported a non-significant difference for chromosome 8p CNVs in the primary tumor and the different growth patterns, in which loss of chromosome 8p was more present in UMs which have an infiltrative growth pattern.[19] We hypothesize that this could be the product of isochromosome 8q formation resulting in chromosome 8q gain with subsequent loss of chromosome 8p, but the precise etiology remains uncertain. However, previous research suggests that metastatic growth properties are modulated by suppression of gene regions specific to chromosome 8p.[20] This not only underlines the importance of genes localized on chromosome 8p for the spread and development of hepatic metastasis in UM, but it is also indicative for the role played by the genetic landscape of the primary tumor in the homing of tumor cells.

Studying UM^{meta} is not only challenging due to the lack of material, but also due to the biases which is created by the methods used to obtain metastasis material. Material is usually available through metastectomy and this is only performed in patients who are suited for this therapy and not for patient with a miliary pattern. However, research into the genetics of metastases remains important especially since there are several reports which state the different metastatic patterns also react differently to therapy.[17,19,21] It has been shown that patient with a nodular metastatic growth pattern whom receive hepatic arterial chemoembolization have a significant longer survival.[19,21] One report even shows that in a patient with a mixture of infiltrative and nodular metastatic growth pattern, the nodular metastasis show reduction in size to hepatic radio-embolization whereas the infiltrative metastasis remain resistant and persist in growth.[17] This highlights that targeted therapy and perhaps also combination therapy is the future in UM^{meta} therapy.

In conclusion, our study has shown that there is an inverse correlation of the number of metastasis with the metastasized survival, indicating separate growth patterns. We could not find an association of metastasis with the mutations status, however loss of chromosome 8p was observed more often in patients harboring more liver metastasis. Future endeavors could focus on discovering different genetic factors including chromosome 8p that influence the propagation and development of hepatic metastases in UM.

References

1. Hu, D.N., Yu, G.P., McCormick, S.A., Schneider, S. & Finger, P.T. Population-based incidence of uveal melanoma in various races and ethnic groups. *Am J Ophthalmol* **140**, 612-7 (2005).
2. Singh, A.D., Turell, M.E. & Topham, A.K. Uveal melanoma: trends in incidence, treatment, and survival. *Ophthalmology* **118**, 1881-5 (2011).
3. McLaughlin, C.C. *et al.* Incidence of noncutaneous melanomas in the U.S. *Cancer* **103**, 1000-7 (2005).
4. Kujala, E., Makitie, T. & Kivela, T. Very long-term prognosis of patients with malignant uveal melanoma. *Invest Ophthalmol Vis Sci* **44**, 4651-9 (2003).
5. Yavuzyigitoglu, S. *et al.* Uveal Melanomas with SF3B1 Mutations: A Distinct Subclass Associated with Late-Onset Metastases. *Ophthalmology* **123**, 1118-28 (2016).
6. Hoglund, M. *et al.* Dissecting karyotypic patterns in malignant melanomas: temporal clustering of losses and gains in melanoma karyotypic evolution. *Int J Cancer* **108**, 57-65 (2004).
7. Trolet, J. *et al.* Genomic profiling and identification of high-risk uveal melanoma by array CGH analysis of primary tumors and liver metastases. *Invest Ophthalmol Vis Sci* **50**, 2572-80 (2009).
8. Meir, T. *et al.* Molecular characteristics of liver metastases from uveal melanoma. *Invest Ophthalmol Vis Sci* **48**, 4890-6 (2007).
9. Griewank, K.G. *et al.* Genetic and clinico-pathologic analysis of metastatic uveal melanoma. *Mod Pathol* **27**, 175-83 (2014).
10. Luscan, A. *et al.* Uveal melanoma hepatic metastases mutation spectrum analysis using targeted next-generation sequencing of 400 cancer genes. *Br J Ophthalmol* **99**, 437-9 (2015).
11. McCarthy, C. *et al.* Insights into genetic alterations of liver metastases from uveal melanoma. *Pigment Cell Melanoma Res* **29**, 60-7 (2016).
12. Singh, P. & Singh, A. Choroidal melanoma. *Oman J Ophthalmol* **5**, 3-9 (2012).
13. Henriquez, F., Janssen, C., Kemp, E.G. & Roberts, F. The T1799A BRAF mutation is present in iris melanoma. *Invest Ophthalmol Vis Sci* **48**, 4897-900 (2007).
14. Yavuzyigitoglu, S. *et al.* Metastatic Disease in Polyploid Uveal Melanoma Patients Is Associated With BAP1 Mutations. *Invest Ophthalmol Vis Sci* **57**, 2232-9 (2016).
15. Grossniklaus, H.E. Progression of ocular melanoma metastasis to the liver: the 2012 Zimmerman lecture. *JAMA Ophthalmol* **131**, 462-9 (2013).
16. Grossniklaus, H.E. *et al.* Metastatic ocular melanoma to the liver exhibits infiltrative and nodular growth patterns. *Hum Pathol* **57**, 165-175 (2016).
17. Halenda, K.M. *et al.* Reduction of Nodular Growth Pattern of Metastatic Uveal Melanoma after Radioembolization of Hepatic Metastases. *Ocul Oncol Pathol* **2**, 160-5 (2016).
18. Liao, A., Mittal, P., Jiang, Y. & Grossniklaus, H.E. Metastatic Uveal Melanoma in the Liver Exhibit Two Distinct Patterns with Different Growth Kinetics. *Investigative Ophthalmology & Visual Science* **58**, 4409-4409 (2017).
19. Dayani, P.N. *et al.* Hepatic metastasis from uveal melanoma: angiographic pattern predictive of survival after hepatic arterial chemoembolization. *Arch Ophthalmol* **127**, 628-32 (2009).
20. Onken, M.D., Worley, L.A. & Harbour, J.W. A metastasis modifier locus on human chromosome 8p in uveal melanoma identified by integrative genomic analysis. *Clin Cancer Res* **14**, 3737-45 (2008).
21. Sharma, K.V. *et al.* Hepatic arterial chemoembolization for management of metastatic melanoma. *AJR Am J Roentgenol* **190**, 99-104 (2008).

Chapter 3

Rare phenotypes in Uveal Melanoma

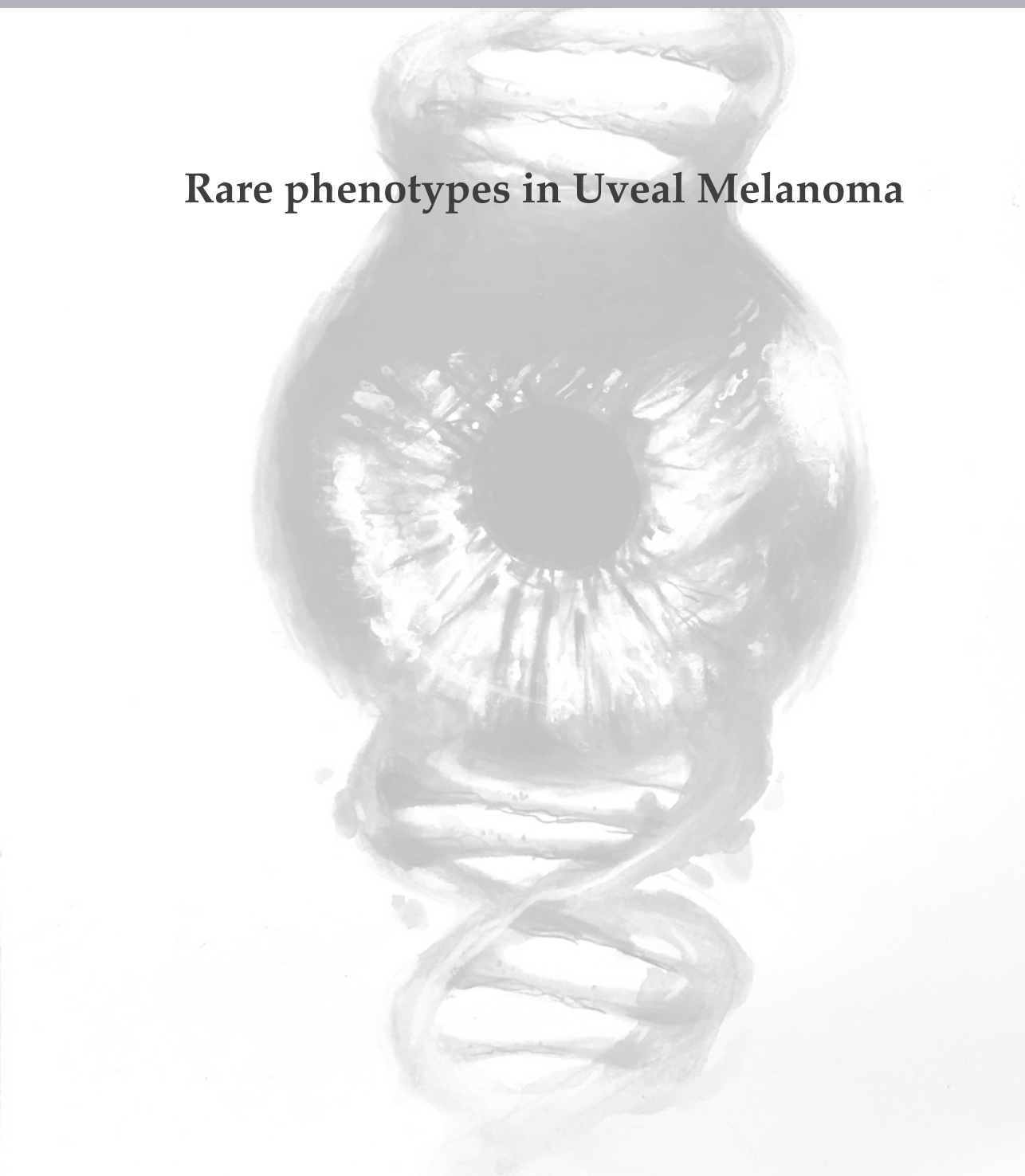

Chapter 3.1

Metastatic Disease in Polyploid Uveal Melanoma Patients Is Associated With *BAP1* Mutations

Serdar Yavuzyigitoglu,* Hanneke W. Mensink,* Kyra N. Smit, Jolanda Vaarwater, Robert M. Verdijk, Berna Beverloo, Hennie T. Brüggenwirth, Ronald van Marion, Hendrikus J. Dubbink, Dion Paridaens, Nicole C. Naus, Annelies de Klein, and Emine Kilic

* These authors contributed equally to this work.

Invest Ophthalmol Vis Sci. 2016 Apr 1;57(4):2232-9. doi: 10.1167/iovs.15-18608.

Abstract

Purpose: Most of the uvea melanoma (UM) display a near-diploid (normal, ~2N) karyotype with only a few chromosomal changes. In contrast to these simple aberrations 18% of the UM samples show a polyploid character (>2N) and this was associated with an unfavorable prognosis. This study attempts to gain insight in the prognostic value of polyploidy in UM.

Methods: In 202 patients the ploidy status of the UM was determined using cytogenetic analysis, fluorescence-in-situ-hybridization (FISH), multiplex ligation dependent probe amplification (MLPA), and/or single nucleotide polymorphism (SNP) array analysis. Immunohistochemistry was used to determine the BAP1 expression and mutation analyses of *BAP1* (coding regions) and the mutation hotspots for the *SF3B1*, *EIF1AX*, *GNAQ*, and *GNA11* genes was carried out using Sanger sequencing or whole-exome sequencing.

Result: Twenty-three patients had a polyploid UM karyotype (11.4%). Patients with a polyploid tumor had larger tumors (15.61 vs. 13.13 mm, $P = 0.004$), and more often loss of heterozygosity of chromosome 3 ($P = 0.003$). No difference in occurrence of mutations between polyploid and diploid tumors was observed for *BAP1*, *SF3B1*, *EIF1AX*, *GNAQ*, and *GNA11*. Polyploidy did not affect survival ($P = 0.143$). BAP1 deficiency was the only significant independent prognostic predictor for patients with polyploid tumors, with a 16- fold increased hazard ratio (HR 15.90, $P = 0.009$).

Conclusion: The prevalence of mutations in the UM related genes is not different in polyploid UM compared with diploid UM. Moreover, similar to patients with diploid UM, *BAP1* mutation is the most significant prognostic predictor of metastasis in patients with polyploid UM.

Introduction

Uveal melanoma (UM) is the most common primary intraocular malignancy in adults with an annual incidence of approximately 7 to 10 per million.[1] In approximately one-half of the patients UM metastasizes via the blood with a preference for the liver.[1] The prognostic factors linked to metastatic disease include clinical variables (increased age, large tumor size), histopathologic findings (epithelioid cell type, closed vascular patterns), genetic, and chromosomal abnormalities (loss of chromosome 3, gain of chromosome 8q).[2–5]

For UM, the karyotype is usually near-normal (diploid) with only few nonrandom chromosomal changes, such as loss of chromosome 3 (monosomy 3) and gain of chromosome 8q.[6] Besides these near-diploid (~2N) tumors, UM with polyploidy (>2N) have also been described. Based on DNA content, a prevalence of 13% to 18% of polyploid UM has been observed.[7–9] In addition to the prevalence, the prognostic value of the ploidy was also described, in which polyploidy was associated with an unfavorable prognosis.[7,9] However, despite the impact on survival, polyploidy in UM is not mentioned in recent literature or investigated with the current knowledge of UM.

Nowadays in UM research, the focus is more on genetic variations. Monosomy 3 in combination with the loss of function of the tumor suppressor *BAP1* (BRCA-associated protein 1) is strongly associated with metastases.[10–13] In contrast, mutations in the *SF3B1* (splicing factor 3 subunit B1) gene and the *EIF1AX* (eukaryotic translation factor 1A) gene are reported mainly in disomy 3 (no loss of chromosome3) tumors.[14–16] Therefore, mutations in *SF3B1* or *EIF1AX* have been suggested as favorable prognostic factors in UM, with low risk of metastasis.[10,14–17] Mutations in the oncogenes *GNAQ* (Guanine nucleotide-binding protein, q polypeptide) and *GNA11* (Guanine nucleotide-binding protein, subunit alpha-11) are present in the majority of UM and are not associated with patient prognosis.[18–20]

This study attempts to describe the differences between polyploid and diploid UM regarding clinical variables, histopathologic findings, chromosomal abnormalities, and genetic mutations (*BAP1*, *SF3B1*, *EIF1AX*, *GNAQ*, and *GNA11*). We also aimed to investigate the prognostic value of polyploidy and prognostic factors within polyploid UM.

Methods

Study Population

Tissue specimens were obtained from 324 patients with UM who were enucleated or had a biopsy between 1993 and 2014. Informed consent was given prior to enucleation and the study was performed according to the guidelines of the Declaration of Helsinki. This study was approved by the local ethics committee. The clinical data from time of diagnosis until December 2014 were updated from the patients' chart. All tumors were histopathologically confirmed. Tumor node metastasis (TNM) classification of the UM was adapted from the AJCC Cancer Staging Manual.[21] Iris melanomas were excluded from this study.

DNA Extraction and Copy Number Analysis

DNA was extracted directly from fresh tumor tissue or frozen tumor using the QIAmp DNA-mini kit (Qiagen, Hilden, Germany) according to the manufacturers' instructions. Chromosome abnormalities were described following the recommendations for cytogenetic nomenclature.[22] The tumors were processed for fluorescence in situ hybridization (FISH), multiplex ligation dependent probe amplification (MLPA), and/or single nucleotide polymorphism (SNP) array analysis (Illumina HumanCytoSNP-12 v2.1 BeadChip and Illumina 610Q BeadChip; Illumina, San Diego, CA, USA), as described previously.[23] Cut-off limits for deletion detected by FISH (>15% of the nuclei with one signal) or amplification (>10% of the nuclei with 3 or more signals) were adapted from the available literature.[23]

Tumor Ploidy

For this study, 202 of 324 patients were included for whom the combination of several techniques was available to determine the ploidy status of the tumor. A threshold of greater than 20% polyploid cells was maintained for cytogenetic analyses. Based on cytogenetic or SNP array analyses, selected chromosomes, which were suspected to be 3N or 4N, were analyzed with FISH to determine the ploidy fraction. A threshold of greater than 10% of the nuclei with three or more signals of these control chromosomes was used to classify a tumor as polyploid.[23] Based on literature, we assumed baseline ploidy of polyploid UM as tetraploid (4N).[24] Chromosomal copy number changes were calculated based on the ploidy baseline. For polyploid samples, chromosomes were treated as loss only in combination with loss of heterozygosity (LOH). For chromo-

some gain, both quantitative gain (>2N) as well as relative gain (>4N) were included in the analyses of polyploid UM.

Mutational Analyses

Mutation analyses using Sanger sequencing or obtained from whole-exome sequencing (WES) was available for 126 samples.[25] Variants found in the WES data were validated by Sanger sequencing. *BAP1*, *SF3B1*, *EIF1AX*, *GNAQ*, and *GNA11* mutation analyses and BAP1 immunohistochemistry (IHC) were carried out as reported previously.[13,18,25,26] For five polyploid samples no fresh or frozen tissue was available, therefore DNA was isolated from formalin-fixed, paraffin-embedded (FFPE) tissue. These DNAs were screened for mutations in the UM genes using the ION Torrent Personal Genome Machine (PGM) with the supplier's materials and protocols (Life Technologies, Carlsbad, CA, USA). A custom primer panel was designed using the ION AmpliSeq Designer 3.2 (Thermo Fisher Scientific, Waltham, MA, USA). Reads were visualized with Integrative Genomics Viewer (v2.3; Broad Institute, Cambridge, MA, USA). Variants were validated with Sanger sequencing using primers (Supplementary Table S1) and protocols for FFPE DNA. Protocols and designs regarding FFPE DNA sequencing are available upon request. De novo missense mutations were investigated with SIFT (in the public domain, http://sift.jcvi.org/) and PolyPhen-2 (in the public domain, http://genetics.bwh.harvard.edu/pph2/index.shtml) for predictions on possible functional impact and pathogenicity of the amino acid change.

Statistical Analyses

Disease-free survival (DFS) was calculated as date of first initial treatment to date of clinically proven metastasis from UM. The Log-rank test was used for categorical variables, and Cox proportional hazard analysis for continuous variables. Statistical significant variables conducted from univariate analysis were analyzed using Cox proportional hazard multivariate analysis. P values of 0.05 or lower were considered significant for survival analyses. Chi-square or Fisher's exact test was used for associations with categorical data; Mann-Whitney U test was used for associations with continuous data. P values of 0.005 or lower were considered significant for correlation analyses. All statistical analyses were performed with SPSS 21.0 Software (IBM, Armonk, NY, USA).

Results

Patient and Tumor Characteristics

Polyploid UM was detected in 23 of 202 patients (11.4%). Nine patients were male and 14 were female with a mean age at diagnosis of 62.5 years. Mean tumor diameter was 15.6 mm with a mean tumor thickness of 8.9 mm. Histopathologically, 19 tumors contained epithelioid cells and 11 formed extracellular matrix patterns. All tumors (n = 23) showed a relative loss of chromosome 3 (<4N), resulting in LOH for chromosome 3 in 20 tumors (Fig. 2), whereas three tumors (S28, S102, and S156) still contained two different alleles despite the relative loss (Figs. 1, 2). For chromosome 8q all polyploid UM had more than two copies, 19 tumors had a relative gain (>4N), all copies were present in three tumors (4N; S147, S156, and S161) and one tumor (S75) had three copies of chromosome 8q (Fig. 1). An overview of the clinical, histopathologic, and chromosomal variables are shown in Table 1.

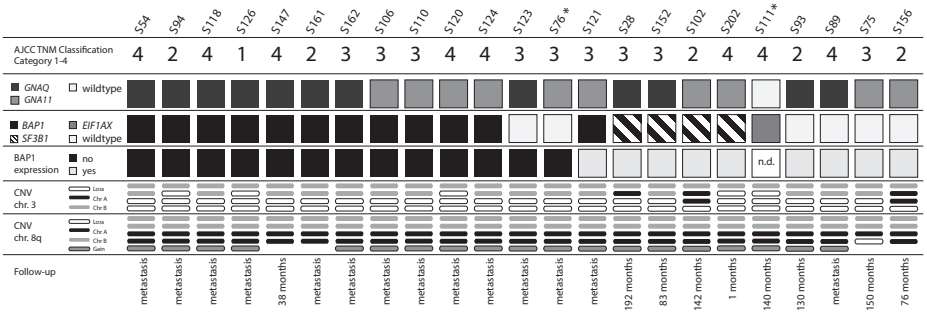

Figure 1. Overview of mutations and copy number variation in polyploid UM. The TNM classification is represented on the first line. First row of blocks represent the *GNAQ* and *GNA11* mutation status; dark gray, *GNAQ* mutation; light gray, *GNA11* mutation; n.d. = not determined; All mutations were exclusive. Second row of blocks represent the *BAP1*, *SF3B1*, and *EIF1AX* mutation status; black, *BAP1* mutation; striped, *SF3B1* mutation; gray, *EIF1AX* mutation; and white, wild-type for the three genes. All mutations were exclusive. Third row of blocks represent the BAP1 expression; white, BAP1 expressed; black, BAP1 not expressed. Fifth row represent the alleles of chromosome 3; CNV ¼ copy number variation (baseline is four copies); black, allele A; light gray, allele B; white, loss of chromosome. Sixth row represent the alleles of chromosome 8q; black, allele A; light gray, allele B; white, loss of chromosome; dark gray, gain chromosome(s). * In these samples the *BAP1* mutation status could not be determined.

Table 1. Patient and tumor characteristics of the study cohort, and associations between ploidy of the tumor with other clinical, histopathological and genetic variables.

	Ploidy status tumor		
Variables (n = 202)	Polyploid	Diploid	
	(mean or n)	(mean or n)	p-value
Age at diagnoses	62.52 ± 2.67	61.17 ± 1.08	0.689†
Gender			
Male	9	90	0.314‡
Female	14	89	
Localization			
Choroid	15	136	0.263‡
Ciliary body	8	43	
Largest tumor diameter	15.61 ± 0.76	13.13 ± 0.25	**0.004**†
Tumor thickness	8.87 ± 0.75	7.68 ± 0.26	0.131†
TNM classification			
Category 1	1	20	-
Category 2	5	66	
Category 3	10	80	
Category 4	7	13	
Cell type			
Spindle	4	59	0.129‡
Epithelioid/mixed	19	120	
Extracellular matrix patterns			
Absent	12	90	0.925‡
Present	11	86	
Chromosome 3			
Relative loss (<4N*)	23	98	**<0.001**‡
Normal (4N*)	0	81	
Chromosome 3			
LOH	20	98	**0.003**‡
No LOH	3	81	
Chromosome 8q			
Normal (2N)	0	69	**<0.001**‡
Absolute gain (>2N)	23	110	
Chromosome 8q			
Normal (4N*)	4	69	0.047‡
Gain (>4N*)	19	110	
BAP1			
Normal	8	69	0.223‡
Deficient	14	68	
SF3B1			
Wild type	19	83	0.546‡
Mutated	4	25	
EIF1AX			
Wild type	22	88	0.125§
Mutated	1	22	

Table 1. Continued.

	Ploidy status tumor		
Variables (n = 202)	Polyploid	Diploid	
GNAQ			
Wild type	11	52	0.946 ‡
Mutated	12	55	
GNA11			
Wild type	13	60	0.969 ‡
Mutated	10	47	

P-values≤ 0.005 was considered significant after correction for multiple testing. Mann-Whitney test † was used for associations with continuous data, Chi-square -test ‡ or Fisher's exact test § was used for associations with categorical data. TNM classification was not compared since tumor diameter and thickness are analyzed separately. *: copy numbers for the polyploid UM.

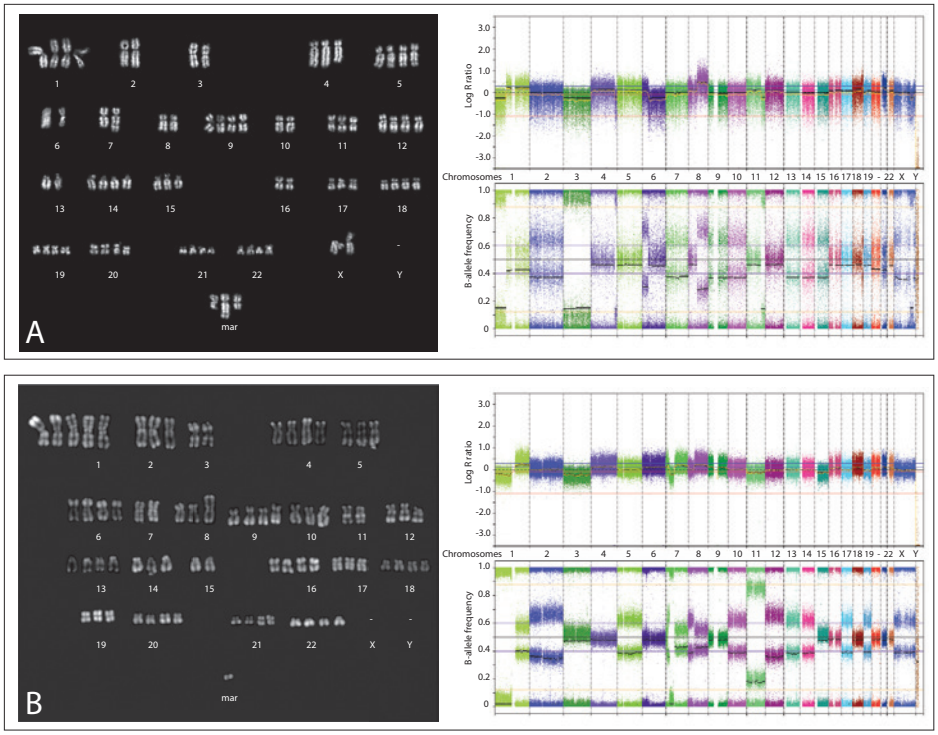

Figure 2. (**A**) Karyogram of S152 demonstrates a polyploid cell with three or four copies of most chromosomes and two copies of chromosome 3; the corresponding whole-genome SNP array (all chromosomes on the X-axis) demonstrates a relative loss of chromosome 3 as observed in the Log R ratio (negative values indicate a relative loss and positive values a relative gain). Loss of heterozygosity of chromosome 3 can be deduced from the B-allele frequency (the B-allele frequency is either 1.0 or 0.0). (**B**) Karyogram of S28 demonstrates a polyploid cell with three or four copies of most chromosomes and two copies of chromosome 3; the corresponding whole-genome SNP array demonstrates a relative loss as observed in the Log R ratio; however, without the loss of heterozygosity as demonstrated by the SNP's (B-allele frequency of ~0.5).

Genetic Analyses UM Genes

Within the patients with polyploid tumors 12 patients harbored a *BAP1* mutation, which were hemi- or homozygous in all cases. In 13 of 22 patients, the tumors did not express BAP1 (examples provided in Fig. 3). In one case (S111) the lack of tumor material restricted us to investigate *BAP1* both for mutations and expression. One patient (S76) could not be investigated for *BAP1* mutations, but did reveal loss of BAP-1expression. In one patient (S123), the tumor did not harbor a mutation in the coding exons, but had a loss of expression of BAP1 in the tumor. One patient (S121) harbored a missense mutation in the tumor, p.E30G, whereas the IHC did show expression of BAP1. This mutation was predicted as 'Deleterious' by SIFT software (J. Craig Venter Institute, Rockville, MD,USA) and 'Probably damaging' by PolyPhen-2 software(Harvard Medical School, Boston, MA, USA). All three patients (S76, S121, and S123) were treated as BAP1-deficient tumors in further analysis. *SF3B1* was mutated in four samples targeting the hotspot p.R625 in three cases and p.V576del in one case. *EIF1AX* harbored a missense mutation, p.G15D, in one case, which was predicted as 'Deleterious' by SIFT software and 'Probably damaging' by PolyPhen-2 software. Twelve tumors harbored a *GNAQ* p.Q209 hotspot mutation, 10 harbored a *GNA11* p.Q209 hotspot mutation, and one tumor was wildtype for exon 4 and 5 of both genes. An overview of the mutations with the corresponding polyploid tumor is shown in Figure 1. Mutations in *BAP1*, *SF3B1*, *EIF1AX*, *GNAQ*, and *GNA11* in the patients with diploid UM were described previously.[13,18,25]

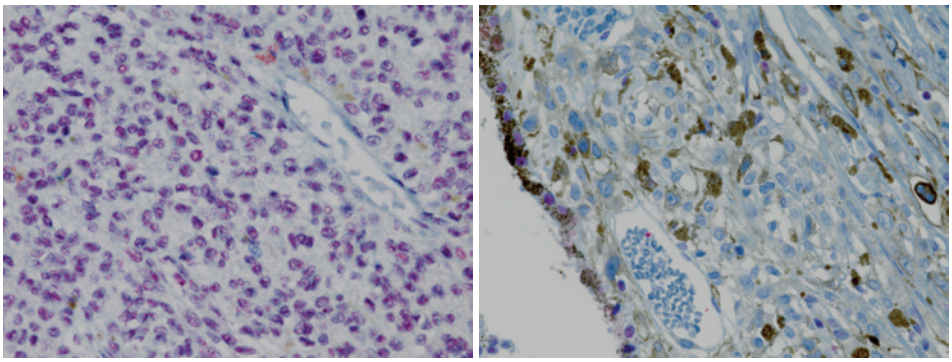

Figure 3. Examples of BAP1 immunohistochemistry of two polyploid uveal melanoma cases. Left picture: BAP1 expression in the tumor cells of S28 (3400). Right picture: lack of BAP1 expression in the tumor cells of the case S162 (3400). Note the positive staining in the retinal pigment epithelium cells and macrophages.

Statistical Analyses

Based on tumor ploidy, patients did not differ in age at diagnoses, sex, tumor localization, tumor thickness, cell type, and presence of extracellular matrix patterns. Patients with a polyploid tumor had significantly larger tumors than patients with a diploid tumor (15.6 vs. 13.1 mm, $P = 0.004$; Table 1). For chromosomal abnormalities we classified the copy number changes for polyploid UM in two ways. For chromosome loss, we determined the relative loss from baseline and also loss with LOH. For chromosome gain, we determined absolute gain from disomy state and relative gain from baseline. Patients with polyploid UM showed more loss of chromosome 3 ($P < 0.001$), which was still significant after correcting for LOH ($P = 0.003$). For chromosome 8q, the polyploid UM contained more often absolute gain (>2N; $P < 0.001$). Relative gain of chromosome 8q was observed more often in polyploid UM ($P = 0.047$), and after correcting the P value for multiple testing to P less than or equal to 0.005 this was not considered significant. Mutational frequencies did not differ between polyploid and diploid UM for *BAP1*, *SF3B1*, *EIF1AX*, *GNAQ*, and *GNA11*.

Survival Analyses

To test whether polyploidy in UM was associated with worse disease-free survival we performed survival analyses for the total group (n = 202). Ploidy was not associated with prognosis, because patients with polyploid tumors, as a group, did not differ from patients with diploid tumors based on the survival (Fig. 4A). Univariate analyses results are shown in Table 2. Also in the multivariate Cox-regression analyses, polyploidy was not associated with disease-free survival. Larger basal tumor diameter (HR 1.110; $P = 0.015$) and BAP1 deficiency (HR 5.132; $P < 0.001$) were the only independent significant predictors for disease-free survival in the total cohort (Table 2). Survival analysis was also performed for patients with polyploid UM to investigate prognostic predictors within this subset (n = 23). Loss of heterozygosity of chromosome 3 ($P = 0.050$), BAP1 deficiency ($P = 0.001$), and *SF3B1* wildtype mutation status ($P = 0.035$) were significantly associated with decreased disease-free survival. Other variables were not significantly associated with disease-free survival (Table 2). Chromosome 3, BAP1, and *SF3B1* status, together with tumor diameter (because this was associated with polyploid UM) were included into the multivariate Cox analyses. This showed BAP1 deficiency as the only significant independent prognostic predictor for patients with polyploid tumors, with a 16-fold increased HR (HR 15.90, $P = 0.009$; Table 2).

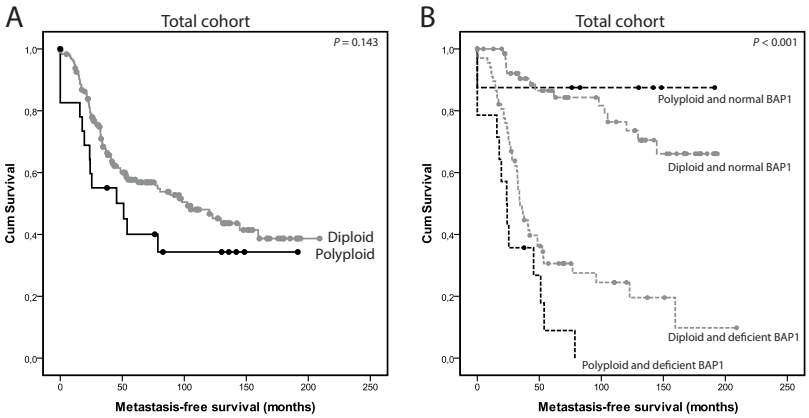

Figure 4. Kaplan-Meier survival analyses for; (**A**) polyploid UM compared to diploid UM ($P = 0.143$) and (**B**) survival analyses between polyploid and diploid UM stratified for BAP1 status ($P < 0.001$).

Table 2. Univariate and multivariate analyses of the uveal melanoma parameters in relation to patient survival for the total cohort and patients with a polyploid tumor karyotype.

Covariate	**Univariate**		**Multivariate**		
Total cohort (n=202)	**95% CI**	**p-value**	**HR**	**95% CI**	**p-value**
Age at diagnoses	1.006-1.036	**0.004**			0.683
Largest tumor diameter	1.030-1.158	**0.003**	1.110	1.021-1.206	**0.015**
Tumor height	0.997-1.113	0.065	-	-	-
Cell type					
Spindle	121.7-160.9	**<0.001**	-	-	0.912
Mixed/epithelioid	77.5-108.6				
Closed vascular loops					
Present	59.4-94.3	**<0.001**	-	-	0.072
Absent	117.1-149.6				
Ploidy					
Diploid	99.6-128.0	0.143	-	-	0.568
Polyploid	49.2-117.9				
Chromosome 3					
Loss (with LOH)	50.6-80.1	**<0.001**	-	-	0.549
Normal	147.1-175.7				
Chromosome 8q					
Normal	155.1-190.7	**<0.001**	2.171	0.958-4.920	0.063
Gain (relative)	60.7-87.9				
BAP1					
Normal	141.2-172.5	**<0.001**	5.132	2.623-10.04	**<0.001**
Deficient	44.4-75.5				
SF3B1					
Wild type	84.3-121.3	**0.028**	-	-	0.166
Mutated	114.9-165.5				
EIF1AX					
Wild type	75.9-106.8	**<0.001**	0.145	0.19-1.116	0.064
Mutated	168.3-214.6				

P-value of P≤0.05 was considered significant. Log-rank test and Cox regression analyses were used to obtain univariate analyses for categorical and continuous data respectively. Multivariate analyses was conducted with Cox regression analyses with variables significantly associated with survival in the univariate analyses. CI: confidence interval of survival (months/HR); HR: hazard ratio (expB). * No statistics could be computed because all cases were censored.

Covariate	Univariate		Multivariate		
Polyploid (n=23)	**95% CI**	**p-value**	**HR**	**95% CI**	**p-value**
Age at diagnoses	0.987-1.073	0.175	-	-	-
Largest tumor diameter	0.937-1.261	0.270	-	-	0.156
Tumor height	0.909-1.229	0.471	-	-	-
Cell type					
Spindle	22.0-149.2	0.624	-	-	-
Mixed/epithelioid					
Closed vascular loops					
Present	17.1-96.2	0.129	-	-	-
Absent	52.5-128.6				
Ploidy					
Diploid					
Polyploid					
Chromosome 3					
Loss (with LOH)	*	**0.050**	-	-	0.357
Normal					
Chromosome 8q					
Normal	66.5-167.4	0.136	-	-	-
Gain (relative)	35.0-107.0				
BAP1					
Normal	123.7-211.5	**0.001**	15.90	1.97-128.3	**0.009**
Deficient	16.4-42.5				
SF3B1					
Wild type	*	**0.035**	-	-	0.294
Mutated					
EIF1AX					
Wild type	*	0.228	-	-	-
Mutated					

Discussion

In our cohort polyploidy occurred in 11.4% of the patients with UM. Previously, we as well as other groups have reported ranges between 13% and 18%,[8,9] and this difference in prevalence can be explained by the different methods which were used to determine the ploidy status and the DNA index (DI) thresholds which were adapted to classify a tumor as polyploid. Meecham et al.[7] report polyploidy in 13% of the UM with flow cytometry measurements and a threshold of DI greater than 1.4 for polyploidy. Toti et al.[9] report polyploidy in18% of the UM cases, while maintaining a threshold of DI greater than 1.3 for polyploidy, which would explain the higher prevalence of polyploidy. Mooy et al.[8] reports tetraploidy (4N) in 17% of the cohort; however, this subset also contains preirradiated tumors, which they also correlate to a higher prevalence of aneuploidy.

When compared with patients with diploid UM, we found larger tumor diameter in the polyploid patient group. Polyploid UM also contained more LOH of chromosome 3. We could not confirm previous findings, which stated that polyploidy as a group is associated with worse patient survival.[7,9] However, we did find that BAP1 deficiency was the most significant factor associated with survival in patients with a polyploid UM, similar to diploid UM.

BAP1 expression has been shown as an independent prognostic marker in UM.[10,12,13] The gene is located on chromosome 3, and is mutated mainly in tumors with loss of chromosome 3,15 resulting in the loss of BAP1 expression.[13] One sample harbored a missense mutation (p.E30G), whereas the staining did reveal BAP1 expression. This mutation was predicted 'Deleterious' and 'Probably damaging' by the prediction software's. Moreover, this mutation is located at the first b-sheet of the protein and also next to three amino acids (p.E31–p.Y33), which form a binding site for ubiquitin,27 making it likely that the replacement of the negatively charged glutamic acid with the neutral glycine causes a structural malformation of the protein resulting in a deficiency of BAP1. The BAP1 expression can be explained, because the mutation is a missense mutation and does not lead to protein degradation. Also, the affected amino acid is located in the N terminal UCH domain, whereas the antibody used for the staining target the C-terminal end of the BAP1 protein.[13] In this study, tumors with *BAP1* mutations and/or loss of BAP1 expression were categorized as deficient BAP1. In this way we observed that deficient BAP1 was the only independent prognostic marker in patients with polyploid UM.

For the other UM relevant genes we found *GNAQ* or *GNA11* mutations in all but one polyploid UM as one would expect based on the occurrence described in diploid UM.[19,20] *SF3B1* mutations were observed in four of our polyploid tumors. Patients with *SF3B1* mutation in the UM have been associated with the low-risk prognostic features; disomy 3, spindle-cell type, and low age at diagnoses.[15,16] None of the patients in our polyploid group with *SF3B1* mutations had developed metastatic disease and were alive at the end of the study (follow-up range, 1–192 months). Nevertheless, both to our own experience as well as by other groups patients can be identified with disomy 3 tumors harboring an *SF3B1* mutation that developedmetastasis.[15,16,25,28] In our polyploid cohort the numbers are too low and the follow-up for some tumors is too short in order to draw conclusions regarding the influence of *SF3B1* mutations in the tumor on disease-free survival. *EIF1AX* mutations are mainly reported in disomy 3 tumors and are correlated with a good prognosis for these patients, and present in the tumor of one patient in our series of polyploid UM, who is metastasis-free and alive at a follow-up of 136 months.[10,16,17,25] The missense mutation found in the tumor of this patient affects amino acid 15 (p.G15D), a missense mutation described in other UM samples as well (the COSMIC database; id=COSM3973544; in the public domain, http://cancer.sanger.ac.uk/cosmic/). The first 18 amino acids at the N-terminus of the eiF1A protein are essential in the interaction with the 40S subunit,[29] thus making it very likely that this mutation results in an altered function of the protein. In this current study, we have shown that the prevalence of mutations in the UM genes do not differ between tumors with diploid and polyploid karyotypes, indicating a similar behavior and progression toward metastatic disease, suggesting polyploid UM are not a subclass in UM.

Caution should be taken in the interpretation of chromosomal abnormalities and using one technique only this could possible lead to misclassifications. Uveal melanoma are characterized by nonrandom recurring chromosomal losses and gains.[6] Loss of chromosome 3 has been correlated to metastasis,[3–5] but in polyploid UM with loss of one or multiple copies of chromosome 3 this does not automatically result in LOH. This is shown in our polyploid tumors, which all contain a relative loss of chromosome 3, while three tumors do not display a LOH (Figs. 1, 2). These three patients without LOH are still alive with a median DFS of 11 years (range, 76–192 months), which is comparable to the survival of patients with disomy 3 tumors.[3] Onken et al.[30] described that LOH of chromosome 3 is superior to quantitative loss of monosomy 3, and that is also the case in polyploid UM in our study. We emphasize the importance of SNP-array to investigate the zygosity of UM, to reduce false-negative (disomy 3

with LOH) and false-positive (relative monosomy 3 without LOH) prognostification. However, we cannot use the same reasoning for chromosome gain. Increase in copies of chromosome 8q is shown to be associated with shorter DFS.[31] In polyploid UM, all tumors contain more than two copies of 8q, while four tumors do not have a relative gain based on the baseline of four copies. One of these four patients developed liver metastasis at 54 months and is still alive after a partial hepatectomy 20 months later, two died due to another cause at 38 and 149 months respectively, and one is alive and metastasis-free at 76 months. Because the survival of these patients is not homogenous we cannot draw conclusions regarding the pathogenicity of absolute gain without relative gain (tri- and tetrasomy) of chromosome 8q.

In conclusion, here we show that polyploid UM do not differ from diploid UM based on prevalence of mutations in the UM genes, and that similar to patients with diploid UM, *BAP1* is the most significant prognostic predictor of metastasis inpatients with polyploid UM (HR 15.90). Yet, the increased chromosome count and frequent losses in polyploid tumors can cause wrongful interpretations of chromosomal data and should therefore be analyzed for ploidy status.

References

1. Bakalian S, Marshall JC, Logan P, et al. Molecular pathways mediating liver metastasis in patients with uveal melanoma. Clin Cancer Res 2008;14:951-956.
2. Kujala E, Makitie T, Kivela T. Very long-term prognosis of patients with malignant uveal melanoma. Invest Ophth Vis Sci 2003;44:4651-4659.
3. Prescher G, Bornfeld N, Hirche H, Horsthemke B, Jockel KH, Becher R. Prognostic implications of monosomy 3 in uveal melanoma. Lancet 1996;347:1222-1225.
4. Tschentscher F, Husing J, Holter T, et al. Tumor classification based on gene expression profiling shows that uveal melanomas with and without monosomy 3 represent two distinct entities. Cancer Res 2003;63:2578-2584.
5. White VA, Chambers JD, Courtright PD, Chang WY, Horsman DE. Correlation of cytogenetic abnormalities with the outcome of patients with uveal melanoma. Cancer 1998;83:354-359.
6. Prescher G, Bornfeld N, Friedrichs W, Seeber S, Becher R. Cytogenetics of 12 Cases of Uveal Melanoma and Patterns of Nonrandom Anomalies and Isochromosome Formation. Cancer Genet Cytogen 1995;80:40-46.
7. Toti P, Greco G, Mangiavacchi P, Bruni A, Palmeri MLD, Luzi P. DNA ploidy pattern in choroidal melanoma: correlation with survival. A flow cytometry study on archival material. Brit J Ophthalmol 1998;82:1433-1437.
8. Mooy C, Vissers K, Luyten G, et al. DNA Flow-Cytometry in Uveal Melanoma - the Effect of Preenucleation Irradiation. Brit J Ophthalmol 1995;79:174-177.
9. Meecham WJ, Char DH. DNA Content Abnormalities and Prognosis in Uveal Melanoma. Arch Ophthalmol-Chic 1986;104:1626-1629.
10. Ewens KG, Kanetsky PA, Richards-Yutz J, et al. Chromosome 3 Status Combined With BAP1 and EIF1AX Mutation Profiles Are Associated With Metastasis in Uveal Melanoma. Invest Ophth Vis Sci 2014;55:5160-5167.
11. Harbour JW, Onken MD, Roberson EDO, et al. Frequent Mutation of BAP1 in Metastasizing Uveal Melanomas. Science 2010;330:1410-1413.
12. Kalirai H, Dodson A, Faqir S, Damato BE, Coupland SE. Lack of BAP1 protein expression in uveal melanoma is associated with increased metastatic risk and has utility in routine prognostic testing. Brit J Cancer 2014;111:1373-1380.
13. Koopmans AE, Verdijk RM, Brouwer RWW, et al. Clinical significance of immunohistochemistry for detection of BAP1 mutations in uveal melanoma. Modern Pathol 2014;27:1321-1330.
14. Furney SJ, Pedersen M, Gentien D, et al. SF3B1 Mutations Are Associated with Alternative Splicing in Uveal Melanoma. Cancer Discov 2013;3:1122-1129.
15. Jackson RJ, Hellen CUT, Pestova TV. The mechanism of eukaryotic translation initiation and principles of its regulation. Nat Rev Mol Cell Bio 2010;11:113-127.
16. Dono M, Angelini G, Cecconi M, et al. Mutation frequencies of GNAQ, GNA11, BAP1, SF3B1, EIF1AX and TERT in uveal melanoma: detection of an activating mutation in the TERT gene promoter in a single case of uveal melanoma. Brit J Cancer 2014;110:1058-1065.
17. Harbour JW, Roberson EDO, Anbunathan H, Onken MD, Worley LA, Bowcock AM. Recurrent mutations at codon 625 of the splicing factor SF3B1 in uveal melanoma. Nat Genet 2013;45:133-135.
18. Martin M, Masshofer L, Temming P, et al. Exome sequencing identifies recurrent somatic mutations in EIF1AX and SF3B1 in uveal melanoma with disomy 3. Nat Genet 2013;45:933-U296.
19. Van Raamsdonk CD, Bezrookove V, Green G, et al. Frequent somatic mutations of GNAQ in uveal melanoma and blue naevi. Nature 2009;457:599-U108.
20. Van Raamsdonk CD, Griewank KG, Crosby MB, et al. Mutations in GNA11 in Uveal Melanoma. New Engl J Med 2010;363:2191-2199.
21. ISCN (2013): An International System for Human Cytogenetic Nomenclature. Basel: S. Karger; 2013.
22. Vaarwater J, van den Bosch T, Mensink HW, et al. Multiplex ligation-dependent probe amplification equals fluorescence in-situ hybridization for the identification of patients at risk for metastatic

disease in uveal melanoma. Melanoma Res 2012;22:30-37.
23. Vandekken H, Pizzolo JG, Reuter VE, Melamed MR. Cytogenetic Analysis of Human Solid Tumors by Insitu Hybridization with a Set of 12 Chromosome-Specific DNA Probes. Cytogenet Cell Genet 1990;54:103-107.
24. Davoli T, de Lange T. The Causes and Consequences of Polyploidy in Normal Development and Cancer. Annu Rev Cell Dev Bi 2011;27:585-610.
25. Koopmans AE, Vaarwater J, Paridaens D, et al. Patient survival in uveal melanoma is not affected by oncogenic mutations in GNAQ and GNA11. Brit J Cancer 2013;109:493-496.
26. Van Beek JG, Koopmans AE, Vaarwater J, et al. Metastatic disease in uveal melanoma: importance of a genetic profile? Melanoma Res 2015.
27. Luscan A, Just PA, Briand A, et al. Uveal melanoma hepatic metastases mutation spectrum analysis using targeted next-generation sequencing of 400 cancer genes. Brit J Ophthalmol 2015;99:437- 439.
28. Onken MD, Worley LA, Person E, Char DH, Bowcock AM, Harbour JW. Loss of heterozygosity of chromosome 3 detected with single nucleotide polymorphisms is superior to monosomy 3 for predicting metastasis in uveal melanoma. Clin Cancer Res 2007;13:2923-2927.
29. van den Bosch T, van Beek JG, Vaarwater J, et al. Higher percentage of FISH-determined monosomy 3 and 8q amplification in uveal melanoma cells relate to poor patient prognosis. Invest Ophthalmol Vis Sci 2012;53:2668-2674.

Chapter 3.2

Chromosomal rearrangements in uveal melanoma: Chromothripsis

Natasha M. van Poppelen, Serdar Yavuzyigitoglu, Jolanda Vaarwater, Bert Eussen, Tom Brands, Dion Paridaens, Emine Kilic and Annelies de Klein

Manuscript submitted

Abstract

Introduction

Uveal melanoma (UM) is the most common primary intraocular malignancy in the Western world. Recurrent mutations in *GNAQ*, *GNA11*, *BAP1*, *EIF1AX* and *SF3B1* are described as well as non-random chromosomal aberrations. Chromothripsis is a rare event in which chromosomes are shattered and rearranged and has been reported in a variety of cancers including UM.

Materials and methods

SNP-arrays of 249 UM from patients who underwent enucleation, biopsy or endoresection were reviewed for the presence of chromothripsis. Chromothripsis was defined as ten or more breakpoints per chromosome involved. Genetic analysis of *GNAQ*, *GNA11*, *BAP1*, *SF3B1* and *EIF1AX* was conducted using Sanger and next-generation sequencing. In addition, immunohistochemistry for BAP1 was performed.

Results

Chromothripsis was detected in seven out of 249 tumors and the affected chromosomes were chromosomes 3, 5, 6, 8, and 12 and 13. The mean total of fragments per chromosome was 39.8 (range 12 – 116). In one UM, chromothripsis occurred simultaneously in two different chromosomes. A *GNAQ* or *GNA11* mutation was present in five tumors. Five out of seven tumors harbored a *BAP1* mutation and/or lacked BAP1 protein expression in immunohistochemistry. Four of these tumors metastasized, from the fifth only short follow-up data is available. One tumor harbored an *SF3B1* mutation and metastasized as well. No *EIF1AX* mutations were detected.

Conclusion

Chromothripsis was observed in 2.8% of the UM with a mean of approximately fourty fragments per chromosome. Chromothripsis occurred concurrently in two different chromosomes in one UM. Five of the seven patients developed metastatic disease, four of these UM harbor a *BAP1* mutation and one an *SF3B1* mutation. Chromothripsis of chromosome 3 was detected in two UM, both having a *BAP1* mutation.

Introduction

Uveal melanoma (UM) is a relative rare disease and has a high mortality rate due to metastasis in about half of all patients within 15 years after diagnosis.[1-3] UM is the most common primary intra-ocular malignancy in adults in the Western world.[4] Uveal melanoma specific mutations in the alpha subunit genes *GNAQ* and *GNA11* are described as well as mutations in *BAP1*, *SF3B1* and *EIF1AX*.[5-7] Mutations in the latter three genes are found in approximately 75% of all UM and useful for prognostication of patients.[8-10] *BAP1* mutated UM give rise to early-onset metastasis whereas *SF3B1*-mutated UM give rise to late-onset metastasis and *EIF1AX*-mutated UM hardly metastasize.[8]

Copy number alterations in chromosomes 1, 3, 6 and 8 are correlated with prognosis of the UM patient.[11, 12] UM with *EIF1AX*, *SF3B1* and *BAP1* mutations are associated with unique chromosomal patterns, suggesting distinct UM subclasses. *BAP1* mutated UM harbor entire chromosome copy number variations (CNVs) and entire chromosome arm CNV anomalies (isochromosomes). UM with an *SF3B1* mutation are characterized by many structural variants, often affecting the terminal ends of chromosomes and thus not entire chromosomes or chromosome arms.[13] Besides these recurrent CNVs, also other chromosomal patterns are described such as polyploidy of the genome, which occurs in approximately 10-15% of all UM.[14] Another chromosomal anomaly described in UM is chromothripsis.[12] This is a phenomenon in which many genomic rearrangements occurs in a single chromosome or chromosome arm. In this case series we report on chromothripsis in seven UM. It has been described in congenital abnormalities, UM and a variety of other cancers such as bone cancer, lung cancer, myelodysplastic syndrome (MDS), colorectal cancer, mammacarcinoma and neuroblastoma.[12, 15-19] Chromothripsis predicts a poor outcome in skin melanoma and occur in high risk neuroblastoma, mammacarcinoma and MDS.[16, 18-20] A positive correlation between chromothripsis and progression free survival was observed in metastatic colorectal cancer.[17] The clinical consequence of this phenomenon in uveal melanoma remains unclear.[12]

The mechanism of chromothripsis remains elusive but several hypotheses are described such as the formation of micronuclei, premature chromosome compaction (PCC), *TP53* mutations and breakage-fusion bridge cycles or irradiation.[21, 22, 23] The formation of chromothripsis involving telomere regions and one chromosome arm is described and supports the hypothesis that events during the cell cycle are involved in the formation

of these chromosomal rearrangements.[24] It is hypothesized that chromothripsis occurs through the formation of micronuclei that arise from lagging chromosomes or chromatid fragments during mitosis.[15, 25-28] Moreover, these micronuclei are more prone to DNA damage, with subsequently DNA nuclease repair by non-homologous end joining (NHEJ), which could explain the chromosome reshuffling.[15, 25, 28, 29]

Materials and methods

Inclusion

Patients with UM that underwent enucleation, endoresection or tumor biopsy at the Erasmus University Medical Center (Rotterdam, The Netherlands) or The Rotterdam Eye Hospital (Rotterdam, The Netherlands) between 1992 and 2017 were selected. SNP (single nucleotide polymorphism) array data of the tumor was available from 249 patients. Chromothripsis was defined as ten or more breakpoints per chromosome detected with SNP-array. This study was approved by the local ethics committee and followed the tenets of the Declaration of Helsinki. Informed consent was obtained prior to treatment.

SNP-array

DNA was extracted from fresh tumor samples using the QIamp DNA-mini kit (Qiagen, Hilden, Germany) following the manufacturer's instructions. SNP-array was performed using 200ng of DNA as input for whole-genome analysis (Illumina 610Q BeadChip, Illumina, San Diego, CA, USA). The data was analyzed with Nexus Copy Number 9.0 software (BioDiscovery Incorporated, El Segundo, California, USA). The amount of copy number gains and losses were used to determine the number of fragments. The total fragments were counted including copy number neutral fragments as separate fragments.

Mutation detection

Mutation analysis for *GNAQ, GNA11, EIF1AX, SF3B1* and *BAP1* was performed with Sanger sequencing and Ion Torrent next-generation sequencing (NGS) (Thermo Fisher Scientific, Waltham, Massachusetts, USA sequencing) as described before.[30] SeqScape Software 3 (Applied Biosystems, Foster City, CA, USA) and Integrative Genomics Viewer (IGV) Version 2.3.68 (97) (Broad Institute, Cambridge, Massachusetts, USA) was used to analyze the data. BAP1 immunohistochemistry (IHC) was performed as described previously.[9]

Results

Patient characteristics

In seven patients chromothripsis was detected in the UM. These seven patients comprised of five women and two men with a mean age at diagnosis of 57.4 years (range 46.2 – 73.4 years). Six patients underwent enucleation as primary treatment. In one patient primary treatment was followed by external beam radiotherapy because of unclear surgical margins. One patient underwent brachytherapy as primary treatment, followed by enucleation almost three years later due to tumor recurrence. Metastasis developed in five patients after 31.9 to 78.7 months. The mean DFS was 51.5 months (range 15.5 – 99.0 months). In Table 1 an overview of patient characteristics is listed.

Tumor characteristics

Six tumors were located in the posterior choroid whereas one UM originated from the ciliary body. Mean largest tumor diameter was 13.5 mm (range 9.5-19 mm) and mean tumor thickness 7.5 mm (range 2 – 12 mm), Table 1. Three UM contained epithelioid cells and four were classified spindle cell type. Closed vascular loops were present in two of the seven UM and extra-ocular extensions were found in two cases. Correlations of chromothripsis with patient and tumor characteristics were not performed due to the limited number of cases.

Table 1.

Patient	Sex	Age	DFS	Metastasis	Tumor diameter (mm)	Tumor thickness (mm)	Primary treatment
UM 1	F	46.3	42.7	Yes	14	10	Enucleation
UM 2	M	46.2	78.7	Yes	13	N.a.	Enucleation
UM 3	F	57.4	47.4	Yes	9.5	2	Brachytherapy
UM 4	F	64.1	31.9	Yes	14	12	Enucleation
UM 5	M	55.8	99.0	No	12	4	Enucleation
UM 6	F	73.4	15.5	No	13	7.5	Enucleation
UM 7	F	58.6	45.4	Yes	19	9.5	Enucleation

F = female; M = male; age = age at diagnosis in years; DFS = disease free survival in months; n.a. = data not available.

BAP1 expression was present in three cases and absent in four cases. Mutation analysis was performed for all seven tumors (Figure 3). A mutation in *GNAQ* was detected in two tumors, a c.626A>C:p.(Gln209Pro) mutation. A *GNA11* c.626A>T:p.(Gln209Leu) mutation was detected in the UM of three patients. One c.1873C>T:p.(Arg625Cys)

mutation in *SF3B1* was found (UM 1) but all tumors were wildtype for *EIF1AX*. *BAP1* mutations were detected in four patients, a c.89A>G:p.(Glu31Gly) (UM 2), a c.172_173del:p.(Ser58Profs*10) (UM 6), a c.206_207insA:p.(Thr69Asnfs*5) (UM 7) and a mutation two base pairs after exon 5 (c.375+2T>C) (UM 4) resulting in alternative splicing with a premature stop before the next predicted splice site (prediction in Alamut Visual, Interactive Biosoftware, Rouen, France). Three of these four *BAP1* mutated UM had an absent BAP1 expression. In one tumor a *BAP1* mutation was not detected with NGS, although IHC revealed lack of BAP1 expression. Moreover, this tumor was irradiated prior to the enucleation. Polyploidy occurred in two out of seven UM. See Figure 3 for an overview of mutation status and BAP1 IHC.

Chromothripsis

In total eight chromosomes showed chromothripsis (Figure 1). One tumor harbored chromothripsis in two separate chromosomes (UM 5; Figure 2). UM 7 (chromothripsis of chromosome 13) showed eight fragments in chromosome 16 as well. However, since this did not meet our criteria of ten fragments, this chromosome was not included for further analysis. Chromosome 3 and 6 were affected in two UM. Regarding chromosome 3, the breaking points were not present in the *BAP1* gene. Other affected chromosomes were chromosome 5, 8, 12 and 13. The mean of the total fragments per chromosome was 39.8 (range 12-116, Figure 3). In four of the eight chromosomes the B-allele frequencies indicates more than two copy number states of the separate chromosome fragments (Figure 1A and Figure 2). In five cases (UM 2, UM 3, UM 4, UM 5 and UM 6) DNA from blood was available for germline analysis using SNP-array. No chromothripsis was observed in these samples.

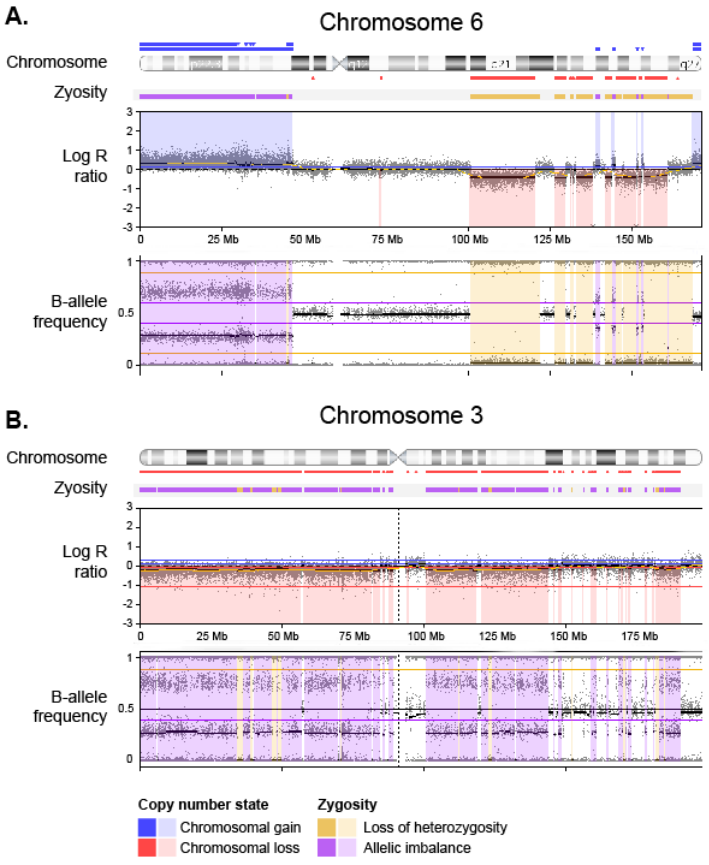

Figure 1. Two examples of chromothripsis. (**A**) UM 1 showing chromothripsis of chromosome 6q with an additional gain of the terminal short (p) arm of chromosome 6. Note the three different copy number states in the chromothriptic chromosome. (**B**) UM 4 showing chromothripsis of chromosome 3.

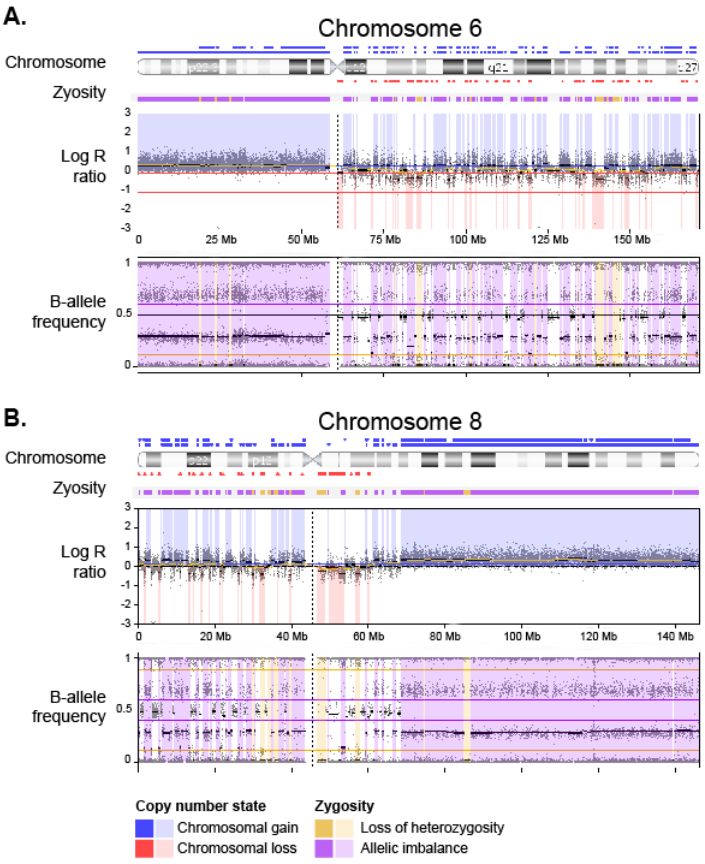

Figure 2. A case with two chromothriptic chromosomes. UM 5 showing chromothripsis of (**A**) chromosome 6 and (**B**) chromosome 8. Note the three copy number states and a general gain of the entire chromosomes.

Discussion

Recurrent chromosomal aberrations have been described in detail in UM, which are strongly correlated to the mutation status.[13, 31, 32] In this paper, another chromosomal aberration, called chromothripsis, is described. Chromothripsis is characterized by ten to hundreds of chromosome fragments that are shattered and randomly rearranged.[15] This is described in numerable type of malignancies with a mean pan-cancer prevalence of 1-2%.[12, 29, 33] Similar to other malignancies, chromothripsis is also rare in UM. In one study chromothripsis was observed in 2/25 UM.[12] We detected chromothripsis in 2.8% of the UM which is in line with the low frequency rate as previously described. A relation between prognosis and chromothripsis has been reported in several studies on different malignancies. In high risk neuroblastoma, mammacarcinoma and MDS, chromothripsis is correlated with a poor outcome while in metastatic colorectal cancer a better progression free-survival has been described.[15,17-19] In this report, metastatic disease was present in five out of seven patients. Four of the metastasizing tumors harbored a *BAP1* mutation and or lacked BAP1 expression and in one tumor an *SF3B1* mutation was present. One of the two patients without metastatic disease did not harbor a *BAP1* or *SF3B1* mutation in the tumor and the IHC showed a positive BAP1 expression while from the other patient (harbouring a *BAP1* mutation in the tumor) only short follow-up data was available (16 months). The overall poor prognosis of this cohort could be explained by the mutations in *BAP1* and *SF3B1* since it is known that mutations in these genes are correlated with a high risk of metastasis.[8, 10]

There are several risk factors known for chromothripsis such as irradiation.[21] In one case, brachytherapy was followed by enucleation. Therefore, the chromothripsis in this UM could be an irradiation effect. Other factors correlated with chromothripsis formation are hyper- and polyploidization.[34, 35] For a long time it was assumed that chromothriptic chromosomes only have two copy number states.[15, 28, 29] However, an observation was made in a subtype of acute lymphoblastic leukemia, in which more copy number states were found in chromothriptic chromosomes.[36] In this study two of the seven UM (29%) were polyploid. Polyploidy occurs in only 11% of all large UM[14] and chromothripsis is a rare event, this could explain the co-occurrence of polyploid UM with chromothripsis. In addition, in our cohort, seven out of eight chromothriptic chromosomes harbored more than two chromosomes. This observation was also made in the only other study that described two cases of UM with chromothripsis.[12] This suggests that chromothripsis occurs in already duplicated chromosomes. Altered

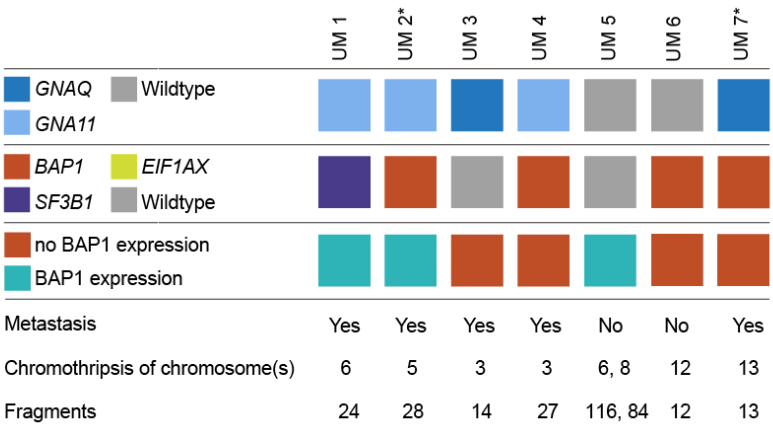

Figure 3. Overview of the affected genes in UM with chromothripsis. The first row of blocks represents the mutation status of *GNAQ* and *GNA11*. In the second row of blocks the mutation status of *BAP1*, *SF3B1* and *EIF1AX* is given. The third row of blocks represents the BAP1 IHC staining. The fourth row indicates whether a patient developed metastasis. In the fifth row the chromosome with chromothripsis is given. The bottom row indicates the number of fragments per chromosome. * = Polyploid tumor

chromosomes might even be more susceptible to chromosome lagging, as 50% of the chromosomes with chromothripsis in this study have more than two copy number states.[36] Furthermore, chromothripsis can occur in more than one chromosome in the same tumor.[15] In our cohort, more than one chromosome was affected in one tumor. It is noteworthy that the affected chromosomes in this study included chromosomes 3, 6 and 8, since copy number variations in these chromosomes are correlated with mutation status in UM.[13] This is in line with other studies in which chromothripsis occur among known cancer driver genes.[23, 37] Nevertheless, chromothripsis-like patterns across different tumor types showed a limited preference according to chromosome size. However, chromosome 17 was most frequently affected and to a lesser degree chromosomes 8,11 and 12 in another study.[24] This could be explained by the fact that chromosome 17 also harbors *TP53*, an important cancer associated gene, which is correlated to chromothripsis as well.[23]

To conclude, chromothripsis is a complex event that occurs in a variety of cancers.[12, 16, 18, 23, 24, 38] This study shows chromothripsis in almost 3% of UM affecting different chromosomes. Limitation of this study was the small number of cases with chromothripsis. Although a large patient cohort was investigated, the rare occurrence of chromothripsis prohibited performing proper statistical analyses. Further studies are needed to investigate the evolutionary advantage of this complex chromosomal aberration.

References

1. Isager P, Osterlind A, Engholm G, et al. Uveal and conjunctival malignant melanoma in Denmark, 1943-97: incidence and validation study. Ophthalmic Epidemiol 2005;12(4):223-32.
2. Kujala E, Makitie T, Kivela T. Very long-term prognosis of patients with malignant uveal melanoma. Invest Ophthalmol Vis Sci 2003;44(11):4651-9.
3. Cohen VM, Carter MJ, Kemeny A, et al. Metastasis-free survival following treatment for uveal melanoma with either stereotactic radiosurgery or enucleation. Acta Ophthalmol Scand 2003;81(4):383-8.
4. Singh AD, Turell ME, Topham AK. Uveal melanoma: trends in incidence, treatment, and survival. Ophthalmology 2011;118(9):1881-5.
5. Dono M, Angelini G, Cecconi M, et al. Mutation frequencies of GNAQ, GNA11, BAP1, SF3B1, EIF1AX and TERT in uveal melanoma: detection of an activating mutation in the TERT gene promoter in a single case of uveal melanoma. Br J Cancer 2014;110(4):1058-65.
6. Onken MD, Worley LA, Long MD, et al. Oncogenic mutations in GNAQ occur early in uveal melanoma. Invest Ophthalmol Vis Sci 2008;49(12):5230-4.
7. Van Raamsdonk CD, Griewank KG, Crosby MB, et al. Mutations in GNA11 in uveal melanoma. N Engl J Med 2010;363(23):2191-9.
8. Yavuzyigitoglu S, Koopmans AE, Verdijk RM, et al. Uveal Melanomas with SF3B1 Mutations: A Distinct Subclass Associated with Late-Onset Metastases. Ophthalmology 2016;123(5):1118-28.
9. Koopmans AE, Verdijk RM, Brouwer RW, et al. Clinical significance of immunohistochemistry for detection of BAP1 mutations in uveal melanoma. Mod Pathol 2014;27(10):1321-30.
10. Decatur CL, Ong E, Garg N, et al. Driver Mutations in Uveal Melanoma: Associations With Gene Expression Profile and Patient Outcomes. JAMA Ophthalmol 2016;134(7):728-33.
11. Aalto Y, Eriksson L, Seregard S, et al. Concomitant loss of chromosome 3 and whole arm losses and gains of chromosome 1, 6, or 8 in metastasizing primary uveal melanoma. Invest Ophthalmol Vis Sci 2001;42(2):313-7.
12. van Engen-van Grunsven AC, Baar MP, Pfundt R, et al. Whole-genome copy-number analysis identifies new leads for chromosomal aberrations involved in the oncogenesis and metastastic behavior of uveal melanomas. Melanoma Res 2015;25(3):200-9.
13. Yavuzyigitoglu S, Drabarek W, Smit KN, et al. Correlation of Gene Mutation Status with Copy Number Profile in Uveal Melanoma. Ophthalmology 2017;124(4):573-5.
14. Yavuzyigitoglu S, Mensink HW, Smit KN, et al. Metastatic Disease in Polyploid Uveal Melanoma Patients Is Associated With BAP1 Mutations. Invest Ophthalmol Vis Sci 2016;57(4):2232-9.
15. Stephens PJ, Greenman CD, Fu B, et al. Massive genomic rearrangement acquired in a single catastrophic event during cancer development. Cell 2011;144(1):27-40.
16. Przybytkowski E, Lenkiewicz E, Barrett MT, et al. Chromosome-breakage genomic instability and chromothripsis in breast cancer. BMC Genomics 2014;15:579.
17. Skuja E, Kalniete D, Nakazawa-Miklasevica M, et al. Chromothripsis and progression-free survival in metastatic colorectal cancer. Mol Clin Oncol 2017;6(2):182-6.
18. Abaigar M, Robledo C, Benito R, et al. Chromothripsis Is a Recurrent Genomic Abnormality in High-Risk Myelodysplastic Syndromes. PLoS One 2016;11(10):e0164370.
19. Molenaar JJ, Koster J, Zwijnenburg DA, et al. Sequencing of neuroblastoma identifies chromothripsis and defects in neuritogenesis genes. Nature 2012;483(7391):589-93.
20. Hirsch D, Kemmerling R, Davis S, et al. Chromothripsis and focal copy number alterations determine poor outcome in malignant melanoma. Cancer Res 2013;73(5):1454-60.
21. Morishita M, Muramatsu T, Suto Y, et al. Chromothripsis-like chromosomal rearrangements induced by ionizing radiation using proton microbeam irradiation system. Oncotarget 2016;7(9):10182-92.
22. Crasta K, Ganem NJ, Dagher R, et al. DNA breaks and chromosome pulverization from errors in mitosis. Nature 2012;482(7383):53-8.
23. Rausch T, Jones DT, Zapatka M, et al. Genome sequencing of pediatric medulloblastoma links catastrophic DNA rearrangements with TP53 mutations. Cell 2012;148(1-2):59-71.
24. Cai H, Kumar N, Bagheri HC, et al. Chromothripsis-like patterns are recurring but hetero-

geneously distributed features in a survey of 22,347 cancer genome screens. BMC Genomics 2014;15:82.
25. Ernst A, Jones DT, Maass KK, et al. Telomere dysfunction and chromothripsis. Int J Cancer 2016;138(12):2905-14.
26. Maciejowski J, de Lange T. Telomeres in cancer: tumour suppression and genome instability. Nat Rev Mol Cell Biol 2017;18(3):175-86.
27. Maciejowski J, Li Y, Bosco N, et al. Chromothripsis and Kataegis Induced by Telomere Crisis. Cell 2015;163(7):1641-54.
28. Storchova Z, Kloosterman WP. The genomic characteristics and cellular origin of chromothripsis. Curr Opin Cell Biol 2016;40:106-13.
29. Rode A, Maass KK, Willmund KV, et al. Chromothripsis in cancer cells: An update. Int J Cancer 2016;138(10):2322-33.
30. Smit KN, van Poppelen NM, Vaarwater J, et al. Combined mutation and copy-number variation detection by targeted next-generation sequencing in uveal melanoma. Mod Pathol 2018.
31. Dogrusoz M, Jager MJ, Damato B. Uveal Melanoma Treatment and Prognostication. Asia Pac J Ophthalmol (Phila) 2017;6(2):186-96.
32. Hoglund M, Gisselsson D, Hansen GB, et al. Dissecting karyotypic patterns in malignant melanomas: temporal clustering of losses and gains in melanoma karyotypic evolution. Int J Cancer 2004;108(1):57-65.
33. Leibowitz ML, Zhang CZ, Pellman D. Chromothripsis: A New Mechanism for Rapid Karyotype Evolution. Annu Rev Genet 2015;49:183-211.
34. Mardin BR, Drainas AP, Waszak SM, et al. A cell-based model system links chromothripsis with hyperploidy. Mol Syst Biol 2015;11(9):828.
35. Notta F, Chan-Seng-Yue M, Lemire M, et al. A renewed model of pancreatic cancer evolution based on genomic rearrangement patterns. Nature 2016;538(7625):378-82.
36. Li Y, Schwab C, Ryan S, et al. Constitutional and somatic rearrangement of chromosome 21 in acute lymphoblastic leukaemia. Nature 2014;508(7494):98-102.
37. Tang MH, Dahlgren M, Brueffer C, et al. Remarkable similarities of chromosomal rearrangements between primary human breast cancers and matched distant metastases as revealed by whole-genome sequencing. Oncotarget 2015;6(35):37169-84.
38. van den Broek E, Dijkstra MJ, Krijgsman O, et al. High Prevalence and Clinical Relevance of Genes Affected by Chromosomal Breaks in Colorectal Cancer. PLoS One 2015;10(9):e0138141.

Chapter 3.3

Lipomatous Change in Uveal Melanoma: Histopathological, Immunohistochemical and Cytogenetic Analysis

Serdar Yavuzyigitoglu, Emine Kilic, MD, Jolanda Vaarwater, Annelies de Klein, Dion Paridaens and Robert M. Verdijk

Ocul Oncol Pathol. 2016 Apr;2(3):133-5. doi: 10.1159/000440981.

Abstract

Purpose: The aim of this study was to describe a case of lipomatous change in uveal melanoma. Procedures: The patient presented with a 2-year history of blurry vision. A full examination

of the right eye revealed a dome-shaped pigmented subretinal mass in the choroid with a thickness of 9 mm and a diameter of 15 mm. The eye was enucleated and prepared for histopathologic, genetic and molecular investigation.

Results: Histopathology revealed a small circumscribed area consisting of mature adipocytic appearing cells with abundant clear cytoplasm and small peripheral flattened nuclei within a spindle-cell melanoma of the uvea. The cytoplasm of the adipocytic cells stained negative for periodic acid- Schiff and Alcian blue and positive for Melan-A, HMB-45 and tyrosinase, confirming melanocytic lineage. Fluorescence in situ hybridization analysis confirmed trisomy of chromosome 6p22 and disomy of chromosome 3p13 in the nuclei of both the tumor spindle type B cells and in the nuclei of lipomatous tumor cells.

Conclusions: Lipomatous change can be added to the many histopathologic faces of uveal melano-ma. To our knowledge, this is the first report of lipomatous change in uveal melanoma performed with cytogenetic investigations.

Introduction

Malignant melanoma is well known for its protean morphologic appearance. Besides the common uveal melanoma types (epithelioid and spindle cell), other histopathologic variants have been reported. Clear cell change of the cytoplasm of uveal melanocytic cells can be observed as balloon cells, signet ring cells and clear cells.[1-3] We describe lipomatous change in uveal melanoma.

Case Description

A 73-year-old male visited the outpatient department of ophthalmology because of a 2-year history of blurry vision, which could not be explained upon two prior visits to an ophthalmologist during these 2 years. At presentation, the best-corrected visual acuity was 20/50 OD and 20/16 OS. On dilated funduscopy (Figure 1A) and ultrasonographic examination of the right eye, a dome-shaped pigmented subretinal mass was seen with a thickness of 9 mm, a diameter of 15 mm and medium-to-low internal reflectivity. No atypical cutaneous pigmented lesions were observed. Systemic radiologic evaluation revealed no metastatic lesions. The patient opted for enucleation. After a follow-up of 12 months, there were no signs of metastases.

Sections of the eye confirmed a dome-shaped tumor composed almost exclusively of spindle type B melanoma cells. A small circumscribed area consisted of mature adipocytic appearing cells with abundant clear cytoplasm and small flattened nuclei at the periphery (Figure 1B). The cytoplasm stained negative for periodic acid-Schiff and Alcian blue stains, excluding glycogen or mucin. Mitotic figures were present at 4 × 8 mm 2 (equivalent to 50 highpower fields). Intracytoplasmic brown pigment stained negative for Prussian Blue iron stain. No closed-loop extracellular matrix pattern was present. The tumor did not show extrascleral extension or invasion of the optic nerve. The lipomatous tumor cells stained positive for Melan-A, HMB-45 (Figure 1C) and tyrosinase, confirming melanocytic lineage. All tumor cell nuclei stained positive for BAP1. The lipomatous tumor cells stained negative for CD34.

Single-nucleotide polymorphism array analysis (HumanCytoSNP-12 v2 BeadChip; Illumina, San Diego, CA, USA) showed gain of chromosome 6p and no loss or gain of chromosomes 3 and 8. Fluorescence in situ hybridization analysis confirmed trisomy

of chromosome 6p22 and disomy of chromosome 3p13 in the nuclei of both the tumor spindle type B cells and in the nuclei of lipomatous tumor cells (Figure 1D). Mutation analysis demonstrated a heterozygous *GNA11* p.Gln209Leu mutation. *GNAQ* , *SF3B1* and *EIF1AX* were wild type.

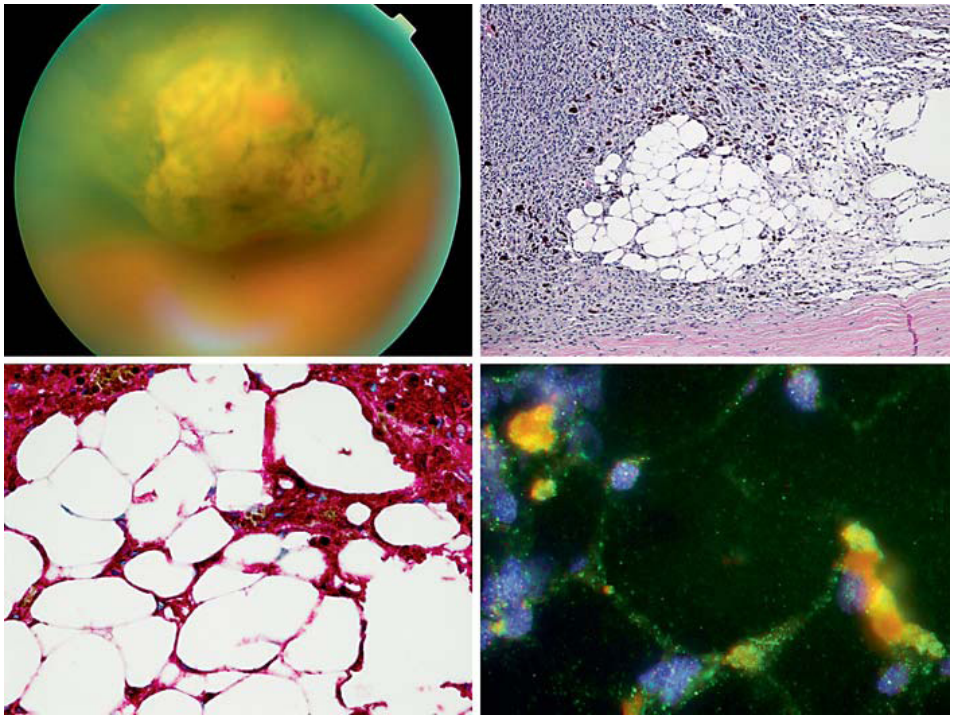

Figure. 1. Fundoscopic, histologic, immunohistochemical and genetic appearance of the tumor. **(A)** Dilated fundoscopic photography of the tumor shows a dome-shaped subretinal mass in the posterior pole. **(B)** The tumor was mainly composed of spindle type B melanoma cells with a focus of lipomatous change (hematoxylin-eosin, original magnification ×100). **(C)** The cytoplasm stained positive for the melanocytic marker HMB-45 (original magnification ×400). **(D)** On fluorescent in situ hybridization, the nucleus of a representative lipomatous tumor cell (arrow) shows three red fluorescent signals for the 6p22 probe and two green fluorescent signals for the 3p13 probe (original magnification ×640).

Discussion

Primary uveal melanoma is classified as spindle cell, epithelioid cell or mixed cell type. The epithelioid cell type is associated with a significantly worse prognosis. Unusual cytomorphologic variants of uveal melanoma have been described, such as oncocytic, neuroendocrine, balloon cell, clear cell, signet ring cell and, as in our case,

lipomatous.[1-5] Although the prognostic significance of these cytomorphologic variants is unknown, they should be recognized in order to avoid misdiagnosis with metastatic neoplasms. The divergent differentiation patterns of neoplastic uveal melanocytes may recapitulate the plasticity of neural crest stem cells. Individual cells from melanoma spheres (melanoma spheroid cells) derived from metastatic cutaneous melanoma can differentiate under appropriate conditions into multiple cell lineages such as melanocytic, adipocytic, osteocytic and chondrocytic lineages.[6] The current case demonstrates that lipomatous change can also be observed in uveal melanoma. The fluorescence in situ hybridization results showed identical changes in the spindle type B melanoma cells and the lipomatous tumor cells. Immunohistochemistry confirmed the melanocytic lineage of the lipomatous change, whereas CD34 staining, commonly positive in adipocytes, was negative. The process of metaplasia implies full expression of the characteristics of the 'new' cell type. In our case, however, the neoplastic cells resembling mature adipocytes retained the immunohistochemical features of melanocytes and lacked specific immunohistochemical features of true adipocytes. Moreover, definite proof of the lipomatous character of the histomorphologic change would require fresh frozen tissue samples for lipid stainings that were not available in our case. We therefore prefer to refer to this phenomenon as lipomatous change. Other neuroectodermal tumors that may contain adipocytes include cutaneous melanocytic nevi, schwannoma, neurofibroma, perineurioma, meningioma and adrenal adenoma.[7-12] In most cases as well as in the current case, the cells retain at least some of the characteristics of their original lineage, which would argue against true metaplasia. Lipomatous change can also be observed in different cardiac pathologic processes, including ischemia, idiopathic dilated cardiomyopathy and arrhythmogenic right ventricular dysplasia.[13] This phenomenon appears to be due to transdifferentiation of multipotential interstitial cells to adipocytes, which would be true metaplasia. Another hypothesis is that lipomatous metaplasia in cardiac muscle may be partially related to progressive myofibril degeneration and lipid accumulation within heart muscle cells, finally leading to phenotypical conversion, or lipomatous change, of cardiac myocytes into adipocyte-like cells.[13] Speculation regarding the cause of lipomatous change in uveal melanoma might include degeneration and lipid accumulation within the melanocytes due to senescence or to chronic injury such as ischemia or inflammation. To our knowledge, this is the first report of lipomatous change in uveal melanoma performed with cytogenetic investigations.

References

1. Riley FC: Balloon cell melanoma of the choroid. Arch Ophthalmol 1974; 92: 131–133.
2. Messmer EM, Hoops JP, Stefani FH: Signet ring malignant melanoma of the choroid. Invest Ophthalmol Vis Sci 1996; 37(suppl):244.
3. Verdijk RM, Koopmans AE, Kilic E, Paridaens D, de Klein A: Histopathologic, immunohistochemical, and cytogenetic analysis of primary clear cell melanoma of the uvea. JAMA Ophthalmol 2013; 131: 814–816.
4. Verdijk RM, van den Bosch T, Naus NC, Paridaens D, Mooy CM, de Klein A: Histopathologic, immunohistochemical, ultrastructural, and cytogenetic analysis of oncocytic uveal melanoma. Arch Ophthalmol 2011; 129: 1501–1502.
5. Pelayes DE, Velazquez-Martin JP, Simpson RE, Zarate JO: Primary choroidal melanoma with divergent neuroendocrine differentiation. J Ophthalmic Pathol 2013; 2: 4.
6. Fang D, Nguyen TK, Leishear K, Finko R, Kulp AN, Hotz S, Van Belle PA, Xu X, Elder DE, Herlyn M: A tumorigenic subpopulation with stem cell properties in melanomas. Cancer Res 2005; 65: 9328–9337.
7. Eng W, Cohen PR: Nevus with fat: Clinical characteristics of 100 nevi containing mature adipose cells. J Am Acad Dermatol 1998; 39: 704–711.
8. Kasantikul V, Brown WJ, Netsky MG: Mesenchymal differentiation in trigeminal neurilemmoma. Cancer 1982; 50: 1568–1571.
9. Val-Bernal JF, Gonzalez-Vela MC: Cutaneous lipomatous neurofibroma: characterization and frequency. J Cutan Pathol 2005; 32: 274–279.
10. Zamecnik M: Perineurioma with adipocytes (lipomatous perineurioma). Am J Dermatopathol 2003; 25: 171–173; author reply 173–174.
11. Roncaroli F, Scheithauer BW, Laeng RH, Cenacchi G, Abell-Aleff P, Moschopulos M: Lipomatous meningioma: a clinicopathologic study of 18 cases with special reference to the issue of metaplasia. Am J Surg Pathol 2001; 25: 769–775.
12. Finch C, Davis R, Truong LD: Extensive lipomatous metaplasia in bilateral macronodular adrenocortical hyperplasia. Arch Pathol Lab Med 1999; 123: 167–169.
13. Nucifora G, Aquaro GD, Masci PG, Barison A, Todiere G, Pingitore A, Lombardi M: Lipomatous metaplasia in ischemic cardiomyopathy: current knowledge and clinical perspective. Int J Cardiol 2010; 146: 120–122.

Chapter 4

General discussion

Over the last years many advances have been made with prognostic testing in patient with UM. Most commonly used parameters are the AJCC classification, gene-expression profiles (GEP), chromosome status, BAP1 immunohistochemistry (IHC) and mutation status of the UM. In this thesis, I focus on chromosomal aberrations and mutation status of the primary tumor to gain insight in the genetics and to discuss the difficulties using these methods. We show in Chapter 2.1 the prognostic value of *SF3B1* mutations, which is correlated to an intermediate risk for metastasis. Next, we show in Chapter 2.2 that besides the different prognostic values, UMs with respectively *BAP1*, *SF3B1* and *EIF1AX* mutations also harbor distinct chromosomal patterns and type of chromosomal aberrations.

Chapter 4.1

Prognostic values of UM specific mutations

Besides the AJCC classification, most prognostic markers divide patients with UM dichotomously in either low-risk or high-risk categories, such as GEP Class 1 versus 2 or disomy 3 versus monosomy 3.[1-3] In this thesis I show that UMs consist of multiple subtypes rather than just two groups. UM patients can be divided in high risk, intermediate risk and low risk for metastasis based on mutations in *BAP1*, *SF3B1* and *EIF1AX* (Figure 1). Patient with *BAP1*^{mut} UMs generally develop metastasis within five years after diagnosis whereas the majority of patients with *SF3B1*^{mut} UMs develop metastasis at a mean of 8 years.[4] This corresponds to the bimodal mortality patterns described by Demicheli and colleagues who show the peaks in mortality are at three years and nine years after treatment.[5] Moreover, although the majority of metastasized *SF3B1*^{mut} UMs manifest after five years, a substantial proportion (36%) is diagnosed within 5 years after diagnosis. Thus, patients with *SF3B1*^{mut} UMs, do require an intensive follow-up even though *SF3B1*^{mut} are not as frequent as *BAP1*^{mut}, and early metastasis does not occur as often as with BAP1^{neg} UMs.

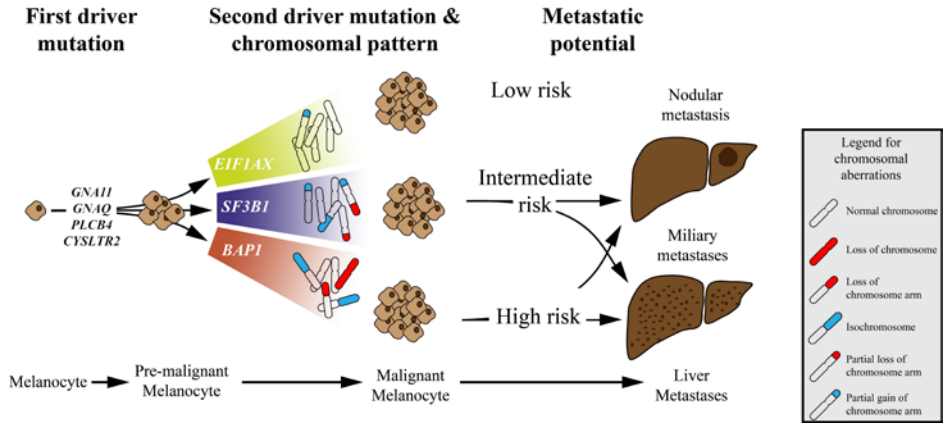

Figure 1. A simplistic schematic overview of the tumorigenesis of UM. *GNAQ*, *GNA11*, *PLCB4* and *CYSLTR2* mutation are considered the first driver mutation in UM. Following, UM develop almost mutual-exclusive mutation in the genes *EIF1AX*, *SF3B1* and *BAP1*. These tumors also harbor specific chromosomal aberrations with either copy number variations of entire chromosomes and chromosome arms or only the terminal ends of the chromosomes. *BAP1*, *SF3B1* and *EIF1AX* have different metastatic risk resulting in metastases.

Another perspective in looking at the prognostic value of an *SF3B1*^{mut}, is the fact that patients with *SF3B1*^{mut} UMs are diagnosed at an earlier median age of 54.5, whereas patients with BAP1^{neg} UMs are diagnosed at a median age of 66.9 years. So, these patients are diagnosed more than ten years earlier than patients with BAP1^{neg} UMs. In Figure 2 we can clearly see that the life-time metastasis-free survival is not different

for patients who develop metastasis with BAP1^{neg} and *SF3B1*^{mut} UMs, respectively. Although not significant, we can even observe that patients with *SF3B1*^{mut} UMs have an earlier life-time onset of metastases. This data shows that *SF3B1* mutations are not to be underestimated as a prognostic value.

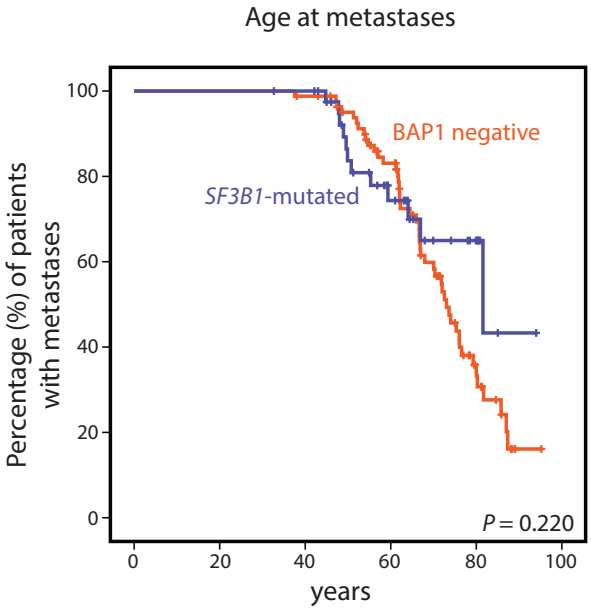

Figure 2. Survival analyses showing that the life-time risk for metastasis occurs at an younger age in patients who develop *SF3B1*-mutated UMs, compared to patients who develop BAP1 negative UMs. However this difference is limited to the first ten years and does not reach significance ($P = 0.220$).

Contrary to *BAP1* and *EIF1AX*, much controversy exists concerning the prognostic values of *GNAQ* and *GNA11* mutations. In concordance with most of the literature, our data shows that mutations in these genes do not correlate to the survival. However, there have been some reports stating that *GNA11* mutations are associated with a worse outcome than patients with *GNAQ* mutations. For example, *GNA11* mutations were found in 57% of the UM metastases, whereas *GNAQ* was mutated in only 22% of the UM metastases, suggesting that *GNA11* mutations are possibly more aggressive. By analyzing specific point mutations in the mutational signatures as shown in Chapter 2.2, we can clearly see different peaks of specific somatic nucleotide variants. When analyzed in more detail we observed that *BAP1*^{mut} UMs are enriched with *GNA11* p.Q209L mutations. For *SF3B1*^{mut} UMs on the other hand, *GNAQ* p.Q209P mutations are enriched. This difference in co-mutations would explain why *GNA11* mutations

are present more often in UM metastases, since most UMs metastases harbor *BAP1*^{mut}. Interestingly, when we stratify for *BAP1* and *SF3B1* (dataset obtained from Chapter 2.1), we observe that patients with *GNA11-SF3B1* mutations have a worse prognosis than patients with *GNAQ-SF3B1* mutations (P = 0.011). We also observe a shorter metastasis-free survival for patients with *GNA11-BAP1* compared to *GNAQ-BAP1* mutations, although this difference does not reach significance (P = 0.690).

Although *GNAQ* and *GNA11* mutations are proposed as the first events in UM tumorigenesis, the difference in co-mutated genes does suggest a different susceptibility to a second mutated gene. Moreover, patients with *GNAQ*^{mut} in the UM are diagnosed at a mean age of 58.9 years whereas patients with *GNA11*^{mut} are diagnosed at a mean age of 66.5 years, which is similar to the age at diagnosis of patients with *SF3B1*^{mut} or *BAP1*^{mut} UMs respectively. *GNAQ* mutations are also found more of in pre-malignant melanocytic lesions, such as blue naevi than *GNA11* mutations (55% versus 7% respectively).[6] It is possible that *GNAQ* hotspot mutations have a slower growth and are less aggressive. It might be that *GNAQ* mutations occur earlier than *GNA11* mutations in the melanocyte and perhaps give rise to choroidal naevi more often. This early occurrence of *GNAQ* mutation would explain the younger age of diagnosis in patients with *SF3B1*^{mut} UMs, and also the slow growing rate of metastases. To date, choroidal nevi have not yet been investigated for *GNAQ* and *GNA11* mutations. It would be interesting to investigate UMs that grow out of precursor lesions, a concept that has been performed for cutaneous melanoma.[7] This would provide more insight in the tumorigenesis and the prognostic value of *GNAQ* and *GNA11* mutations.

A challenge in prognostication based on the mutation status is the interpretation of mutations in two or more of the prognostic predicting genes (*BAP1*, *SF3B1* and *EIF1AX*). Although rare, these co-mutations are not absent. In Chapter 2.1 we describe a handful of *SF3B1* and *EIF1AX*-mutated UMs. Do these patients have an intermediate risk (*SF3B1* mutation) for metastases or the favorable effect of an *EIF1AX* mutation? The same applies to patients with BAP1^{neg} UMs that harbor *EIF1AX* mutations. We would expect that co-mutations would make a tumor more aggressive. If the tumor would not have an advantage with the co-mutated gene the rest of the tumor that doesn't harbor co-mutations would outgrow this subpopulation. However, our data does not support this assumption. For *SF3B1* and *EIF1AX* co-mutated UMs none of the patients developed metastases (range follow-up, 36-167 months). For patients with

BAP1^{neg} with *EIF1AX*^{mut} UMs, one patient did develop metastasis within five year after diagnosis whereas the other two were metastasis-free after five years. This shows that large numbers of such cases are needed to draw conclusions about co-mutations.

Despite these limitations, mutation analyses provide robust results for prognostification. In Chapter 3.1 we describe an easy method to sequence all UM related genes with one panel using the ION torrent sequencer. Especially compared to gene expression profiling (GEP), that uses a 15-gene panel to classify patients with UMs in only two risk classes (high risk versus low risk). However for both methods the major limitation is prognosticating patients for which no tumor material is available for genetic testing. I will discuss this subject later on in this Chapter.

Chapter 4.2

Difficulties in using the mutations status for prognosis

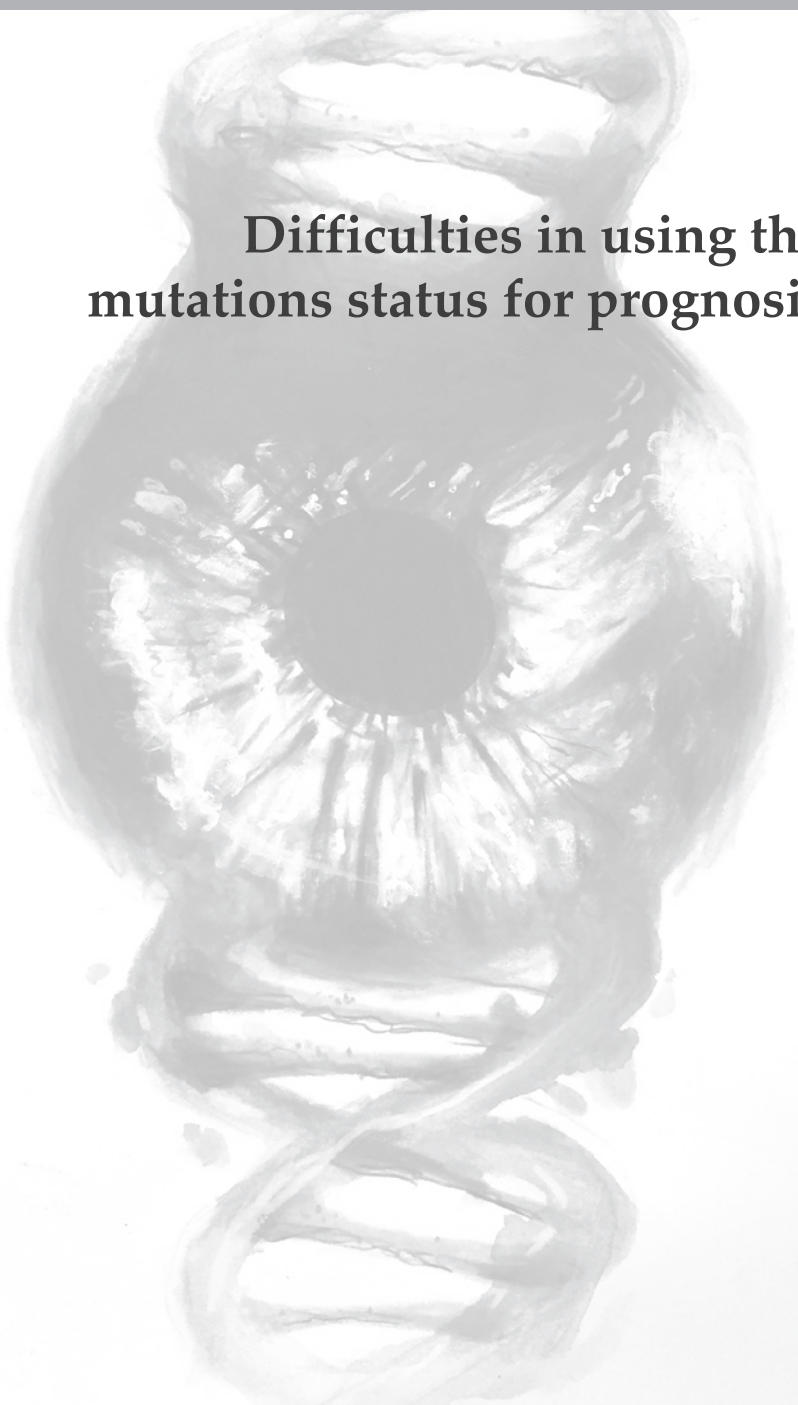

In Chapters 2.1 and 3.1 *BAP1* is shown to be the most accurate prognostic marker for patients with UMs. In our cohort, BAP1 is determined using immunohistochemistry in almost all cases. Although this technique is a quick and cheap method for prognostication, it also has its limitations.[8] *BAP1* is located on chromosome 3p, and is inactivated by a double hit.[8,9] Loss of BAP1 expression is almost congruent with monosomy 3, however this is not always the case. In some cases, we observe a BAP1 negative expression whereas there are still two copies of chromosome 3. This is either by isodisomy 3 formation or local deletion of the *BAP1* gene. Furthermore, we also observe a proportion of monosomy 3 UMs that do express BAP1. For these cases we also did not observe *SF3B1* and *EIF1AX* mutations, and thus classified them as 'No Recurrent Mutation' (NRM) UMs as described in Chapter 2.2. Secondary mutation analyses of *BAP1*, revealed somatic non-truncating mutations in most cases, which would explain why BAP1 is still expressed. Moreover, these tumors display the same chromosomal patterns as BAP1^{neg} UMs and also develop metastases at the same rate as BAP1^{neg} UMs. This indicates that in these BAP1^{pos} UMs with *BAP1* mutations, BAP1 is very likely impaired resulting in the same pathogenicity as in BAP1^{neg} UMs. Since *BAP1* is a tumor suppressor gene, infinite amount of mutations are possible to inactive BAP1. Thus when mutated, *BAP1* can contain large and complex deletions and insertions that are hard or even impossible to detect with conventional Sanger or Targeted-exome sequencing.[10] Moreover, exon 1 of *BAP1* is hardly covered with our next-generation sequencing techniques (ION torrent and WES) and is also hardly covered in the WES samples of UMs in The Cancer Genome Atlas (TCGA) database. Even with conventional Sanger sequencing exon 1 requires a different protocol than all other exons. Thus for *BAP1* no method is perfect and cases that do not fit the profile (e.g. monosomy 3 with BAP1 expression) should be investigated in more thoroughly.[10]

So, some of the NRM UMs can be explained by a non-truncating mutation in *BAP1*, however many NRM UMs do not harbor a *BAP1* mutation. Thus for these cases the novel gene discovery phase is not over yet. For this, publicly available genomic data such as The Cancer Genome Atlas (TCGA) and data-sharing initiatives by several publishers may play a huge role. Since several independent groups published WES and WGS data online, larger datasets could be made to investigate UMs for rare recurring mutated genes. In this way, mutations in *CYSLTR2* and *PLCB4* were found UMs that are wildtype for *GNAQ* and *GNA11*.[11,12] Collectively, these four genes explain the early proliferative event (first mutated gene) in almost all UM.

However, for the second mutated gene in UM more genes are yet to be discovered. In our cohort of 133 UMs (**Chapter 2.1**) we show that 17% of the UMs are wildtype for *BAP1*, *SF3B1* and *EIF1AX*. For this a selections of UMs can be made for sequencing. A method would be to analyze UMs with *BAP1*-like, *SF3B1*-like or *EIF1AX*-like chromosomal patterns. In breast cancer it has already been shown that based on chromosomal patterns the tumors can be divided into *BRCA*-like and non *BRCA*-like breast cancers.[13] Interestingly, a large proportion of these *BRCA*-like breast cancers do not harbor *BRCA* mutations or methylation, but do display similar molecular characteristics and also benefit from the same therapies as the tumors with *BRCA* mutations.[14] In the case of UMs, tumors which harbor *SF3B1*-like chromosome patterns should be analyzed for other splicing factors, especially since mutations in splicing factors such as *SRSF2*, *U2AF1* and *ZRSR2* are common in other malignancies.[15] We also show that isochromosome formation is a characteristic of BAP1^{neg} UMs. However, some UMs with isochromosomes are BAP1^{pos} and lack *BAP1* mutations. For these UMs it would be interesting to analyze other genes that are known to be involved in DNA integrity, chromosome segregation or isochromosome formation. For example, *BAP1* mutations are also found in a considerable proportion (5%) of hepatocellular carcinomas (HCCs).[16] These *BAP1*^{mut} HCCs also harbor isochromosomes (n = 15 of the 24), in particular isochromosome 8q. Moreover, HCCs without *BAP1*^{mut} also harbor isochromosomes.[16] Recurrent mutated genes in these *BAP1*-like HCCs might also be mutated in *BAP1*-like UM.

Concluding, the novel gene discovery phase in UM research has made great advances, however there are still UMs that cannot be explained by the currently known genes. These cases pose a challenge in patient prognostication and might be a challenge in future targeted therapies. Therefore, sequencing selected UMs that harbor similar chromosomal patterns should lead to the discovery of *de novo* mutated genes involved in UM tumorigenesis.

Chapter 4.3

Uveal melanoma: genetically one tumor type or different tumor types?

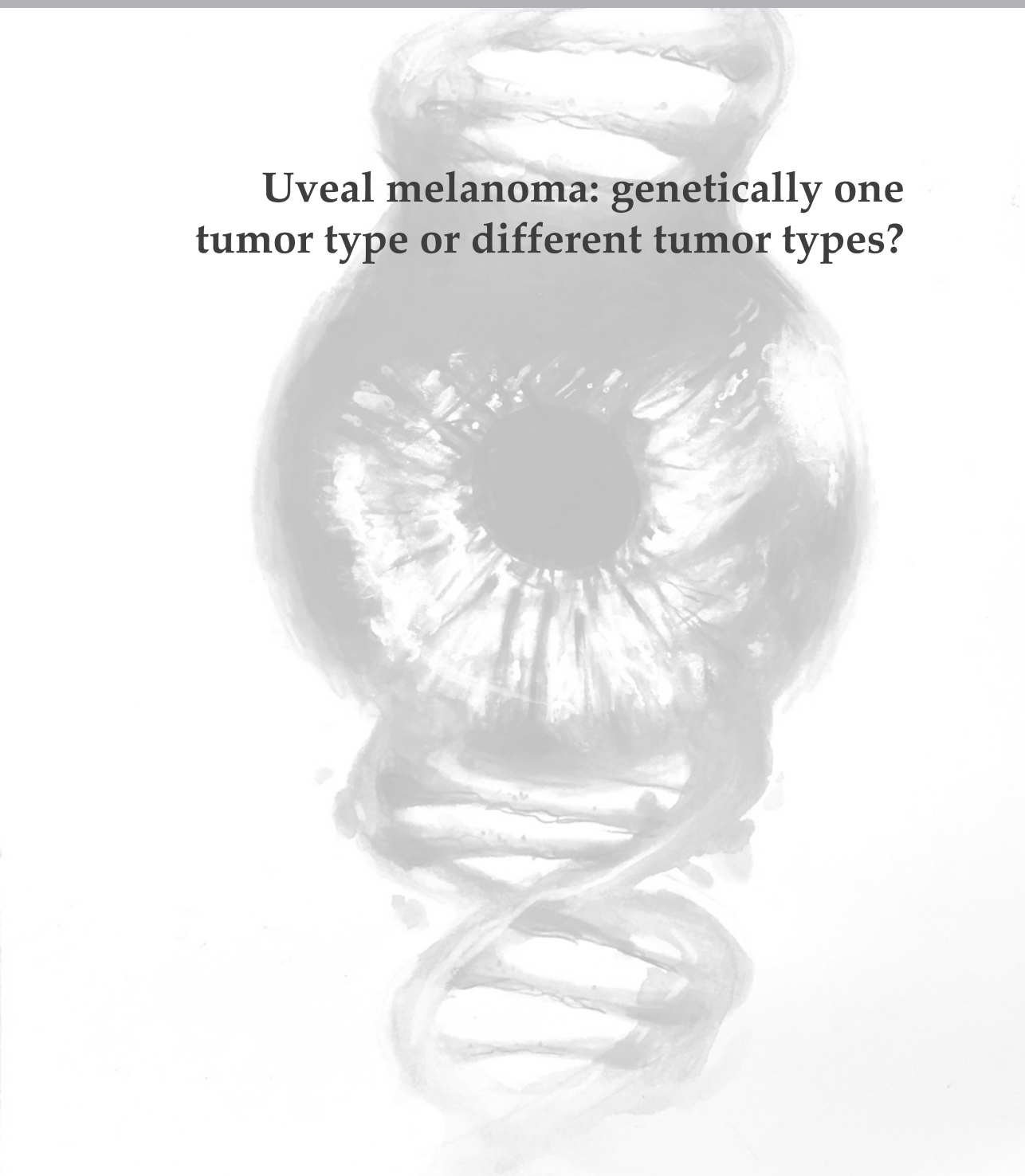

We clearly show that the chromosomal patterns for *BAP1*^{mut}, *SF3B1*^{mut} and *EIF1AX*^{mut} UMs differ based on the different types of chromosomal aberrations.[17] This observation, together with the mutual exclusivity of mutated genes, shows that UMs with different mutated genes are genetically distinct and are not part of one evolutionary process. For example, if one would expect that intermediate risk UMs (*SF3B1*^{mut}) are predecessors of high risk UMs (*BAP1*^{mut}), the latter group should harbor co-mutations. However we and others only rarely describe co-mutations.[4,18-20]

BAP1^{mut} UMs are characterized by numerical and whole chromosome arm aberrations such as isochromosomes and *SF3B1*^{mut} UMs are characterized by structural CNVs (Figure 1). Singh and colleagues state that, evolutionary, the gain of the terminal end of 8q is the first event that is then followed by the gain of the centromeric part of 8q resulting in a gain of the entire chromosome 8q arm.[21] According to our results in Chapter 2.2, gain of the entire arm of chromosome 8q is one event, resulting from isochromosome formation.[17] This observation is confirmed by karyograms of UMs by looking at individual cells. This highlights that these conventional techniques are still useful and informative in research, since these observations contradicted purely mathematical analyses. Another hypothesis in UM research is that chromosome 8q gain precedes monosomy 3.[22] This is based on calculation of the load of chromosome 8q and chromosome 3 in the tumor samples. By assuming that chromosome 8q gain in UMs is based on three copies, and monosomy 3 is based on one copy, it is shown that most UMs have more tumor cells containing three copies of chromosome 8q than cells containing monosomy 3. Concluding that chromosome 8q gain precedes monosomy 3. However, this assumption is false since it has been described that UMs do not contain just three copies of chromosome 8q but usually more than three copies in most UM cells.[23] Not taking this into count overestimates the amount of cells with chromosome 8q gain. Besides, we clearly show that *BAP1* mutations are associated with isochromosome formation. Therefore it is much more likely that BAP1 deficiency (caused by loss of chromosome 3) causes isochromosome formation and thus chromosome 8q gain. UMs with different mutated genes have other pathways involved in generating chromosomal aberrations and also give different risks for metastasis. Therefore, UMs can be divided in at least three subtypes based on the mutations status of *BAP1*, *SF3B1* and *EIF1AX*.

How about polyploidy? Are UMs with polyploidy a subtype, or is polyploidy part of an already defined evolutionary pathway? Polyploidy is a state of the cell in which

genome doubling has occurred.[24] Polyploidy in other malignancies is shown to be associated with worse outcome and these polyploid malignancies also tend to be more therapy resistant due to their genomic instability.[24,25] In UM patients we did observe a slight worse survival in polyploid BAP1^{neg} UMs compared to diploid BAP1^{neg} UMs. This would suggest that polyploid UMs are more aggressive, however we believe that this is a bias. No single sample harbored heterozygous *BAP1* mutations even though some UMs contained two copies of chromosome 3, indicating that *BAP1* mutations and the loss of chromosome 3 precedes the genome doubling (polyploidization). We hypothesize polyploidization is a late event in the tumorigenesis. This hypothesis is supported by the fact that polyploid BAP1^{neg} UMs are larger than diploid BAP1^{neg} UM at time of diagnosis. We believe that polyploidy is a late event in UM tumorigenesis, and thus does not represent a separate subtype. However, polyploidy can cause false results if prognostification is based on chromosome analyses. Therefore, the genome should be checked for polyploidy. Also, polyploidy might cause therapy resistance as in other malignancies. Unfortunately, no successful treatment of UM metastases is yet available.

Chapter 4.4

Clinical implications and therapeutic options

BAP1 and *SF3B1* are described in many cellular mechanisms. BAP1 is a deubiquinitase of Histone A2 (H2A). BAP1 deficiency is shown to increase the ubiquitinase of H2A, that might lead to anti-apoptotic features.[26] *In silico* screens of therapeutic compounds in UM cell lines showed that Histone deacytelase (HDAC) inhibitors might be potential candidates for BAP1 deficient UM.[27] *In vivo* experiments show that these HDAC inhibitors indeed cause cell cycle arrest and also induce melanocytic cell differentiation.[27] Malignant pleural mesothelioma also harbor *BAP1* mutations resulting in loss of BAP1 expression.[28] A clinical phase III trial, using the HDAC inhibitor vorinostat showed that this compound is unfortunately ineffective in patients with malignant pleural melanoma.[29] Another consequence of loss of BAP1 is the increase of enhancer of zeste 2 polycomb repressive complex 2 subunit (EZH2) in the tumors of patients with malignant pleural mesothelioma.[30] Although mesothelioma with BAP1 deficiency showed sensitivity to EZH2 inhibitors, this effect was not found in BAP1 deficient UM cells.[31,32] These findings show that BAP1 deficiency between different malignancies do not need to results in the same molecular effects.

Most well-known function of *SF3B1* is the role in splicing.[33] *SF3B1* mutations in uveal melanoma almost always target hotspot codon p.R625.[4,20,33,34] For this mutation, and for the less occurring hotspot mutation p.K666, it is shown that mutant *SF3B1* does not function as an oncogene or tumor suppressor gene, but rather as a change-of-function mutant gene.[35] *SF3B1*^{mut} results in an alternative use of 3' splice site recognition sites and use of an alternative branch point, resulting in alternative spliced products, which may give rise to tumorigenesis. [35,36] Also, there are also reports on how cancer cells harboring mutation in genes encoding for splicing factors are dependent on the wild-type allele of the gene to prevent apoptosis.[37,38] This does not only provide possibilities by targeting alternative splicing in cancer but also targeting the normal functioning splicing factors.[39,40] Similar to the DNA damage repair pathway targeted therapies, this might also push the cell 'over the edge', making it too unstable to survive.

Targeting the downstream pathways of *GNAQ* and *GNA11* have also been investigated extensively. *GNAQ* and *GNA11* hotspot mutations result in a continuous activation of Gα and its downstream pathways. A major downstream effector is the MEK-ERK1/2 pathway, which is shown to be targetable in UM cell lines by MEK1/2 inhibitors such as selumetinib or trametinib.[41,42] Unfortunately, in clinical trials, these inhibitors were not successful in treating metastatic disease in UM patients.[43-45] Hepatocyte growth factor (HGF) is highly expressed in liver microenvironment, and is shown to cause

MEK-inhibitor resistance in UM cell lines.[41] *Ex vivo* experiment showed that co-targeting HGF with MEK inhibitors might be successful in treating metastatic disease.[46] Another downstream activated protein is Yes-associated protein (YAP). YAP is an effector protein of the Hippo pathway, a pathway involved in organ growth. In UM cell lines *GNAQ* and *GNA11* mutations stimulate YAP through a Hippo-independent manner.[47,48] YAP inhibition with verteporfin causes growth arrest in *GNAQ*^{mut} and *GNA11*^{mut} UM cell lines.[49] YAP is also identified as a cause for resistance in several malignancies and targeting YAP is shown to sensitize malignancies to MEK inhibitors.[50] This emphasizes that co-targeting several pathways simultaneous might potentially provide success in treating metastatic disease.

Many potential pathways are targetable in patients with UM. Yet, no treatment is successful. Recent years, progress has been made in the field of oncology targeting DNA damage repair (DDR) impaired malignancies.[51] Malignancies with impaired DNA damage pathways are more error-prone to genetic alterations. By targeting these pathways, cancer cells accumulate mutations and chromosomal aberrations, that make the already unstable cancer cells highly unstable for chromosomal aberrations, causing apoptosis.[51,52]

BAP1 encodes for a deubiquitinase involved in chromatin remodeling and *SF3B1* encodes for a splicing factor as described earlier. However besides these functions, both genes are also involved in DDR.[35,53-56] It is shown that *BAP1* is involved in homologous recombination (HR), an error-free DNA repair mechanism.[56] BAP1 deficient cells that become HR deficient might make use of the error-prone non-homologous end-joining (NHEJ) repair mechanism, resulting in chromosomal aberrations and mutational insertions and deletions (InDels).[56] Also mutated *SF3B1* in chronic lymphocytic leukemia is known to be involved in DDR.[54] One might thus expect impaired DDR in UMs with mutations in *BAP1* or *SF3B1*. Is this the case?

In several malignancies, DDR deficiencies lead to an accumulation of mutations and promote genome instability.[57,58] WGS of UM samples show that the mutational burden per cell is less than one mutation per Mb of genome. On average only 20 coding single-nucleotide variations (SNVs) are found, placing UMs between pediatric malignancies which also have a very low mutational load.[33,59] Second argument in spite of DDR deficiency in UMs, is the chromosomal aberrations and the tumor heterogeneity. DDR deficiencies cause tumor heterogeneity due to the genomic instability and rapidly

changing genome.[57,60] We show in **Chapter 2.2** that *BAP1*^{mut} UMs are characterized by the lack of structural variants making it very unlikely that these cells make use of NHEJ. Moreover, monosomy 3 UMs are shown to be quite homogenous.[61] As *SF3B1*^{mut} harbor more structural chromosomal aberrations, it might be that these tumors make use of NHEJ. Mutational signatures analysis is a recently developed method to gain more insight in the mutational spectrum of malignancies by analyzing somatic SNVs and the flanking nucleotides.[62] In UM research this has also been performed in several studies. Although, signatures associated with DDR pathways are present in UMs, all three publications on this topic display a discrepancy in the found signatures.[11,33,59]

Summarizing, the mutational load and the lack of chromosomal instability suggest that DDR is not impaired or only slightly impaired, whereas the mutational signatures and functional experiments on non-UM cells do suggests impaired DDR in UM.

Chapter 4.5

Future prospect and experimental considerations

In this Chapter I describe and discuss several insights in the genetics of UM. Using genetic data we draw conclusions regarding the prognosis and molecular processes. However, this also means that there is a bias towards larger tumors that are investigated in this thesis. In our cohort, material from the primary tumors is almost always obtained by enucleation and hardly by biopsies. Medium-sized and small-sized UMs are generally treated using eye-saving irradiation techniques such as protonbeam, stereotactic radiotherapy and brachytherapy. In these patients, no material of the primary tumor is available unless a biopsy is taken. Currently, no other method than the AJCC classification is available to prognosticate these patients.

Luckily, many advances are made in the field of liquid biopsies.[63] These techniques are already clinical used for analyzing fetal circulating free DNA (cfDNA) in the mothers' plasma.[64] Also for patients with solid malignancies it is shown that the load of cfDNA is higher compared to healthy subjects.[65] Targeting specific somatic mutations of the primary tumor, the mutational load in the circulation can be calculated and used for monitoring.[63]

Taking advantage of the fact that roughly 95% of the UMs harbor a hotspot mutation (*GNAQ* p.Q209 and p.R184, *GNA11* p.Q209 and p.R184, *CYSLTR2* p.L129 and *PLCB4* p.D630), these mutations may be picked up using a handful of allele-specific PCRs on patient' blood sample for whom the mutation status is unknown. This can also be used for *SF3B1* since in UMs with *SF3B1*^{mut} amino acid p.R625 is targeted in the majority of cases. However, for *BAP1* and *EIF1AX* this cannot be applied. Since *BAP1* is a tumor suppressor gene, infinite possible mutations can cause a loss of BAP1. For these UMs is would be perhaps be more useful to detect the monosomy 3 of the primary tumor. For fetal DNA it is possible to detect e.g. trisomy 21 in the maternal plasma.[64] This would be more challenging for circulating tumor DNA, since a loss of a chromosome would require different algorithms and also UMs contain more chromosomal aberrations which would make the analyses more difficult.[66] Other methods using liquid biopsies are also possible and investigated in UM research. Achberger and colleagues describe the detection of circulating immune cells and microRNA as biomarkers for metastatic disease.[67]

Another development in the field of oncology is the use of exosomes obtained from patients' plasma. Exosomes are small vesicles secreted by cells, which carry messenger RNA (mRNA), microRNA (miRNA) and also DNA.[68,69] This provides novel transla-

tional possibilities for surveillance of UM patients by harvesting exosomes secreted by primary or the metastatic tumor. Recent research also showed that exosomes play a part in the metastatic process. For gastric cancer it is shown that the membrane protein epidermal growth factor receptor (EGFR) of the exosomes can be transferred to liver stromal cells and activate HGF.[70] Besides the role of HGF in MEK-inhibitor resistance in UM cell lines, HGF also plays a role in providing a suitable microenvironment for cancer cells.[46,70] Yet again, this highlights that the metastatic process of UMs is complicated and that more research is required for a better understanding.

Considering future treatment options for UM metastases we have touched upon the topic of using splicing inhibitors, targeting DNA-damage pathways, downstream pathways of *GNAQ/11* and others. A more recent developed technique on gene level is using the clustered regularly interspaced short palindromic repeats (CRISPR) and CRISPR-associated System (cas); CRISPR-cas. Chen and colleagues used this technique in liver cancer and prostate cancer cells by exploiting cancer-specific genetic abnormalities.[71] They used a method that implemented 'suicide' genes in the fusion gene, and thus replacing the cancer gene that is responsible for tumor invasion and rapid growth by a suicide gene that causes cell death. This method proved to be effective in mice.

For UM this would be an applicable technique as almost all UM harbor a cancer-specific hotspot mutation in *GNAQ* or *GNA11*. By targeting this hotspot location replacing the oncogene by a suicide gene would result in apoptosis rather than proliferation. Unfortunately, this highly exciting new technique still has its limitations. In theory only cancer cells would be targeted since only these cell harbor the mutation. However, non-specific targets (non-cancer cells) and off-target binding are serious challenges that still need to be overcome.[72] Another described problem is resistance/immunity against the (viral) vector that carry the CRISPR system.[73] The CRISPR technique is promising, but needs to be investigated in more detail.

Concluding, although uveal melanoma have limited number of mutations the tumorigenesis has not been completely unraveled, and additional research is needed to move forward for an efficient approach to treat metastatic disease in UM patients.

References

1. Onken, M.D., Worley, L.A., Ehlers, J.P. & Harbour, J.W. Gene expression profiling in uveal melanoma reveals two molecular classes and predicts metastatic death. *Cancer Res* **64**, 7205-9 (2004).
2. Prescher, G., Bornfeld, N. & Becher, R. Nonrandom chromosomal abnormalities in primary uveal melanoma. *J Natl Cancer Inst* **82**, 1765-9 (1990).
3. Sisley, K. *et al.* Non-random abnormalities of chromosomes 3, 6, and 8 associated with posterior uveal melanoma. *Genes Chromosomes Cancer* **5**, 197-200 (1992).
4. Yavuzyigitoglu, S. *et al.* Uveal Melanomas with SF3B1 Mutations: A Distinct Subclass Associated with Late-Onset Metastases. *Ophthalmology* **123**, 1118-28 (2016).
5. Demicheli, R., Fornili, M. & Biganzoli, E. Bimodal mortality dynamics for uveal melanoma: a cue for metastasis development traits? *BMC Cancer* **14**, 392 (2014).
6. Van Raamsdonk, C.D. *et al.* Mutations in GNA11 in uveal melanoma. *N Engl J Med* **363**, 2191-9 (2010).
7. Shain, A.H. *et al.* The Genetic Evolution of Melanoma from Precursor Lesions. *N Engl J Med* **373**, 1926-36 (2015).
8. Koopmans, A.E. *et al.* Clinical significance of immunohistochemistry for detection of BAP1 mutations in uveal melanoma. *Mod Pathol* **27**, 1321-30 (2014).
9. Harbour, J.W. *et al.* Frequent mutation of BAP1 in metastasizing uveal melanomas. *Science* **330**, 1410-3 (2010).
10. van de Nes, J.A. *et al.* Comparing the Prognostic Value of BAP1 Mutation Pattern, Chromosome 3 Status, and BAP1 Immunohistochemistry in Uveal Melanoma. *Am J Surg Pathol* **40**, 796-805 (2016).
11. Johansson, P. *et al.* Deep sequencing of uveal melanoma identifies a recurrent mutation in PLCB4. *Oncotarget* **7**, 4624-31 (2016).
12. Moore, A.R. *et al.* Recurrent activating mutations of G-protein-coupled receptor CYSLTR2 in uveal melanoma. *Nat Genet* **48**, 675-80 (2016).
13. Lips, E.H. *et al.* Quantitative copy number analysis by Multiplex Ligation-dependent Probe Amplification (MLPA) of BRCA1-associated breast cancer regions identifies BRCAness. *Breast Cancer Res* **13**, R107 (2011).
14. Severson, T.M. *et al.* BRCA1-like signature in triple negative breast cancer: Molecular and clinical characterization reveals subgroups with therapeutic potential. *Mol Oncol* **9**, 1528-38 (2015).
15. Bejar, R. Splicing Factor Mutations in Cancer. *Adv Exp Med Biol* **907**, 215-28 (2016).
16. Cancer Genome Atlas Research Network. Electronic address, w.b.e. & Cancer Genome Atlas Research, N. Comprehensive and Integrative Genomic Characterization of Hepatocellular Carcinoma. *Cell* **169**, 1327-1341 e23 (2017).
17. Yavuzyigitoglu, S. *et al.* Correlation of Gene Mutation Status with Copy Number Profile in Uveal Melanoma. *Ophthalmology* **124**, 573-575 (2017).
18. Decatur, C.L. *et al.* Driver Mutations in Uveal Melanoma: Associations With Gene Expression Profile and Patient Outcomes. *JAMA Ophthalmol* **134**, 728-33 (2016).
19. Dono, M. *et al.* Mutation frequencies of GNAQ, GNA11, BAP1, SF3B1, EIF1AX and TERT in uveal melanoma: detection of an activating mutation in the TERT gene promoter in a single case of uveal melanoma. *Br J Cancer* **110**, 1058-65 (2014).
20. Martin, M. *et al.* Exome sequencing identifies recurrent somatic mutations in EIF1AX and SF3B1 in uveal melanoma with disomy 3. *Nat Genet* **45**, 933-6 (2013).
21. Singh, N., Singh, A.D. & Hide, W. Inferring an Evolutionary Tree of Uveal Melanoma From Genomic Copy Number Aberrations. *Invest Ophthalmol Vis Sci* **56**, 6801-9 (2015).
22. de Lange, M.J. *et al.* Heterogeneity revealed by integrated genomic analysis uncovers a molecular switch in malignant uveal melanoma. *Oncotarget* **6**, 37824-35 (2015).
23. van den Bosch, T. *et al.* Higher percentage of FISH-determined monosomy 3 and 8q amplification in uveal melanoma cells relate to poor patient prognosis. *Invest Ophthalmol Vis Sci* **53**, 2668-74 (2012).
24. Davoli, T. & de Lange, T. The causes and consequences of polyploidy in normal development and cancer. *Annu Rev Cell Dev Biol* **27**, 585-610 (2011).

25. Kuznetsova, A.Y. *et al.* Chromosomal instability, tolerance of mitotic errors and multidrug resistance are promoted by tetraploidization in human cells. *Cell Cycle* **14**, 2810-20 (2015).
26. Wang, A., Papneja, A., Hyrcza, M., Al-Habeeb, A. & Ghazarian, D. Gene of the month: BAP1. *J Clin Pathol* **69**, 750-3 (2016).
27. Landreville, S. *et al.* Histone deacetylase inhibitors induce growth arrest and differentiation in uveal melanoma. *Clin Cancer Res* **18**, 408-16 (2012).
28. Yoshikawa, Y. *et al.* Frequent inactivation of the BAP1 gene in epithelioid-type malignant mesothelioma. *Cancer Sci* **103**, 868-74 (2012).
29. Krug, L.M. *et al.* Vorinostat in patients with advanced malignant pleural mesothelioma who have progressed on previous chemotherapy (VANTAGE-014): a phase 3, double-blind, randomised, placebo-controlled trial. *Lancet Oncol* **16**, 447-56 (2015).
30. LaFave, L.M. *et al.* Loss of BAP1 function leads to EZH2-dependent transformation. *Nat Med* **21**, 1344-9 (2015).
31. LaFave, L.M. *et al.* Reply to "Uveal melanoma cells are resistant to EZH2 inhibition regardless of BAP1 status". *Nat Med* **22**, 578-9 (2016).
32. Schoumacher, M. *et al.* Uveal melanoma cells are resistant to EZH2 inhibition regardless of BAP1 status. *Nat Med* **22**, 577-8 (2016).
33. Furney, S.J. *et al.* SF3B1 mutations are associated with alternative splicing in uveal melanoma. *Cancer Discov* **3**, 1122-9 (2013).
34. Harbour, J.W. *et al.* Recurrent mutations at codon 625 of the splicing factor SF3B1 in uveal melanoma. *Nat Genet* **45**, 133-5 (2013).
35. Alsafadi, S. *et al.* Cancer-associated SF3B1 mutations affect alternative splicing by promoting alternative branchpoint usage. *Nat Commun* **7**, 10615 (2016).
36. Kesarwani, A.K. *et al.* Cancer-associated SF3B1 mutants recognize otherwise inaccessible cryptic 3′ splice sites within RNA secondary structures. *Oncogene* **36**, 1123-1133 (2017).
37. Lee, S.C. *et al.* Modulation of splicing catalysis for therapeutic targeting of leukemia with mutations in genes encoding spliceosomal proteins. *Nat Med* **22**, 672-8 (2016).
38. Zhou, Q. *et al.* A chemical genetics approach for the functional assessment of novel cancer genes. *Cancer Res* **75**, 1949-58 (2015).
39. Effenberger, K.A., Urabe, V.K., Prichard, B.E., Ghosh, A.K. & Jurica, M.S. Interchangeable SF3B1 inhibitors interfere with pre-mRNA splicing at multiple stages. *RNA* **22**, 350-9 (2016).
40. Lee, S.C. & Abdel-Wahab, O. Therapeutic targeting of splicing in cancer. *Nat Med* **22**, 976-86 (2016).
41. Cheng, H. *et al.* Paracrine Effect of NRG1 and HGF Drives Resistance to MEK Inhibitors in Metastatic Uveal Melanoma. *Cancer Res* **75**, 2737-48 (2015).
42. Khalili, J.S. *et al.* Combination small molecule MEK and PI3K inhibition enhances uveal melanoma cell death in a mutant GNAQ- and GNA11-dependent manner. *Clin Cancer Res* **18**, 4345-55 (2012).
43. Carvajal, R.D., Schwartz, G.K., Mann, H., Smith, I. & Nathan, P.D. Study design and rationale for a randomised, placebo-controlled, double-blind study to assess the efficacy of selumetinib (AZD6244; ARRY-142886) in combination with dacarbazine in patients with metastatic uveal melanoma (SUMIT). *BMC Cancer* **15**, 467 (2015).
44. Carvajal, R.D. *et al.* Effect of selumetinib vs chemotherapy on progression-free survival in uveal melanoma: a randomized clinical trial. *JAMA* **311**, 2397-405 (2014).
45. Falchook, G.S. *et al.* Activity of the oral MEK inhibitor trametinib in patients with advanced melanoma: a phase 1 dose-escalation trial. *Lancet Oncol* **13**, 782-9 (2012).
46. Cheng, H. *et al.* Co-targeting HGF/cMET Signaling with MEK Inhibitors in Metastatic Uveal Melanoma. *Mol Cancer Ther* **16**, 516-528 (2017).
47. Feng, X. *et al.* Hippo-independent activation of YAP by the GNAQ uveal melanoma oncogene through a trio-regulated rho GTPase signaling circuitry. *Cancer Cell* **25**, 831-45 (2014).
48. Yu, F.X. *et al.* Mutant Gq/11 promote uveal melanoma tumorigenesis by activating YAP. *Cancer Cell* **25**, 822-30 (2014).
49. Lyubasyuk, V., Ouyang, H., Yu, F.X., Guan, K.L. & Zhang, K. YAP inhibition blocks uveal melanogenesis driven by GNAQ or GNA11 mutations. *Mol Cell Oncol* **2**, e970957 (2015).
50. Lin, L. *et al.* The Hippo effector YAP promotes resistance to RAF- and MEK-targeted cancer therapies. *Nat Genet* **47**, 250-6 (2015).
51. Kelley, M.R., Logsdon, D. & Fishel, M.L. Targeting DNA repair pathways for cancer treatment:

what's new? *Future Oncol* **10**, 1215-37 (2014).
52. Pavey, S., Spoerri, L., Haass, N.K. & Gabrielli, B. DNA repair and cell cycle checkpoint defects as drivers and therapeutic targets in melanoma. *Pigment Cell Melanoma Res* **26**, 805-16 (2013).
53. Carbone, M. *et al.* BAP1 and cancer. *Nat Rev Cancer* **13**, 153-9 (2013).
54. Te Raa, G.D. *et al.* The impact of SF3B1 mutations in CLL on the DNA-damage response. *Leukemia* **29**, 1133-42 (2015).
55. Yu, H. *et al.* The ubiquitin carboxyl hydrolase BAP1 forms a ternary complex with YY1 and HCF-1 and is a critical regulator of gene expression. *Mol Cell Biol* **30**, 5071-85 (2010).
56. Yu, H. *et al.* Tumor suppressor and deubiquitinase BAP1 promotes DNA double-strand break repair. *Proc Natl Acad Sci U S A* **111**, 285-90 (2014).
57. Broustas, C.G. & Lieberman, H.B. DNA damage response genes and the development of cancer metastasis. *Radiat Res* **181**, 111-30 (2014).
58. Toyota, M. & Suzuki, H. Epigenetic drivers of genetic alterations. *Adv Genet* **70**, 309-23 (2010).
59. Royer-Bertrand, B. *et al.* Comprehensive Genetic Landscape of Uveal Melanoma by Whole-Genome Sequencing. *Am J Hum Genet* **99**, 1190-1198 (2016).
60. Bartek, J., Bartkova, J. & Lukas, J. DNA damage signalling guards against activated oncogenes and tumour progression. *Oncogene* **26**, 7773-9 (2007).
61. Mensink, H.W. *et al.* Chromosome 3 intratumor heterogeneity in uveal melanoma. *Invest Ophthalmol Vis Sci* **50**, 500-4 (2009).
62. Alexandrov, L.B. & Stratton, M.R. Mutational signatures: the patterns of somatic mutations hidden in cancer genomes. *Curr Opin Genet Dev* **24**, 52-60 (2014).
63. Wan, J.C. *et al.* Liquid biopsies come of age: towards implementation of circulating tumour DNA. *Nat Rev Cancer* **17**, 223-238 (2017).
64. Hill, M. *et al.* Evaluation of non-invasive prenatal testing (NIPT) for aneuploidy in an NHS setting: a reliable accurate prenatal non-invasive diagnosis (RAPID) protocol. *BMC Pregnancy Childbirth* **14**, 229 (2014).
65. Leon, S.A., Shapiro, B., Sklaroff, D.M. & Yaros, M.J. Free DNA in the serum of cancer patients and the effect of therapy. *Cancer Res* **37**, 646-50 (1977).
66. Oellerich, M. *et al.* Using circulating cell-free DNA to monitor personalized cancer therapy. *Crit Rev Clin Lab Sci* **54**, 205-218 (2017).
67. Achberger, S. *et al.* Circulating immune cell and microRNA in patients with uveal melanoma developing metastatic disease. *Mol Immunol* **58**, 182-6 (2014).
68. Thakur, B.K. *et al.* Double-stranded DNA in exosomes: a novel biomarker in cancer detection. *Cell Res* **24**, 766-9 (2014).
69. Valadi, H. *et al.* Exosome-mediated transfer of mRNAs and microRNAs is a novel mechanism of genetic exchange between cells. *Nat Cell Biol* **9**, 654-9 (2007).
70. Zhang, H. *et al.* Exosome-delivered EGFR regulates liver microenvironment to promote gastric cancer liver metastasis. *Nat Commun* **8**, 15016 (2017).
71. Chen, Z.H. *et al.* Targeting genomic rearrangements in tumor cells through Cas9-mediated insertion of a suicide gene. *Nat Biotechnol* **35**, 543-550 (2017).
72. Zhang, X.H., Tee, L.Y., Wang, X.G., Huang, Q.S. & Yang, S.H. Off-target Effects in CRISPR/Cas9-mediated Genome Engineering. *Mol Ther Nucleic Acids* **4**, e264 (2015).
73. Peng, R., Lin, G. & Li, J. Potential pitfalls of CRISPR/Cas9-mediated genome editing. *FEBS J* **283**, 1218-31 (2016).

Chapter 5

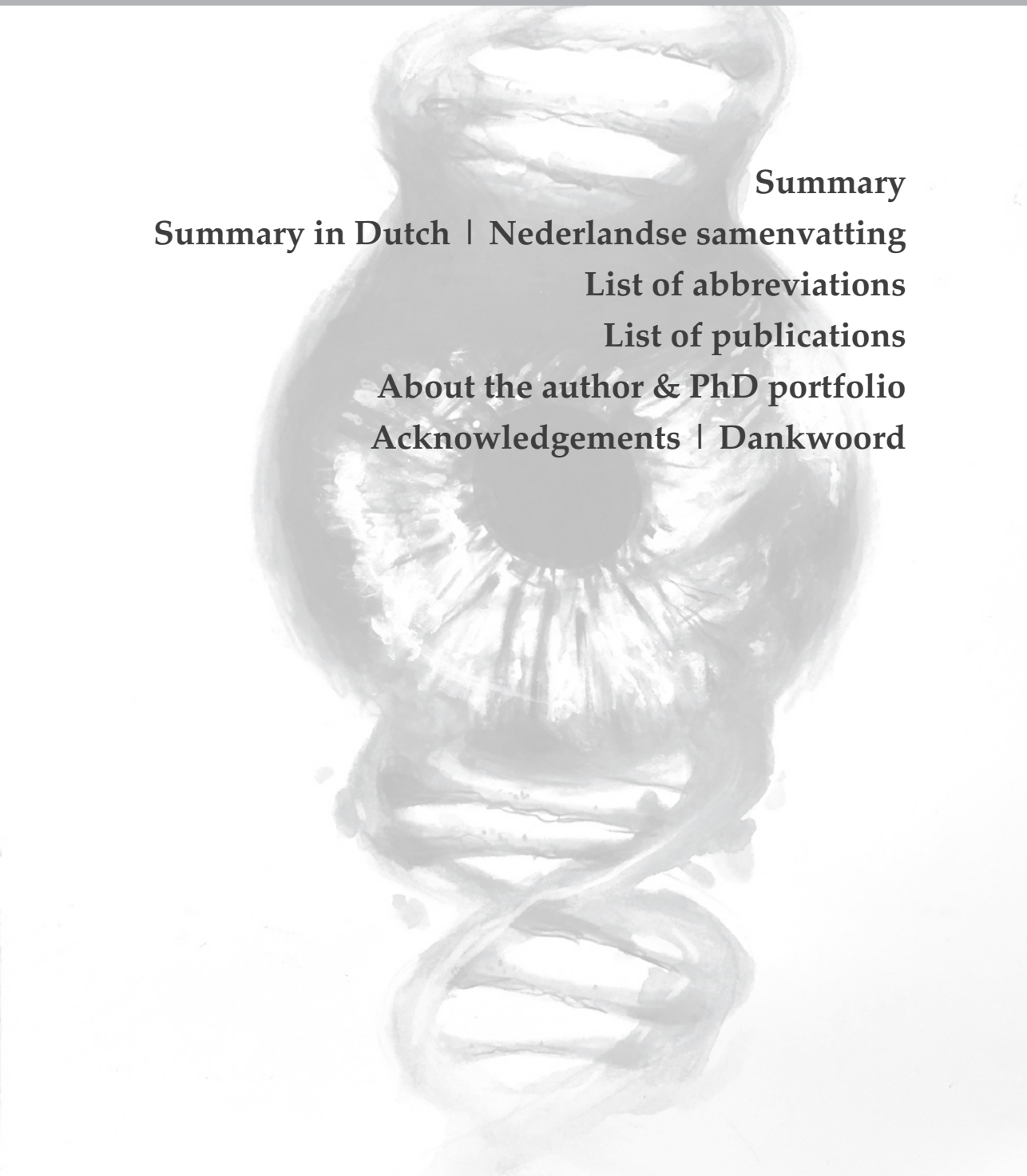

Summary

Summary in Dutch | Nederlandse samenvatting

List of abbreviations

List of publications

About the author & PhD portfolio

Acknowledgements | Dankwoord

Summary

Uveal melanoma (UM) is a rare malignancy derived from the melanocytes in the choroid, ciliary body and iris. Although treatment of the primary tumor has a high (>90%) local tumor control, up to 50% of the patients still develop metastasis within 15 years after diagnosis. The liver is affected typically, with two different metastasis patterns; nodular metastases and a miliary (innumerable small) metastases pattern. Metastases are lethal within a year in almost all patients. Several markers are known to predict patient prognosis. Besides the AJCC TNM classification, these markers classically divide patients in UM with high-risk and low-risk for metastasis.

Historically, the chromosomal aberrations in UM were the best predictors of metastatic disease. Monosomy 3 (loss of chromosome 3) occurs in the UM of half of the patients, and has the strongest chromosomal association with an unfavorable prognosis. Besides monosomy 3 also chromosome 8q gain is correlated with unfavorable outcome, whereas chromosome 6p gain predicts a favorable outcome. In the recent years, with the development of massive sequencing, many genes involved in UM tumorigenesis were discovered. Of these genes, the three genes correlating to survival were BAP1, SF3B1 and EIF1AX.

Patients with monosomy 3 and BAP1 mutations in the remaining allele (BAP1 is located on chromosome 3), predispose to a high risk for metastasis. The majority of the patients develop metastases within five years after diagnosis. A second group are the patients with SF3B1 mutations in combination with disomy 3 (no chromosome 3 loss). These patients seem to have a favorable prognosis within the first years after diagnosis, however these patients typically develop metastases after five years. The third group is comprised of patients with EIF1AX mutations, also in combination with disomy 3. These patients have a very low risk of developing metastases.

Besides the differences in prognosis these almost-mutually exclusive mutated genes are also characterized by typical chromosomal patterns. BAP1-mutated UM contain copy number variations (CNVs) that affect entire chromosomes or chromosome arms. Also isochromosomes (two short or long arms of the same chromosome attached to each other) are almost only observed in BAP1-mutated UM. SF3B1-mutated UM on the other hand have more CNVs, however these CNV are smaller in size since they only affect the chromosome telomere. And finally, EIF1AX-mutated UM only harbor

very few CNVs, most typically only entire chromosome 6 gain or gain of a small terminal part of chromosome 6p. This highlights that UM with mutations in these genes reflect different UM subtypes that differ in prognosis and chromosomal patterns. An association of the mutated genes and the metastases patterns (nodular versus miliary) could not be made.

Besides these genetic aberrations, patients with UM can also harbor rare chromosomal phenotypes such as polyploidy (genome doubling) and chromothripsis (shattered and randomly rearranged chromosomes). When analyzed in a dichotomous way (present versus absent), these chromosomal aberrations both correlate to worse patient survival. However, when corrected for the mutation status, this difference does not remain significant. These chromosomal aberrations occur more often in the BAP1-mutated patients, perhaps due to chromosomal imbalance, and therefor skew the prognosis towards an unfavorable outcome.

In conclusion, survival of UM patients is strongly correlated to mutations in the genes BAP1, SF3B1 and EIF1AX. These UM represent molecular distinct subclasses. These differences may provide patient and gene specific targets for future therapies.

Summary in Dutch | Nederlandse samenvatting

Uvea melanomen (UM) zijn zeldzame maligniteiten die ontstaan vanuit de melanocyten in het choroid (vaatvlies), corpus ciliare (straalvormig lichaam) en iris (regenboogvlies). De behandeling van de primaire tumor leidt tot een goede lokale tumorcontrole (>90%). Desondanks ontwikkelt de helft van de patiënten levermetastasen binnen 15 jaar na diagnose. Bij deze groep patiënten is de overlevingsduur gemiddeld korter dan één jaar. Echter, ook binnen deze groep zijn de verschillen wat betreft overleving aanzienlijk. Om de prognose nader te bepalen wordt gebruik gemaakt van diverse markers. Naast de AJCC 'Tumor Node Metastases' (TNM) classificatie, verdelen de markers patiënten met UM in twee groepen; hoog risico en laag risico voor het ontwikkelen van metastasen.

Eén van de tumorkenmerken die helpen bij het voorspellen van metastasen zijn chromosoomafwijkingen. Chromosomen komen normaal gesproken altijd in paren (disomie). Wanneer één heel chromosoom verloren gaat spreekt men van een monosomie. Monosomie van chromosoom 3 heeft de sterkste associatie met een korte survival en wordt gezien in de helft van de tumoren. Naast verlies van een chromosoom kan het ook zijn dat er juist een (deel van) een chromosoom bij komt. Hierbij zien we dat winst van de lange arm van chromosoom 8 is gecorreleerd met een ongunstige uitkomst, terwijl winst van de korte arm van chromosoom 6 juist is geassocieerd met een gunstige overleving. Met behulp van nieuwe DNA sequentietechnieken zijn er ook genen ontdekt die betrokken zijn in het ontstaan (tumorgenese) van UM. Mutaties in drie van deze genen , *BAP1*, *SF3B1* en *EIF1AX* correleren met de overleving van de patiënt.

Van deze genen geeft de *BAP1* mutatie in de tumor het hoogste risico op metastasen. Het merendeel van deze patiënten ontwikkelt metastasen binnen 5 jaar na diagnose. Een gunstiger profiel wordt gezien bij patiënten met een *SF3B1* mutatie in de tumor. Bij hen ontwikkelen metastasen zich na 7-10 jaar. De *EIF1AX* mutaties tenslotte, geven een zeer laag risico op het ontwikkelen van metastasen.

Naast het feit dat deze mutaties effect hebben op de overleving, zien we ook dat mutaties in deze genen gepaard gaan met een karakteristiek chromosomenpatroon. *BAP1* gemuteerde UM bevatten chromosoomafwijkingen waarbij hele chromosomen of chromosoomarmen veranderd zijn . In UM met deze *BAP1* mutatie worden ook isochromosomen gevonden, waarbij twee dezelfde chromosoomarmen aan elkaar vast

zitten. De tumoren met een *SF3B1* mutatie hebben juist meer en kleinere chromosoom afwijkingen, waarbij alleen de uiteinden (telomeren) van de chromosomen zijn aangedaan. De tumoren met een *EIF1AX* mutatie hebben weinig chromosoom afwijkingen, hoewel winst van heel chromosoom 6 of alleen winst van een kleine terminale einde van chromosoom 6p relatief vaak voorkomt.

Tenslotte hebben we gekeken naar twee bijzondere vormen van chromosoomafwijkingen: polyploidie (verdubbeling van het genoom) en chromothripsis (herschikking van een [deel van] een chromosoom). Beide genetische veranderingen zien we vaak in combinatie met een *BAP1* mutatie hetgeen geassocieerd is met een ongunstige prognose.

Concluderend: De overleving van patiënten met een uvea melanoom is sterk gecorreleerd met mutaties in *BAP1*, *SF3B1* en *EIF1AX* genen. Daarnaast leiden de verschillende mutaties tot een verschillend chromosoom patroon. Met behulp van het genetisch profiel van een uvea melanoom kan zodoende een goede inschatting van de prognose gemaakt worden.

List of abbreviations

AJCC	American Joint Committee on Cancer
ANOVA	Analysis of Variance
BAP1	BRCA1-associated Protein 1
CAS	CRISPR-associated System
CBI	Ciliary Body Involvement
cfDNA	Circulating free DNA
CLL	Chronic Lymphocytic Leukemia
CN	Copy Number
CNV	Copy Number Variation
COMS	Collaborative Ocular Melanoma Study
CRISPR	Clustered Regulatory Interspaced Short Palindromic Repeats
CSV	Chromosomal Structural Variants
CT	Computed Tomography
CYSLTR2	Cysteinyl Leukotriene Receptor 2
DDR	DNA Damage Repair
DFS	Disease-Free Survival
DI	DNA Index
EIF1AX	Eukaryotic Translation Initiation Factor 1A, X-linked
EMT	Epithelial-to-Mesenchymal Transition
EXE	Extraocular Extension
EZHZ	Enhancer of Zester 2 Polycomb Repressive Complex 2, subunit
FAG	Fluorescence Angiography
FFPE	Formalin-Fixed Paraffin-Embedded
FISH	Fluorescence in-situ Hybridization
FNAB	Fine-Needle Aspiration Biopsy
GEP	Gene Expression Profiling
GNA11	Guanine Nucleotide Binding Protein, subunit 11
GNAQ	Guanine Nucleotide Binding Protein, subunit q
H2A	Histone 2A
HC	Hierarchical Clustering
HDAC	Histone Deacytelase
HGF	Hepatocyte Growth Factor
HR	Homologous Recombination
ICG	Indocyanine Green Chorioangiography

IHC	Immunohistochemistry
InDel	Insertion and/or Deletion
LOH	Loss of Heterozygosity
LUMPO	Liverpool Uveal elanoma Prognosticator Online
MDS	Myelodysplastic Syndrome
MLPA	Multiplex Ligation Dependent Probe Amplification
MRI	Magnetic Resonance Imaging
miRNA	Micro RNA
mRNA	Messenger RNA
NHEJ	Non-Homologous End Joining
NRM	No Recurrent Mutation
OCT	Optical Coherence Tomography
PCC	Premature Chromosome Compaction
PLCB4	Phospholipase C Beta 4
PRAME	Preferentially Expressed Antigen in Melanoma
RASSF1A	Ras-associated Domain Family Member 1
ROMS	Rotterdam Ocular Melanoma Studygroup
SF3B1	Splicing Factor 3b, subunit 1
SKY	Spectral Karyotyping
SNP	Single NucleotidePpolymorphism
SNV	Single Nucleotide Variation
SRT	Stereotactic Radiation Therapy
TCGA	The Cancer Genome Atlas
TNM	Tumor Node Metastasis
UM	Uveal Melanoma
US	Ultrasonography
WES	Whole-Exome Sequencing
WGS	Whole-Genome Sequencing
YAP	Yes-associated Protein

List of publications

Serdar Yavuzyigitoglu*, Anna. E. Koopmans*, Robert M. Verdijk, Jolanda Vaarwater, Bert Eussen, Alice van Bodegom, Dion Paridaens, Emine Kilic and Annelies de Klein. Uveal Melanoma with SF3B1 mutations; A Distict Subclass Associated with Late-Onset Metastases. *Ophthalmology. 2016 May;123(5):1118-28.*

S. Yavuzyigitoglu*, Hanneke W. Mensink*, Kyra N. Smit, Jolanda Vaarwater, Robert M. Verdijk, Berna Beverloo, Hennie T. Brüggenwirth, Ronald van Marion, Hendrikus J. Dubbink, Dion Paridaens, Nicole C. Naus, Annelies de Klein and Emine Kilic. Metastatic disease in polyploid uveal melanoma patients is associated with BAP1 mutations. *Invest Ophthalmol Vis Sci. 2016 Apr 1;57(4):2232-9.*

S. Yavuzyigitoglu, Emine Kilic, Jolanda Vaarwater, Annelies de Klein, Dion Paridaens and Robert M. Verdijk. Lipomatous Change in Uveal Melanoma: Histopathological, Immunohistochemical and Cytogenetic Analysis. *Ocul Oncol Pathol 2016;2:133–135.*

S. Yavuzyigitoglu*, Wojtek Drabarek*, Kyra N. Smit, Natasha van Poppelen, Anna E. Koopmans, Jolanda Vaarwater, Tom Brands, Bert Eussen, Hendrikus J. Dubbink, Jov van Riet, Harmen J.G van de Werken, Berna Beverloo, Robert M. Verdijk, Nicole Naus, Dion Paridaens, Emine Kilic and Annelies de Klein. Correlation of Gene Mutation Status with Copy Number Profile in Uveal Melanoma. *Ophthalmology. 2017 Apr;124(4):573-575.*

* These authors contributed equally to this work.

About the author

Serdar Yavuzyigitoglu was born on the 24th of December 1988 in Hellevoetsluis, the Netherlands. He graduated from Atheneum at the GSG Helium, Hellevoetsluis in 2007. The same year he started his study Medicine at the Erasmus University Rotterdam. During his study he worked as a research assistant under the supervision of Dr. Tahlita Zuiverloon and Prof. Dr. Ellen Zwarthoff at the Department of Pathology of the Erasmus Medical Centre, Rotterdam. In 2011 he moved to Tilburg for his internships. In 2013 he returned to Erasmus MC for his research internship under the supervision of dr. Emine Kilic at the Department of Ophthalmology. After obtaining his medical degree, he began his PhD study in February 2018 under the supervision of Dr. Annelies de Klein and Dr. Emine Kilic. During his PhD study he also took part of the PhD committee of Erasmus MC. In June of 2016, he started his residency in Ophthalmology at the Department of Ophthalmology at the Erasmus Medical Centre, headed by Prof. Dr. Hans Vingerling.

PhD Portfolio

Summary of PhD training and teaching

Name PhD student: Serdar Yavuzyigitoglu Erasmus MC Department: Ophthalmology & Clinical Genetics Research School: MGC	PhD period: 01-02-2014 Promotor(s): Prof. dr. J.R. Vingerling & Prof. dr. A.D.A. Paridaens Supervisor: Dr. J.E.M.M. de Klein & Dr. E. Kiliç

1. PhD training

	Year	Workload (Hours/ ECTS)
General courses		
- Safe Laboratory Techniques, 25 June 2014, Leiden (MGC)	2014	8 hours
- Research Integrity, 22 May 2015, Rotterdam	2015	0.3 ECTS
- Biomedical English Writing and Communication	2015	4 ECTS
- Biostatistical Methods I: Basic Principles (CCO2), 21 September – 16 October 2015	2015	5.7 ECTS
In-depth courses		
- Genetics Crouse (MGC)	2014	3 ECTS
- Biochemistry and Biophysics Course (MGC)	2015	3 ECTS
- Chromatin Day (MGC)	2015	1 ECTS
Specific courses (e.g. Research school, Medical Training)		
- The Annual Course on Molecular Medicine, 18-19 February 2014, Rotterdam (MolMed)	2014	0.7 ECTS
- A broad spectrum of NGS Applications in Molecular Medicine, 23-24 April 2014, Rotterdam (MolMed)	2014	16 hours
- Biomedical Research Techniques XIII, 13-17 October 2014, Rotterdam (MolMed)	2014	1.5 ECTS
- NGS in DNA Diagnostics Course, 28-30 October 2014, Rotterdam (MolMed)	2014	1.0 ECTS

Seminars and workshops		
- The Photoshop and Illustrator CS6 Workshop for PhD-students and other researchers, 8 April 2014, Rotterdam	2014	0.3 ECTS
- Workshop on NCBI & other open source software, 12-14 May 2014, Rotterdam	2014	20 hours
- Survival Analysis Course, 18-19 December 2014, Rotterdam (MolMed)	2014	0.5 ECTS
- Erasmus MC mini-symposium, 'a beauty contest', 6 June 2014, Rotterdam (MolMed)	2014	5 hours
- The 24th MGC Symposium, 19 September 2014, Rotterdam (MGC)	2014	8 hours
- New tests in oncology and diseases of the vitreous, 28 November 2014, Utrecht (ARVO-Ned)	2014	5 hours
- 3rd Daniel den Hoed Day, 18 February 2015, Rotterdam (MolMed)	2014	8 hours
Presentations		
- Weekly scientific seminars at the department of Clinical Genetics, Erasmus MC, Rotterdam (oral presentations)	2014-2015	15 hours
- Weekly scientific and clinical seminars at the department of Ophthalmology, Erasmus MC, Rotterdam (oral presentations)	2014-2015	10 hours
(Inter)national conferences		
- The 45th Ophthalmic Oncology Group (OOG) meeting, 7-9 March 2014, Krakow, Poland; oral presentation 'The FileMaker database of ROMS'	2014	40 hours
- The 24th Genetics Retreat meeting, 19-21 March 2014, Kerkrade; oral presentation '*SF3B1* and *EIF1AX* mutations in uveal melanoma, protective or not?'	2014	30 hours
- Nederlands Oogheelkundig Gezelschap (NOG) jaarvergadering 2014, 26-28 March 2014, Maastricht	2014	24 hours
- CGC.nl meeting 'Cellular Signalling and Cancer Therapeutics', 13-14 November 2014, Amsterdam	2014	16 hours
- Dutch Ophthalmology PhD Students (DOPS), 6-7 March 2015, Nijmegen; poster contribution '*BAP1* correlates with metastasis in polyploid uveal melanoma'	2015	16 hours
- The 47th Ophthalmic Oncology Group (OOG) meeting, 12-14 March 2015, Moscow, Russia; oral presentation '*BAP1* correlates with metastasis in polyploid uveal melanoma' (awarded with travel prize)	2015	40 hours
- From Discovery to Diagnostics: Translational research in medical genetics, 26 March 2015, Nijmegen	2015	8 hours
- Nederlands Oogheelkundig Gezelschap (NOG) jaarvergadering 27, March 2015, Groningen; oral presentation '*BAP1* correleert met metastasen in polyploïde uvea melanomen'	2015	8 hours
- The 25th Genetics Retreat meeting, 22-24 April 2015, Kerkrade; oral presentation '*BAP1* correlates with metastasis in polyploid uveal melanoma'	2015	30 hours
- PhD student workshop (MGC), 15-18 June 2015, Maastricht; poster contribution '*BAP1* correlates with metastasis in polyploid uveal melanoma'	2015	30 hours
- NCRI Cancer Conference, 1-4 November 2015, Liverpool, United Kingdom; poster contribution '*SF3B1* and *EIF1AX* mutations in uveal melanoma' (awarded with EACR Travel Award for abstract)	2015	30 hours
- Nederlands Oogheelkundig Gezelschap (NOG) jaarvergadering 27, March 2017, Maastricht: oral presentation 'Molecular classification of uveal melanoma subtypes using integrative mutational and whole-genome copy number analyses'	2017	24 hours

(Inter)national conferences (Continued) - The Association for Research in Vision and Ophthalmology (ARVO) Annual Meeting, 7-11 May 2017, Baltimore, United States of America; oral presentation 'Molecular classification of uveal melanoma subtypes using integrative mutational and whole-genome copy number analyses'	2017	40 hours
Other - Travel price for best presentation at the 47th Ophthalmic Oncology Group (OOG) meeting, Moscow, Russia. Presentation: '*BAP1* correlates with metastasis in polyploid uveal melanoma'. - European Association of Cancer Research Travel award for abstract at the NCRI Cancer Conference, Liverpool, United Kingdom. Poster '*SF3B1* and *EIF1AX* mutations in uveal melanoma'. - Bayer Ophthalmology Research Award (BORA) prior to Nederland Oogheelkundig Gezelschap (NOG) conference. Second price (€10.000) for project 'Whole-exome sequencing of matched primary uveal melanoma and metastasis : unravelling the genetics'.	2015 2015 2016	
2. Teaching		
	Year	**Workload (Hours/ ECTS)**
Lecturing -		
Supervising practicals and excursions, Tutoring -		
Supervising Master's theses - Mentor 4th year technical analyst student Esra Bekdaş: 'Pathway analysis of whole-exome sequencing identifies *de novo* mutations in uveal melanoma' - Mentor 4th year medical student Miguel Jansen; 'Correlation of imaging findings in liver metastasis and genetic profiles of uveal melanoma' - Mentor 6th year medical student Wojtek Drbarek: 'Correlation between copy number variation and mutation status of *EIF1AX*, *SF3B1* and *BAP1* genes in uveal melanoma' - Supervising 4th year technical analyst student Rolf Barkmijer: 'The prognostic value of MUC4, ATRX, RKIP, YAP, pYAP and β-catenin in uveal melanoma: an immunohistochemical analysis' - Mentor 6th year medical student Michael Tang; 'Analysis of metastatic disease of uveal melanoma in relation to tumor profile'	2014-2015 2014-2015 2015 2014-2015 2017	7 months 2 years 6 months 7 months 5 months
Other - Tutor Junior Medschool Students: 'Biomarkers in uveal melanoma'	2015	1 month

Acknowledgements | Dankwoord

Elhamdülillah! Eindelijk is het dan zo ver. Ik ben vele mensen dankbaar voor het tot stand komen van mijn proefschrift. Het was een periode waarin ik veel heb geleerd over oogheelkunde, genetica, oncologie, statistiek, ethiek en met name ook over mezelf. Ik heb gedurende mijn promotie traject een nieuwe passie ontwikkeld, het doen van wetenschappelijk onderzoek. Voor dit wil ik vele mensen bedanken die hier direct of indirect aan hebben bijgedragen.

Allereerst mijn ouders. Sevgili annem ve babam. Sonunda bitti! Sizlerin sayesinde inşAllah doktoramı alacağım. Bu başarıda benim emeğim olduğu kadar sizinde emeğiniz var. Bilgilerinizi ve özelliklerinizi bana yansıtarak beni ben yaptığınız için teşekkur ederim.Daarnaast wil ik ook mijn broers Süleyman en Mehmet en zusje Hilal bedanken. Ik leerde goed discussiëren en beargumenteren door onze vele gesprekken over politiek, geschiedenis, religie en Dragonball Z.

Mijn copromotoren, dr. Annelies de Klein en dr. Emine Kılıç. Beste Annelies, als er iets is wat ik langer had willen doen is het onderzoek doen onder jouw supervisie. Jouw kennis, doorgrondende eerlijkheid, oprechtheid, perfectionisme, 'thinking outside the box' en vele andere kwaliteiten hebben mij gevormd tot de onderzoeker die ik ben. We hebben moeilijke periodes doorgemaakt, echter ben ik van mening dat die onze relatie alleen maar sterker hebben gemaakt. Ik ben je ongelooflijk dankbaar voor je begeleiding en de mogelijkheid om iedere dag langs te komen met mijn vragen en problemen. Beste Emine, je bent mijn nummer 1 voorbeeld! Als anderen vragen naar mijn toekomstplannen zeg ik altijd 'werken zoals Emine het doet'. Het combineren van wetenschap en kliniek in een academische setting om het beste te kunnen bieden voor patiënten. Sinds mijn keuzeonderzoek heb je me onder je vleugel genomen en hiervoor ben ik je dankbaar. Ik kon altijd bij je terecht voor wetenschappelijke, medische en niet-medische zaken. Ik hoop nog veel van je te leren in de kliniek.

Mijn promotoren, prof. dr. Hans Vingerling en prof. dr. Dion Paridaens. Beste Hans, bedankt voor het vertrouwen dat je in mij had sinds dat ik als oudste coassistent op de afdeling rondliep. Je leiderschap op de afdeling en de kansen die je biedt voor persoonlijke ontplooiing zorgden ervoor dat ik mijn opleiding tot oogarts en het afronden van mijn proefschrift goed kon combineren. Beste Dion, hartelijk dank voor je input voor alle manuscripten en je betrokkenheid bij alle projecten. Dankzij mijn stage in

het Oogziekenhuis heb ik je expertise mogen meemaken in de kliniek. Ik kijk uit naar onze toekomstige samenwerkingen!

De leden van de kleine commissie prof. dr. Ellen Zwarthoff, prof. dr. Robert Hofstra en prof. dr. Jeroen Klevering wil ik hartelijk bedanken voor het deelnemen aan mijn leescommissie en het beoordelen van mijn proefschrift.

Daarnaast wil ik prof. Dr. Martine Jager, prof. dr. Stefan Sleijfer en dr. Victoria Cohen bedanken voor hun deelname aan mijn grote commissie. Dr. Cohen, thank you for taking part in the doctoral committee.

Mijn mede PhD kandidaten van uvea melanoom onderzoek. Beste Anna, bedankt voor de begeleiding toen ik nog student was en voor het vervolgens overdragen van het stokje. Beste Kyra, Natasha en Jackelien, bedankt voor alle samenwerkingen, discussies en overleggen. Ik wens jullie allen succes met het afronden van jullie trajecten. Woj-tek Dra-ba-rek! Mijn protegé! Wat heb jij een moeilijke taak gekregen om mij op te volgen! Zet mijn filosofie voort van tien uur beginnen met werken en buiten uitgebreid lunchen!

Dr. Verdijk, beste Rob, je vormt een onmisbaar en ongelooflijk groot deel uit van de research groep Rotterdam Ocular Melanoma Studygroup (ROMS). Bedankt voor alle input en aanvullende onderzoeken. Mijn dank gaat ook uit naar alle andere leden van de ROMS; Hanneke Mensink, Nicole Naus, Caroline van Rij, Kaspar Geul en iedereen die erbij betrokken is. De ROMS vormt een geweldige Rotterdamse samenwerking tussen meerdere afdelingen van het Erasmus MC, het Oogziekenhuis en het St Franciscus Gasthuis ziekenhuis.

Collega's van de afdelingen Klinische Genetica en Oogheelkunde. Jolanda, je bent onvervangbaar voor het onderzoek en een stabiel factor binnen de groep, bedankt voor alle samenwerkingen. Bert en Tom, jullie wil ik ook van harte bedanken voor alle hulp met technologie, informatica en de database. Kamergenoten op de 20e, Hannie, Erwin en Daphne, bedankt voor alle hulp op het lab. Kamergenoten en verdiepinggenoten op de 16e, Jan-Roelof, Magda, Elizabeth, Frea en prof. Huib Simonsz, bedankt voor alle gezelligheid.

Daarnaast wil ik alle collega's bedanken van de 9e, 20e en 24e verdieping voor alle gezelligheid, besprekingen en hulp op het lab. Hardcore muziek tijdens het sequensen houd je altijd geconcentreerd. Robert van de Helm bedankt voor alle hulp met de SNP-arrays. Guido en Bianca, bedankt voor alle hulp bij PCR'en en Sanger sequensen. Ook wil ik de afdeling Biomics bedanken voor alle hulp rondom het NGS werk. Askar, Harmen en Job bedankt voor alle hulp met bio-informatica. Het tumor cytogenetisch laboratorium ook hartelijk dank voor alle hulp.

De vele studenten die ik heb mogen begeleiden; Alice, Esra, Rolf, Lieke, Remon, Stanley, Wojtek, Miguel en Michael. Bedankt voor al jullie bijdrages! Ik wens jullie allen succes met het vervolgen van jullie carrière.

Alle arts assistenten, stafartsen en andere medewerkers van de poli Oogheelkunde , hartelijk dank dat jullie me uithouden op de poli! Ik zal weer broodjes regelen bij Grillig! Nicole van Basten en Tanja Bovenkamp bedankt voor alle administratieve regelzaken rondom mijn promotie en opleiding! Mijn mede PhD kandidaten van de oogheelkunde (EMCRO), bedankt voor de gezelligheid! En voor het controleren en verbeteren van mijn Nederlandse tekst ook veel dank aan Gijsbert.

Elia Pellegrini (@elia_pelle), thank you very much for the cover. You are an amazing artist! Dr. Lardenoije en de rest van de oogartsen en de medewerkers van de polikliniek Oogheelkunde van het St. Elisabeth ziekenhuis wil ik ook bedanken. Dankzij jullie ben ik in aanraking gekomen met de oogheelkunde en door jullie enthousiasme was ik er van overtuigd dat dit vakgebied ook voor mij was.

Extra bedankje voor mijn twee paranimfen. Beste Kyra, ik wil je hartelijk bedanken voor alle samenwerkingen en gezelligheid. Het was me altijd een genoegen om ideeën met je uit te wisselen over oncologie en genetica (en ethiek en vrouwenvoetbal en religie en het nieuwe album van Justin Bieber, which totally rocks!). Succes met het afronden van je PhD! Aleksander (Leksieboo), waddup boy? We zijn vrienden sinds Geneeskunde jaar 2 … sinds dat we samen veel cash verdienden werkende voor dr. Tahlita Zuiverloon en prof. Dr. Ellen Zwarthoff. Ik zal de tijden van de Sixpack, Romeo en Cesco nooit vergeten! En nu samen oogarts worden!

Mijn matties!!! De shisha boys (grapje Dilek, ik gebruik geen shisha!), Askin, Heybet, Riza, Mehmet, Fatih, Ayhan en Umut! De Opa Soldiers, Aleksander, Stefan, Serhat, Jay, Matthijs, Musti, Niri en Rushil! De SpareRibs boys, Nedim, Annas, Willem, Gijsbert, Wojtek, Mesut, Ünal, Ramazan, Tim en Onur! Boys bedankt voor alle bromance!

Lieve Dilek, Sevgili Dileğim, hayatıma okdar güzellik getirdin ve inşAllah dahada çok güzel günlerimiz olacaktır. Senin güzelliğinle, aklınla, çalışkanlığınla gurur duyuyorum ve senin için kendimde daha başarılı olmak istiyorum. Herşey için sağol. #couplegoals.